VIRAL GLYCOPROTEINS AND ENDOPLASMIC RETICULUM-ASSOCIATED DEGRADATION

By

Dylan Alexander-Aldo Frabutt

A DISSERTATION

Submitted to
Michigan State University
in partial fulfillment of the requirements
for the degree of

Microbiology and Molecular Genetics–Doctor of Philosophy

2018

ABSTRACT

VIRAL GLYCOPROTEINS AND ENDOPLASMIC RETICULUM-ASSOCIATED DEGRADATION

By

Dylan Alexander-Aldo Frabutt

Enveloped viruses are responsible for many virulent diseases of critical concern to public health. As a prerequisite for infectivity, enveloped viruses must mount viral proteins into host membranes in order to facilitate binding and entry into their target cell population. These membrane proteins are often heavily glycosylated and are subject to the unique folding environment in the endoplasmic reticulum, which consists of the host machinery necessary for maintaining the protein homeostasis either through folding assistance or degradation of proteins unable to fold properly. I have investigated both of these aforementioned roles through the characterization of HIV-1 and influenza A virus envelope interactions with the endoplasmic reticulum chaperones calnexin and calreticulin and the roles that class I α 1,2-mannosidases play in the degradation of these viral envelope glycoproteins. Additionally my work has sought to characterize how different viruses activate the unfolded response when producing their envelope glycoproteins and how this activation may influence viral infections.

TABLE OF CONTENTS

LIST OF TABLES

LIST OF FIGURES

KEY TO ABBREVIATIONS

HIV	Human immunodeficiency virus
ERAD	Endoplasmic reticulum-associated degradation
IAV	Influenza A virus
EDEM	Endoplasmic reticulum-associated degradation enhancing α-mannosidase-like
ERManI	Endoplasmic reticulum class I α-mannosidase
UPR	Unfolded protein response
HA	Hemagglutinin
NA	Neuraminidase
NGS	N-glycosylation sites
ER	Endoplasmic reticulum
UPS	Ubiquitin/proteasome system
IRE1	Inositol-requiring enzyme 1
PERK	Protein kinase-like ER kinase
ATF6	Activating transcription factor 6
Man	Mannose
CNX	Calnexin
CRT	Calreticulin

CHAPTER 1 - Arms Race between Enveloped Viruses and the Host ERAD Machinery

Dylan A. Frabutt and Yong-Hui Zheng

Originally published in Viruses, 2016 September; Volume 8(9):255

Introduction

Enveloped viruses represent a significant category of pathogens that cause serious diseases in animals. These viruses express envelope glycoproteins that are singularly important during the infection of host cells by mediating fusion between the viral envelope and host cell membranes. Despite low homology at protein levels, three classes of viral fusion proteins have, as of yet, been identified based on structural similarities. Their incorporation into viral particles is dependent upon their proper sub-cellular localization after being expressed and folded properly in the endoplasmic reticulum (ER). However, viral protein expression can cause stress in the ER, and host cells respond to alleviate the ER stress in the form of the unfolded protein response (UPR); the effects of which have been observed to potentiate or inhibit viral infection. One important arm of UPR is to elevate the capacity of the ER-associated protein degradation (ERAD) pathway, which is comprised of host quality control machinery that ensures proper protein folding. In this review, we provide relevant details regarding viral envelope glycoproteins, UPR, ERAD, and their interactions in host cells.

Enveloped Viruses

Despite their vast diversity, animal viruses can be simply divided into two categories: non-enveloped viruses and enveloped viruses (1). While non-enveloped viruses are wrapped with naked shells made of viral capsid proteins, enveloped viruses are covered with a lipid-bilayer, which is called a viral envelope. The viral envelope is obtained from progenitor host cells during the budding process, which can be a portion of plasma membrane or intracellular membrane. On the surface of the enveloped viruses, there are peplomers that project from the viral envelope, and play a critical role in viral infection. These peplomers are also described as spikes, which are made of viral envelope glycoproteins. Envelope spikes serve to identify and bind to viral receptors on the host cell surface, allowing viral entry into cells and the initiation of infection by mediating virus-cell fusion. Thus, the infectivity of enveloped viruses is absolutely dependent on the integrity of the viral envelope, and the functionality of the viral glycoproteins found therein.

Enveloped viruses are more stable than non-enveloped viruses under physiological conditions, at the expense of their sensitivity to high-temperature, low-pH, desiccation, or detergent-treatment, which limits their ability to withstand severe environments (2). The entry of enveloped viruses requires the formation of a fusion pore between the viral envelope and the cell membrane, through which the viral genome is released into the cell. This fusion process is triggered by interactions between viral glycoproteins on the viral envelope and viral receptors on the cell surface, which can occur directly at the plasma membrane at neutral pH or in endocytic compartments at either low or neutral pH (3). In addition, enveloped viruses can also enter cells through direct cell-to-cell contacts via virological synapses to provide a means by which the virus can cross the biophysical and immunological obstacles to infection (4). The membrane penetration mechanism differs fundamentally in non-enveloped viruses, but similar strategies are used for their entry (5). In general,

enveloped animal viruses possess greater adaptability than non-enveloped animal viruses, and consequently, cause a number of severe diseases, such as acquired immunodeficiency syndrome (AIDS), influenza, severe acute respiratory syndrome (SARS), hemorrhagic fever, hepatitis, encephalitis, and microcephaly.

Virus Envelope Glycoproteins

The fusion between viral envelope and cell membranes is absolutely critical for the entry of enveloped viruses, which is usually triggered by the insertion of a viral envelope glycoprotein's (Env) fusion peptide into the host membrane. The vast majority of viral fusion proteins are type I transmembrane proteins, which have a single transmembrane domain (TMD), with their *N*-terminus outside cells and *C*-terminus inside cells. Most viral envelope proteins have been modeled as existing in a less stable pre-fusion state or a stable post-fusion state. Many of these proteins also oligomerize into trimeric fusogenic complexes in their post-fusion states, forming trimeric hairpin structures on the viral envelope.

Based on their structural and mechanistic properties, viral fusion proteins have been classified into three distinct classes (6). Class I fusion proteins are found in influenza viruses, paramyxoviruses, retroviruses, and filoviruses. These envelope proteins are first expressed as a polypeptide precursor and then cleaved by cellular proteases, yielding a transmembrane protein with an amino-terminal fusion peptide and a surface protein, which are attached either non-covalently or by a disulfide-bond. The core of the class I protein fusogenic domain is predominantly composed of α-helices, which contain an *N*-terminally located fusion peptide. These proteins trimerize and form a central coiled-coil structure with a three-α-helix bundle in the pre-fusion state, which refolds into a six-α-helix bundle in the post-fusion state.

Class II fusion proteins are found in flaviviruses, hepaciviruses, alphaviruses, togaviruses, and Rift Valley fever viruses. They depend on a viral chaperone for folding, which is produced from the same polypeptide precursor where they are arrayed in tandem. When the

chaperone is cleaved off, the fusion protein gains the fusogenic activity. These fusion proteins are mostly made of β-sheets and exist as homo- or hetero-dimers with the fusion peptides buried in internal loops in the pre-fusion state. In the post-fusion state, these proteins undergo self-rearrangement into stable trimeric hairpins, exposing the fusion peptide and resulting in viral and host membrane fusion.

Class III fusion proteins are found in rhabdoviruses, herpesviruses, and baculoviruses. These proteins are directly translated as a single protein from viral mRNA without protease cleavage, and trimerize in both pre- and post-fusion states. Notably, they combine structural signatures found in both classes I and II, which include a central trimeric coiled coil, three domains predominantly made of β-sheets, and internal fusion peptides in the pre-fusion state. However, unlike in class I and II fusion proteins, the pre-fusion and post-fusion states are reversible in class III fusion proteins.

In addition to these structural features, viral fusion proteins are subject to *N*-glycosylation at varying degrees. Although some viral envelope proteins such as the dengue virus (DENV) E protein are glycosylated at relatively low levels (7), most of the other important human viruses are subject to heavy glycosylation. For example, human immunodeficiency virus type 1 (HIV-1) Env precursor gp160 has ~34 potential *N*-linked glycosylation sites (PNGSs): ~30 in gp120 and ~4 in gp41 (8); influenza hemagglutinin (HA) molecules have 5 to 11 PNGSs depending on subtypes, with the majority of sites residing in the globular head of the molecule (9); hepatitis C virus (HCV) E1 has 4 PNGSs and E2 has 9 PNGSs (10); and Ebola virus envelope glycoprotein (GP) has 17 PNGSs (15 in GP1 and 2 in GP2) (11). HIV-1 Env and HCV E1 and E2 are so heavily glycosylated that ~50% of their respective molar masses are derived from *N*-linked glycans. Most of the critical sites in these viral glycoproteins are conserved during viral evolution, suggesting the important function of glycosylation in viral infections.

Glycosylation, which is one of the most common post-translational modifications in eukaryotic cells, is required for protein folding and maintaining protein structure. Viruses have taken advantage of this benefit at nearly every step of the viral life cycle (12). *N*-glycosylation significantly promotes their folding and solubility, enhances subsequent trafficking of these viral proteins to their destinations, and ensures that they are properly processed and incorporated into virions. Nevertheless, glycosylation can have distinct effects that are both advantageous and detrimental to viral fitness. For example, if glycosylation occurs close to the glycoprotein processing sites, it may block the precursor cleavage by proteases and inhibit viral infection (13); if glycosylation occurs adjacent to the receptor-binding site, it may enhance the binding affinity and promote viral infection (14, 15). In addition, the high density of glycans on virions may form a shield to impede antibody attack and promote immune evasion. However, these glycans can also become epitopes for stimulating neutralizing antibodies and the innate immune response, making viruses more vulnerable to immune clearance (16). Thus, there are multiple selective pressures on viral envelope glycosylation that can influence the pattern of glycosylation in order to achieve the optimal fitness in their hosts (17).

Glycosylation and the Unfolded Protein Response

Viruses are obligate intracellular parasites, and their glycoprotein biosynthesis and modification rely entirely on host cell machinery in the secretory pathway. Therefore, viral and host proteins are glycosylated in a similar manner by the same mechanism. Although glycans can be attached to polypeptide structures via several different mechanisms, asparagine *N*-linked glycosylation represents a fundamental and well characterized post-translational modification in eukaryotic organisms (18).

N-linked glycosylation starts from the membrane of the endoplasmic reticulum (ER), where the tetradecasaccharide precursor is assembled. This precursor consists of two

N-acetylglucosamine (GlcNAc), nine mannose (Man, 4 are α1,2-linked), and three terminal glucose (Glc) residues distributed on three extended Man branches: a, b, and c ($Glc_3Man_9GlcNAc_2$) (Figure 1A) (19, 20). When nascent polypeptides enter the ER lumen, the precursor is en bloc attached to Asn residues of a nascent polypeptide in a consensus Asn-X-(Ser/Thr) motif. After the attachment, these precursors are processed by a series of enzymes in both the ER and the Golgi apparatus to remold the core oligosaccharide into diverse *N*-linked glycan structures (Figure 1B). The first step in this process is the sequential removal of the two outermost Glc residues on branch A. The first Glc residue is removed by glucosidase I (GI), resulting in the di-glycosylated oligosaccharide $Glc_2Man_9GlcNAc_2$, which is recognized by an ER transmembrane lectin malectin (21). The second Glc residue is then removed by glucosidase II (GII), resulting in the mono-glucosylated oligosaccharide $Glc_1Man_9GlcNAc_2$, which is recognized by two other ER lectins, the membrane-bound calnexin (CNX) and/or soluble calreticulin (CRT). Interaction with these two chaperones segregates the newly formed glycoprotein and provides access to protein disulfide isomerases (PDIs) such as ERp57, which promotes disulfide bond formation, resulting in protein folding into a native conformation. Once a protein is properly folded, GII cleaves the last Glc residue on branch A, which releases the protein from the CNX/CRT cycle. The ER class I α-mannosidase (ERManI) then cleaves the outermost Man residue on branch b on native proteins, resulting in the oligosaccharide $Man_8GlcNAc_2$. These high-Man glycans are then recognized by lectins including ER-Golgi intermediate compartment-53 (ERGIC-53), vesicular integral membrane protein of 36Kda (VIP36), and VIP36-like (VIPL), which promote trafficking from the ER to the Golgi (22). The remaining Man residues are cleaved by the Golgi mannosidases, and the glycan remolding process is continued through the remainder of the *N*-glycosylation pathway, which generates functional glycoproteins that are delivered to the cell surface (Figure 1B).

In addition to these chaperones and enzymes that promote protein folding, the ER is also equipped with a unique quality control mechanism that extracts and degrades proteins that are not correctly folded or assembled into their native conformation, which is called ER-associated protein degradation (ERAD) (23). In fact, the folding efficiency of glycoproteins in the ER is very low, which requires cycles of association and dissociation from CNX/CRT to ensure proper glycoprotein maturation. If glycoproteins with the $Man_9GlcNAc_2$ oligosaccharide display non-native conformations, they are reglucosylated by the UDP-Glc:unfolded glycoprotein glucosyltransferase (UGT1 or UGGT), and are subject to additional rounds of re-engagement with the CNX/CRT machinery until folding is achieved. However, if a certain time frame for the folding is exceeded, proteins may never fold properly. Misfolded proteins are sequestered into coat protein complex II (COP-II) -dependent, highly mobile ER-derived quality control vesicles (QCVs), where ERManI is enriched (Figure 1B) (24). Because ERManI is able to excise all α1,2-Man residues when it is expressed at much higher levels in vitro (25), the enzyme may catalyze extensive demannosylation, resulting in the production of low-Man oligosaccharide $Man_5GlcNAc_2$-containing glycoprotein precursors. The removal of the a branch terminal Man residue, which is the acceptor for Glc transferred by UGGT, disables these proteins from reengagement with CNX/CRT and re-entering into the folding cycle. Importantly, the low-Man *N*-glycans represent a tag for defective glycoproteins, targeting them to ERAD (26).

With only one-tenth of the total cell volume, the ER is responsible for the synthesis of the vast majority of the secreted or membrane proteins, which account for one-third of total cellular proteins. Therefore, the ER has extremely high protein concentrations (100 mg/mL), which renders this organelle very susceptible to protein aggregation (27). In addition, the protein folding is error prone, and this process can be further compromised by physiological and pathological perturbations. Moreover, genetic mutations may prohibit proteins from

being folded properly. All these factors may cause the accumulation of unfolded or misfolded proteins. When the level of these aberrant proteins exceeds the folding and clearance capacity of the ER, known as ER homeostasis, it leads to a cellular stress response termed “ER stress”, which in turn activates the unfolded protein response (UPR) to restore the ER homeostasis (28). ER stress is sensed by three ER transmembrane receptors: double-stranded RNA (dsRNA)-activated protein kinase (PKR)-like ER kinase (PERK), inositol-requiring enzyme 1 (IRE1), and activating transcription factor 6 (ATF6). PERK and ATF6 are in association with another ER chaperone, the binding immunoglobulin protein (BiP, or GRP78), when the cell is not under stress. BiP preferentially binds to misfolded proteins and dissociates from PERK and ATF6 under ER stress, resulting in their activation and UPR to mitigate this stress (29, 30). IRE1 is activated by the direct binding of unfolded proteins (31). IRE1 then activates the transcription factor X-Box Binding Protein 1 (XBP-1), which in turn up-regulates ER chaperones to assist in the folding capacity of the ER as well as ERAD components to boost protein degradation. PERK phosphorylates the eukaryotic initiation factor (eIF)-2α and halts protein translation, and ATF6 up-regulates protein expression to boost the ER protein folding capacity and ERAD. However, if these objectives are not achieved within a certain time span or if the disruption is prolonged, UPR also activates pathways leading to cell death. Although PERK activation causes global inhibition of protein translation by blocking eIF-2α activity, it paradoxically enhances translation of the transcription factor ATF4. ATF4 then *trans*-activates the CCAAT/enhancer-binding protein-homologous protein (CHOP), which is a pro-apoptotic transcription factor, resulting in cell death by apoptosis (32).

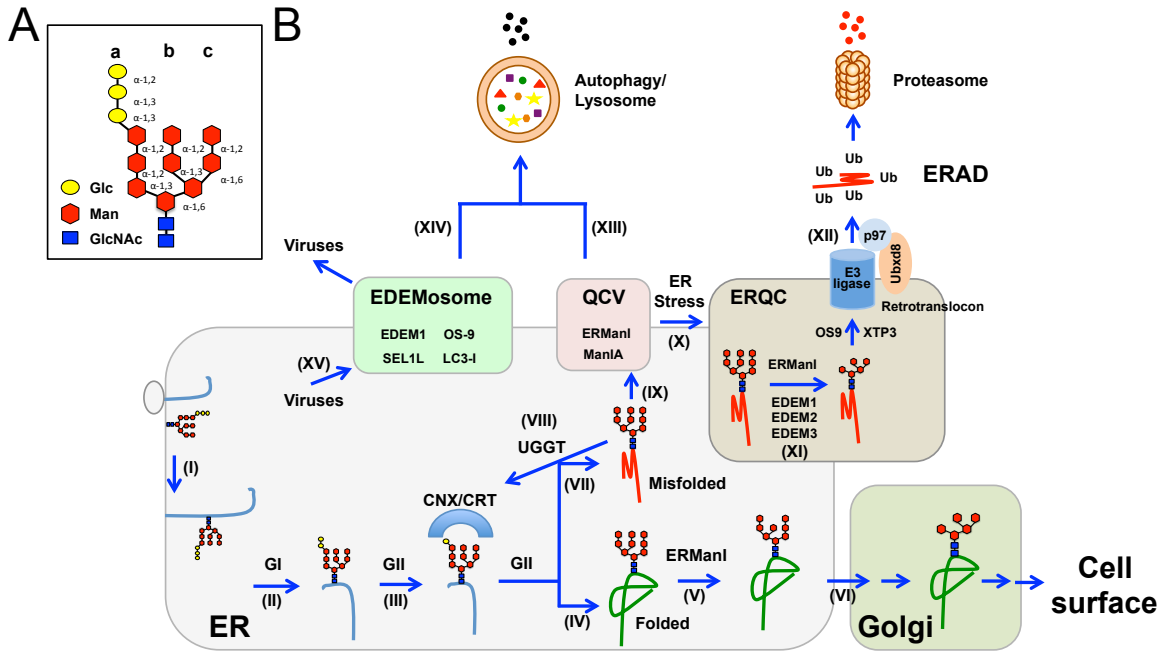

Figure 1.1. N-linked glycosylation and ERAD. (A) Schematic presentation of the *N*-linked core oligosaccharide structure. The core is composed of two *N*-acetylglucosamine (GlcNAc, *blue*), nine mannose (Man, *red*), and three glucose (Glc, *yellow*) residues. a, b, and c are three oligosaccharide branches. (B) Schematic description of *N*-glycosylation, endoplasmic reticulum-associated protein degradation (ERAD), and endoplasmic reticulum (ER) stress pathways. Nascent polypeptides are translocated through Sec61 into the rough ER, where the core oligosaccharide is transferred from a dolichol phosphate onto asparagine residues in asparagine-X-serine/threonine (NXS/T) motifs (I). The two terminal glucose residues on the core oligosaccharide are trimmed by glucosidase I, (GI) (II), and GII (III), respectively, allowing for the association with the chaperones, membrane-bound calnexin (CNX) and and/or soluble calreticulin (CRT), which promote folding to a native conformation. Eventually, the last terminal glucose residue will be trimmed by GII, and the glycoprotein will attain a native conformation (IV), or misfold (VII). Glycoproteins that reach a native conformation will have the terminal α1,2-Man residue on the b branch removed by ER class I α-mannosidase (ERManI) (V), as a signal to allow it to traverse the canonical secretory pathway for surface presentation or secretion (VI). Polypeptides unable to reach a native conformation (VII) will engage in multiple rounds of the CNX/CRT cycle, facilitated by reglucosylation of the terminal glucose by UDP-Glc:unfolded glycoprotein glucosyltransferase (UGGT) (VIII), and trafficking between quality control vesicles (QCV) (IX) and the the ER-derived quality compartments (ERQC) (X) under ER stress. Terminally misfolded glycoproteins will be demannosylated to remove all α1,2-Man residues (XI), followed by association with lectins osteosarcoma amplified 9 (OS9) and XTP3-transactivated gene B protein (XTP3-B) for ERAD (XII). ERManI containing QCV are rapidly recycled through autophagy/lysosome pathways (XIII). Without interactions with client glycoproteins, EDEMosome components are degraded through an autophagy-like mechanism (XIV). Viruses can hijack EDEMosomes to form double membrane vesicles (DMVs) that serve as platforms for their replication (XV).

ER-Associated Protein Degradation

ERAD is a protein quality control mechanism conserved in all eukaryotic cells, which is an important arm of UPR, necessary to alleviate ER stress (33). ERAD results in the selective dislocation of unfolded and misfolded proteins from the ER to the cytosol via specific membrane machinery. ERAD targets are subsequently degraded by the cytosolic ubiquitin proteasome system (UPS) (34). Quality control of functional proteins produced from the ER is also critical for maintenance of the ER homeostasis by eliminating unfolded and misfolded proteins. Thus, ERAD is a central element of both the secretory pathway and UPR, which targets a number of physiological and pathological substrates such as the T cell antigen receptor (TCR) (35), 3-hydroxy-3-methylglutaryl coenzyme-A (HMG-CoA) reductase (HMGCR) (35), squalene monooxygenase (SQLE) (36), Inositol 1,4,5-trisphosphate (IP_3) receptor (37), diacylglycerol acyltransferase 2 (DGAT2) (38), heme oxygenase-1 (HO-1) (39), alpha-1 antitrypsin (35), and cystic fibrosis transmembrane regulator (CFTR) (40). So far, more than 60 human diseases have been attributed to this pathway (41).

Although the vast majority of secreted proteins are glycosylated, the ER is responsible for the folding and assembly of both glycosylated and non-glycosylated proteins into functional complexes, which are subjected to ERAD quality control if they are misfolded. The process of ERAD can be divided into three steps: substrate recognition, retrotranslocation, and ubiquitylation/proteasomal degradation. In fact, extensive excision of α1,2-Man residues from *N*-glycans sends an important signal to trigger misfolded glycoprotein degradation, which is dependent on class I mannosidases (42).

Class I mannosidases belong to the glycoside hydrolase family 47 (GH47), which are exo-acting α1,2-mannosidases that are divided into three subfamilies (43). The first subfamily consists of ERManI, which is supposed to cleave the outmost α1,2-Man residue on the ‘b’ branch from *N*-linked glycans in the ER. The second subfamily consists of three Golgi

α-mannosidase I, including GolgiManIA, GolgiManIB, and GolgiManIC, which cleave the remaining three α1,2-Man residues in the Golgi complex for *N*-glycan maturation. The third subfamily consists of the ER degradation-enhancing α-mannosidase-like proteins (EDEM) 1, 2, and 3. Although some EDEM orthologs in lower eukaryotes have detectable α1,2-mannosidase activity, such activity has not been reported for any mammalian EDEM proteins in vitro. Nevertheless, there is evidence suggesting that these EDEM proteins should have enzymatic activity in vivo (44, 45). Indeed, the extent of Man excision determines the fate of a glycoprotein, which could be either targeted to ERAD for degradation or sent to the Golgi for normal trafficking. ERManI exhibits a slow rate of enzymatic activity, which allows nascent proteins to perform multiple rounds of reglucosylation and achieve proper folding (46). Properly folded glycoproteins should have one Man residue trimmed off from *N*-glycans by ERManI. These glycoproteins then interact with the high-Man binding lectin, ER-Golgi intermediate compartment 53 kDa protein (ERGIC-53) (47), for trafficking from the ER to the Golgi (Figure 1B). However, if glycoproteins are misfolded terminally, the remaining three α1,2-Man residues are excised from these molecules, which targets misfolded proteins for degradation (48).

It is still not completely understood how misfolded glycoproteins are subjected to such extensive demannosylation in the ER and then targeted for ERAD. Although ERManI alone may be able to complete this task, there is evidence suggesting that additional GH47 enzymes are involved. Elevation of the Golgi mannosidases has been shown to accelerate ERAD, so these enzymes may possibly be responsible for such extensive excision, likely by trafficking back to the ER via an unknown mechanism (49). In fact, the localization of the GolgiManIA has recently been observed in QCV with other canonical ERAD machinery such as ERManI, and overexpression and knockdown can, respectively, increase or retard trimming of misfolded glycoproteins from $Man_9GlcNAc_2$ to $Man_5GlcNAc_2$ in vitro (50). In addition, upon

ER stress, QCV converge to form the ER-derived quality compartments (ERQC), where EDEM proteins are also sequestered (Figure 1B) (48). EDEM1 and EDEM3 boost mannose trimming when overexpressed (45, 51, 52). In addition, using a genomic knockout approach, it has been recently proposed that EDEM2 plays a central role in the trimming of the outmost Man residue on the b branch, whereas EDEM1 and EDEM3 should be responsible for trimming of the remaining α1,2-Man residues. Accordingly, a "double check" model for misfolded glycoproteins has been proposed, which suggests that EDEM2 catalyzes the first step of Man trimming, and EDEM1 and EDEM3 contribute the second step (44). Under these joint actions, all four α1,2-Man residues are removed from the oligosaccharide, which is then recognized by the lectins osteosarcoma amplified 9 (OS9) and XTP3-transactivated gene B protein (XTP3-B) via the mannose 6-phosphate receptor homology (MRH) domain (Figure 1B) (53, 54). Misfolded proteins are targeted to specific translocation channels (retrotranslocons) for retrotranslocation in an energy-dependent manner. This process is facilitated by p97, a member of the ATPases associated with the diverse cellular activities (AAA) family, by catalyzing ATP hydrolysis (55). The p97 ATPase is recruited by the ubiquitin-like (UBX)-domain-containing protein Ubxd8, an ER-membrane protein that plays a role in ERAD (56).

It is still mysterious how these retrotranslocons are formed and how integral membrane and lumenal ERAD substrates are exported across the ER membrane through these retrotranslocons. The first candidate channel is composed of the Sec61 complex, which is comprised of α, β, and γ subunits. The α subunit crosses the membrane 10 times, and forms a channel with the other subunits. The Sec61 heterotrimeric channel is the main translocon involved in co-translational protein transport into the ER (57). However, there is evidence suggesting that the Sec61 translocon is also involved in retrotranslocation of ERAD substrates, implying the non-specificity and bi-directional property of this channel (58). The

second candidate is a member of the Derlin family (Derlin-1, -2, and -3) (59, 60). Derlins are integral membrane proteins that likely span the ER membrane four times and contain a rhomboid-like domain (61). The third candidate includes the ERAD-specific E3 ligases. They have a large number of transmembrane domains, which are not only responsible for polyubiquitylation, but could act as potential exit channels for ERAD substrates (62).

In *Saccharomyces cerevisiae*, there are two major types of Really Interesting New Gene (RING)-finger E3 ligase complexes, Hrd1 and Doa10, which mediate ERAD by targeting discrete substrates (63). Hrd1 was the first E3 enzyme identified in the ERAD pathway during the study of HMG-CoA reductase degradation (Hrd) (64). Hrd1 has 6 transmembrane helices in its *N*-terminal transmembrane domain and a catalytic RING domain in the soluble *C*-terminal region extended to the cytosol. Using an elegant ERAD assay reconstituted in vitro, the Hrd1-mediated formation of ubiquitin-gated protein-conducting membrane channels has been demonstrated (65, 66). Hrd1 has two mammalian orthologs named HRD1 and gp78, and its functioning E2 enzyme is known as Ubc7, which also has two mammalian orthologs, Ube2g2 and Ube2g1 (67). Hrd1 is unstable, and must be stabilized by its co-factor Hrd3 in an equimolar ratio (68). The mammalian ortholog of Hrd3 is SEL1L, which is required for ERAD substrate retrotranslocation (69). Hrd1 interacts with Der1, and the Der1-Hrd1 interaction is bridged by another integral membrane protein Usa1, which is also required for Hrd1 oligomerization (70). The Usa1 mammalian ortholog is called Herp, which also interacts with HRD1 and Derlin-1 and plays an important role in ERAD (71).

Doa10 was identified in degradation studies of Mating Type (MAT)-α2-10 (doa), which is a yeast transcription factor. Doa10 is a ~150 kDa protein that has 14 transmembrane domains, which requires both Ubc6 and Ubc7 as E2 enzymes. The Doa10 mammalian ortholog is TEB4 (MARCH6), which functions in the ERAD pathway with similar

subcellular distribution and topology (72). The Ubc6 E2 enzyme has two mammalian orthologs, Ube2j1 and Ube2j2; both are involved in ERAD (73, 74).

In *Saccharomyces cerevisiae*, ERAD is executed synergistically by Hrd1 and Doa10 with minimal redundancy because they exhibit different substrate specificity. Doa10 mainly triggers ubiquitylation of specific soluble proteins and membrane proteins with degrons exposed to the cytosol; a process referred to as ERAD-C (75, 76). Hrd1 interacts with two other types of substrates, whose degradation is termed ERAD-L and ERAD-M. ERAD-L includes soluble lumenal proteins in the ER and transmembrane proteins with degrons exposed to the ER lumen; ERAD-M includes transmembrane proteins with degrons embedded into the ER membrane (63). Simultaneous inactivation of both genes has been shown to increase the sensitivity to heavy metal-induced cellular stress and exhibit an elevated UPR.

The regulation of protein folding and the functional relation between ERAD and the UPR are much more complex in mammalian cells. In *Saccharomyces cerevisiae*, the CNX cycle does not exist due to the lack of UGGT. In addition, protein synthesis is tightly controlled at the translational level by determination of the stoichiometry to avoid surplus production, resulting in minimal dependence on the post-translational regulation of protein expression. Moreover, although the yeast ERManI ortholog Mns1p and EDEM ortholog Htm1p are indispensable for ERAD, only one EDEM ortholog is present in yeast (77, 78). Because overly active ERAD may interfere with the regular protein folding process in the ER, mammalian cells have evolved mechanisms to tightly regulate this quality control device by a combination of compartmentalization and tuning.

EDEM1 is segregated into ER-derived, LC3-I-associated vesicles, which are called EDEMosomes, where EDEM1, OS-9, and SEL1L are concentrated when they lack client glycoproteins to dislocate (Figure 1B) (79). Notably, unlike chaperones and the other

enzymes, many ERAD regulators including ERManI, EDEM1, OS-9, HERP, and SEL1L are short-lived proteins, and ERManI, EDEM1, SEL1L, and OS-9 are targeted to the lysosomal pathway for degradation (79, 80). Thus, EDEMosomes are called ERAD tuning vesicles, which deliver their content to lysosomes for disposal via an autophagy-like pathway to reduce the ERAD capacity under natural conditions (81). Additionally, lysosomal inhibitors are able to cause the accumulation of an aggregating mutant of dysferlin in the ER when compared to the wild-type, which was used as evidence to propose that large protein aggregates are disposed of via an autophagy/lysosomal pathway, dubbed ERAD II (82). However, under ER stress, most of these factors are highly induced, including the EDEM proteins, but not ERManI (45, 83, 84). Under stress, QCV are recruited to the ERQC, resulting in the accumulation of ERManI and its glycoprotein substrates (85). Moreover, many other ERAD components, including EDEM1, HRD1, Derlin-1, Sec61β, and Herp, are also concentrated in ERQC. Importantly, it has been found that EDEM1 stabilizes ERManI and increases its protein expression at steady-state levels (86). Such enrichment of these critical components accelerates efficient assembly of the ERAD machinery, potentiating the degradation of misfolded glycoproteins and alleviating ER stress.

Viruses and UPR

During infection, viruses are able to hijack the host translational machinery and saturate the ER with viral proteins. Not only do viruses use the ER to generate their glycoproteins, but some even utilize the ER as their site to assemble progeny particles (87). Such accumulation of viral proteins in the ER places a heavy demand on the protein folding machinery, which may cause ER stress, and in turn, activate the UPR, resulting in restoration of the ER homeostasis or apoptosis. So far, at least 36 viruses have been found to be able to induce ER stress, and activate the three UPR stress signaling pathways (88).

Enveloped viruses may bud through the plasma membrane or an intracellular compartment. In addition, their envelope glycoproteins are targeted to the ER for post-translational modifications and folding. Not surprisingly, many viral envelope glycoproteins are significant inducers of the UPR, which includes HCV (89), hepatitis B virus (HBV) (90), coronaviruses (91), chikungunya virus (CHIKV) (92), and retroviruses (93). As introduced earlier, the UPR utilizes three different mechanisms to alleviate ER stress: reducing global protein translation, increasing the ER folding capacity, and enhancing ERAD by activating the PERK, ATF6, or IRE1-XBP1 pathways, respectively.

Viral infections may activate these pathways, resulting in the inhibition or enhancement of viral replication (Table 1). For example, the PERK-mediated global translation shutdown is a very effective antiviral mechanism, and a similar shutdown by PKR has been used in the interferon pathway to defend against viral infection (94). Conceivably, viruses have evolved a number of strategies to circumvent the detrimental effect of UPR to establish productive infection. HCV is still able to produce viral proteins even when the cellular translational machinery is shut down, because these viruses have their own internal ribosome entry site (IRES) to recruit and assemble the ribosomal initiation complex for protein expression (95). Epstein-Barr virus (EBV), herpes simplex virus (HSV), and African swine fever virus (ASFV) can counteract the PERK-mediated eIF2α phosphorylation by activating an eIF2α phosphatase PP1 (96-98). In another example, the HCV E2 protein directly interacts with PERK to prevent ER stress sensing by acting as a pseudo-substrate to block PERK activity (99). In addition to combating the UPR, viruses also take advantage of the UPR pathways to benefit their replication. For example, influenza A virus (IAV) replication is promoted by activation of the IRE1-XBP1 pathway (100); ATF6 activation promotes ASFV, lymphocytic choriomeningitis virus (LCMV), DENV, human cytomegalovirus (HCMV), and Japan encephalitis virus (JEV) replication (101, 102), and ATF4 activation enhances HIV-1

replication (103). Thus, despite the detrimental effects, viruses have evolved to manipulate host UPR signaling pathways to promote viral infections.

Below, we will focus on the roles of ERAD played in virus replication, which is the main target of this review.

Table 1.1. Viral manipulations of unfolded protein response (UPR).

Virus	UPR Pathway	Description	Ref.
HIV-1	PERK	ATF4 enhances HIV-1 replication synergistically with Tat.	(103)
IAV	IRE1	IAV infection induces IRE1. Treatment with an IRE1 inhibitor reduces viral replication. An alternate splice variant of the PB1 polymerase subunit (PB1-F2) from an avian influenza A strain has been implicated in the induction of IRE1 in chickens. ΔPB1-F2 mutant virus displayed enhanced virulence in chickens.	(100, 104)
HCV	PERK	HCV E2 glycoprotein binds to PERK as a pseudo-substrate to repress PERK activation.	(99)
DENV	PERK, ATF6, IREI	PERK-mediated eIF2α phosphorylation is reversed through the viral-induced expression of GADD34, which works with PP1 to dephosphorylate eIF2α. ATF6 is activated by PERK in a cell-type specific manner. PERK and IREI knockout producer cells have decreased production of virus.	(105)
ASFV	PERK, ATF6	Ectopic DP71L expression dephosphorylates eIF2α in vitro. DP71L mutant viruses lack increased eIF2α phosphorylation, suggesting redundant viral factors. ATF6 activation by virus is implicated in caspase activation and early apoptosis required for viral exit.	(98, 101)
EBV	PERK, IRE1, ATF6	LMP1 activates all three UPR sensors through an unknown mechanism. ATF4 is induced by the activation of PERK binding to the LMP1 promoter to stimulate LMP1 expression.	(96)
HSV1	PERK	Viral infection induces PERK and PKR, causing eIF2α phosphorylation. The HSV1 gamma(1)34.5 protein is involved in the dephosphorylation of the eIF2α through an interaction with the phosphatase PP1	(97)
CHIKV	PERK	NSP4, the viral polymerase, reduces PERK-mediated eIF2α phosphorylation.	(92)
HCMV	IRE1	HCMV late protein UL50 down-regulates IRE1 protein expression.	(106)
SARS-CoV	PERK	SARS coronavirus protein 3a activates PERK independently of IRE1 and ATF6.	(107)

Abbreviations: HIV-1, human immunodeficiency virus type 1; IAV, influenza A virus; HCV, hepatitis C virus; DENV, dengue virus; ASFV, African swine fever virus; EBV, Epstein-Barr virus; HSV1, herpes simplex virus 1; CHIKV, chikungunya virus; HCMV, human cytomegalovirus; SARS-CoV, severe acute respiratory syndrome coronavirus; PEKR, double-stranded RNA-activated protein kinase (PKR)-like ER kinase; IRE1, inositol-requiring enzyme 1; ATF6, activating transcription factor 6; Tat, trans-activator of transcription; eIF2α, eukaryotic initiation factor-2α; PP1, protein phosphatase 1; GADD34, growth arrest and DNA damage-inducible protein 34; LMP1, latent membrane protein 1.

Roles of ERAD in Promotion of Virus Replication

As introduced earlier, ERAD transports unfolded/misfolded proteins from the ER into the cytosol for proteasomal degradation. Conceivably, viruses can manipulate and exploit this cellular machinery to degrade several important host factors to promote their propagation.

Herpesviruses have evolved multiple mechanisms to suppress the host immune response via ERAD. Major histocompatibility complex (MHC) molecules play an indispensable role in triggering an immediate immune response to inhibit virus infections. Herpesviruses inhibit MHC class I (MHC-I) expression by targeting these molecules to ERAD for degradation. For example, HCMV produces two transmembrane proteins, US2 and US11, and each is sufficient to bind to MHC-I heavy chains, causing their dislocation from the ER to the cytosol for degradation (108). Notably, US2 and US11 use different mechanisms to degrade MHC-I. US2-dependent MHC-I degradation is mediated through an interaction with the E3 ligase, TRC8. This US2/TRC8 complex has been implicated in the degradation of other membrane proteins including multiple alpha-integrins, the interleukin 12 receptor (IL-12R), thrombomodulin (THBD), protein tyrosine phosphatase receptor type J (PTPRJ), and CD112 (109). Although the signal peptide peptidase (SPP) has been shown to bind to TRC8, the US2/TRC8 complex maintains its MHC-1 degradation activity in SPP−/− knockout cells, suggesting that SPP binding is not related to MHC-1 degradation (110, 111). Recent reports now regard the US2/TRC8 complex as a multifunctional hub that is able to degrade a multitude of targets in order to further HCMV immune evasion (109, 112). A complex formed between US11, Derlin-1, and the E3 ligase, TMEM129, mediates MHC-I degradation via US11 (113). Initial reports concerning US11 found an association with SEL1L and assumed that US11 mediated MHC-1 degradation could be SEL1L/HRD1 dependent. Recent literature has confirmed that while the US11/TMEM129 complex degrades MHC-1, US11 itself is degraded through a SEL1L/HRD1 axis in the absence of the client MHC-1 (113, 114). Recruitment of p97 by Ubxd8 is also crucial for US11-mediated MHC-I degradation (115). With regard to US11, HCMV utilizes ERAD to dispose of MHC-I and its own effector protein using discrete axes for ubiquitination. Mouse gammaherpesvirus 68 (MHV68) uses another mechanism to inhibit MHC-I. MHV68 produces a protein termed MK3, which is a

Ring-finger E3 ligase anchored on the ER membrane. MK3 interacts with MHC-I heavy chain molecules, and it also associates with the transporter associated with antigen processing (TAP), p97, Derlin-1, and the E2 Ube2J2. Association with Ube2J2 results in an interesting pattern of ubiquitination of non-lysine residues (the MK3/Ube2J2 complex can ubiquitinate serines as well as lysines) that leads to rapid degradation of the MHC-I by proteasomes (73, 116). Thus, herpesviruses have evolved numerous strategies to block the MHC antigen presentation and evade the host immune response to establish a persistent infection.

Primate lentiviruses also harness the ERAD pathway to promote their replication via downregulation of their receptor CD4. CD4 downregulation prevents superinfection and promotes viral release by interrupting viral receptor-envelope interactions on the plasma membrane, leading to a controlled and productive viral infection and immunodeficiency (117). These viruses produce two accessory proteins, Nef and Vpu, to trigger CD4 degradation via two distinctive mechanisms (118). Nef uses the endocytic pathway to redirect CD4 from the cell surface, or to interfere with the transport of newly synthesized CD4 from the trans-Golgi network (TGN) to the cell surface, resulting in CD4 dislocation to endosomes and degradation by lysosomes (119). However, Vpu interacts with CD4 in the ER and induces CD4 proteasomal degradation via ERAD (120). Vpu is a small transmembrane protein encoded by HIV-1 and some simian immunodeficiency virus (SIV) isolates. Vpu forms ion conductive membrane pores; it also interacts with β-transducin repeat-containing proteins (βTrCP), which are F-box/WD repeat-containing proteins that are part of the Skp1-Cul1-F-box (SCF) E3 ubiquitin ligase complex (121). The Vpu-induced CD4 degradation is strictly dependent on the SCF-β-TrCP complex (122). Notably, this E3 ligase complex is not associated with the ER membrane, and therefore does not normally function in ERAD. However, the degradation also requires the cytosolic ATPase p97 and its cofactors UFD1L and NPL4, which are key components of the ERAD machinery, suggesting that CD4

is degraded via ERAD (122). Nevertheless, the degradation is not dependent on HRD1, SEL1L, and UBC7.

In addition to degradation, viruses may harness ERAD components to benefit their replication. First, ERAD can promote viral protein expression. Mouse mammary tumor virus (MMTV) is a betaretrovirus, which expresses the Rem protein in the ER. Rem has a *N*-terminal 98-amino acid signal peptide (SP), which is cleaved off by signal peptidase and retrotranslocated in a p97-dependent manner (123). Rem SP then promotes the nuclear export of viral unspliced RNAs to the cytosol for protein expression. Similarly, hepatitis E virus (HEV) ORF2 is an *N*-linked glycoprotein, but functions as the major capsid protein. Although ORF2 is expressed in the ER, it depends on ERAD components to exit from the ER to the cytoplasm without being polyubiquitylated (124).

Second, ERAD can promote virus entry. Polyomaviruses (PyV) enter cells through the ER and then replicate in the nuclei (125). To get from the ER to the nucleus, these viruses can cross the ER membrane into the cytosol via the ERAD retrotranslocons (126). An example of this is mouse PyV, which uses Derlin-2, whereas simian virus 40 (SV40) uses Derlin-1 and the SEL1L complex for dislocation (126, 127). In addition, the proteasome machinery is also required for the human BK PyV exit from the ER (127).

Third, ERAD can promote virus replication. The replication of positive-strand RNA viruses normally involves the formation of double-membrane vesicles (DMVs) and convoluted membranes (CMs) by rearrangement of cellular membranes, which segregates and protects viral proteins and genomes from the host's innate immune response. As introduced earlier, the ERAD activity can be adjusted by ERAD tuning vesicles termed EDEMosomes (Figure 1B), which display non-lipidated LC3 and segregate the ERAD factors EDEM1, OS-9, and SEL1L from the ER lumen (81). By comparing the similarity between DMVs and EDEMosomes, it has been discovered that mouse hepatitis virus (MHV), equine

arteritis virus (EAV), and JEV indeed replicate in these ERAD tuning vesicles (128). Thus, these viruses can subvert EDEMosomes as their replication vesicles to promote infection (129).

Roles of ERAD in Inhibition of Virus Replication

Although ERAD has been frequently manipulated by a number of viruses to promote infection or attenuate immune responses, it may also function directly as an antiviral device to protect host cells from infection. Because viral envelope glycoprotein production and folding take place in the ER, these viral proteins may become the primary targets for ERAD, resulting in the inhibition of viral infection.

Primate lentiviruses, including HIV and SIV, have low levels of envelope glycoproteins on their surface, and the average copy number is ~14 Env trimers per virion (130, 131). In contrast, IFA, Sendai virus, HSV, and Moloney murine leukemia virus (MoMuLV) have much more envelope glycoproteins on their surfaces (132-135). The exceptionally low number of Env spikes may protect HIV-1 from host immune responses (136) since almost 85% of Env proteins are retained in the ER and are degraded (137-139). This degradation mechanism was not clear until we recently reported that HIV-1 Env glycoproteins are targeted for ERAD.

From completely unrelated studies, we isolated HIV-1 non-permissive (NP) and permissive (P) T cell clones N2-NP and N5-P from the original CEM.NKR human T cell line (140). Our initial analysis uncovered that HIV-1 replication is restricted from the second round of the viral life cycle in N2-NP cells, resulting in ~1000-fold inhibition when compared to N5-P. Further transcriptome analysis by microarrays revealed that N2-NP cells overexpress the mitochondrial translocator protein (TSPO), which strongly inhibits HIV-1 Env expression (141). TSPO interacts with the mitochondrial permeability transition pore (mPTP) complex, which includes the outer membrane protein voltage-dependent anion

channel (VDAC) protein, the inner membrane protein adenine nucleotide translocase (ANT), and the mitochondrial matrix protein cyclophilin D (CypD) (142). TSPO binds to VDAC and contributes to the regulation of the mitochondrial membrane permeability by the mPTP complex (143). Our results suggested that TSPO overexpression could reduce the oxidative redox status in the ER, which interferes with the Env oxidative folding process, resulting in Env degradation. Consistently, the rapid Env degradation in N2-NP cells was rescued by kifunesine, an effective inhibitor of glycoside hydrolase family 47 (GH47) enzymes (144), suggesting that HIV-1 is degraded via ERAD in N2-NP cells.

To further explore the Env degradation mechanism, we investigated which of those four ER-associated GH47 enzymes was responsible for the Env degradation. Notably, when ERManI, EDEM1, EDEM2, and EDEM3 were ectopically expressed in 293T cells, only ERManI strongly inhibited Env expression in a dose-dependent manner. In addition, when the endogenous ERManI was knocked out by CRISPR/Cas9, TSPO was no longer able to suppress the Env expression (145). These results demonstrated that ERManI should be responsible for the initiation of HIV-1 Env degradation via ERAD. Human ERManI is a 699-amino-acid, 79.5-kDa, type II membrane protein, which is divided into an *N*-terminal cytoplasmic domain (CD), transmembrane (TM) helix, lumenal 'stem' region, and a catalytic domain (146, 147). Using an immunoprecipitation assay, we found that HIV-1 Env interacts with the catalytic domain of ERManI (145). The structure of this catalytic domain shows an $(\alpha\alpha)_7$-barrel composed of 14 consecutive helices (148). In the catalytic domain, there are seven residues that are critical for ERManI function. C527 and C556 form a highly conserved disulfide bond and were reportedly critical for protein folding (149), whereas E330, D463, and E599 were proposed as catalytic residues (148). R334C and E397K mutations are found in nonsyndromic autosomal-recessive intellectual disability (NS-ARID) disease (150), and the R334C mutation is also found in the congenital disorders of glycosylation (151). All these

residues are required for HIV-1 Env degradation, suggesting that the mannosidase activity is important for the ERManI activity. ERManI also targets the terminally misfolded human alpha1-antitrypsin variant null (Hong Kong) (NHK) for degradation via ERAD, but neither its catalytic activity nor its catalytic domain is required for this degradation, suggesting that different mechanisms are involved in HIV-1 Env and NHK degradation (152). We have also found that the viral protein R (Vpr) of HIV-1 enhances viral replication in monocyte-derived macrophages (MDMs) and dendritic cells (MDDCs) by rescuing Env from ERAD degradation through the ERAD (II) autophagy pathway. Compounds known to facilitate glycoprotein folding (PK11195 and As_2O_3) and inhibit ER α-mannosidases crucial for ERAD (Kifunensine), and those that block lysosomal proteases (Bafilomycin) rescued envelope expression and infectivity in a ΔVpr background to that of wild-type virus (153).

As aforementioned, unlike ERManI, whose expression is not responsive to UPR, the expression of the EDEMs is induced upon UPR via the IRE1/XBP activation pathway, which boosts ERAD and alleviates ER stress. Although ectopic expression of EDEMs did not inhibit HIV-1 Env expression (145), these proteins inhibit the expression of some other envelope glycoproteins. HBV expresses three surface glycoproteins, the large (L), middle (M), and small (S), which are translated from different initiation codons within the same open reading frame (ORF) and share the tetra-spanning transmembrane domains in the S protein. The *N*-terminus of the M and L protein contain additional preS2 and preS1-preS2 domains, respectively. The common S domain has an *N*-glycosylation site, and the M preS2 domain has another site. Overexpression of the surface proteins is sufficient to activate the IRE1/XBP1 pathway and elevate EDEM1, EDEM2, and EDEM3 expression. Importantly, EDEM1 overexpression destabilizes S, M, and L, and EDEM1 silencing stabilizes their expression (154). In addition, the autophagy/lysosomal pathway, but not the proteasomal

pathway, is involved in the degradation of HBV surface glycoproteins, further complicating our understanding of the viral protein degradation process via ERAD (154).

HCV has two *N*-glycosylated envelope proteins E1 and E2 on the surface of virions, which are type I transmembrane proteins expressed from a common viral polyprotein precursor. HCV infection strongly induces the activation of the IRE1 stress sensor, resulting in elevation of EDEM1, EDEM2, and EDEM3, but not the ERManI expression. Both EDEM1 and EDEM3, but not EDEM2, interact with E2, and overexpression of these two proteins induces E2 polyubiquitylation and degradation. Conversely, knockdown of EDEM1 expression or treatment with kifunesine increases E2 expression, and also reduces the interaction of EDEM1 and EDEM3 with SEL1L (155). Taken together, these results strongly suggest that EDEM proteins are able to extract viral polypeptides from the ER quality control cycle, and degrade them via ERAD. However, since none of these proteins can target the JEV E protein to ERAD for degradation, not every viral glycoprotein is recognizable by these proteins (155). In vivo experiments on patients with chronic liver injury were unable to identify up-regulation of UPR and ERAD elements in diseased versus control patients (156).

ERAD has also been implicated in the degradation of HCMV glycoproteins, gH and gL, via the 26S proteasome. HCMV produces at least 65 unique glycoproteins, with four homologues to the HSV glycoproteins, gH, gB, gL, and gM (157). The glycoproteins, gH and gL, are constituents of the gcII type complexes found on the surface of HCMV virions. The gcII trimeric complex between gH, gL, and gO can initiate pH independent fusion (158). In addition, a pentameric complex between gH, gL, and the gene products U128, U130, and U131 is able to mediate entry into different cell types via pH-dependent receptor-mediated endocytosis; a process that requires the trimeric gH/gL/gO complex (159). Although previous studies have shown that the glycoprotein gL stabilizes the expression of gH and potentiates its surface localization (160), recent work revealed that gH is degraded via ERAD in the

absence of gL (161). Replacement of the cytoplasmic tail of gH with that of the human CD4 protein subverted gH degradation via ERAD, potentiating surface expression.

Current studies describe two paradigms for ERAD to target viral glycoproteins for degradation: ERManI-mediated, which targets HIV-1 Env, and EDEM-mediated, which can target HCV and HBV surface glycoproteins. GH47 family members share a common catalytic mannosidase homology domain of ~440-residues (52), and the three catalytic residues E330, D463, and E599 found in ERManI are all conserved in these proteins (43). Nevertheless, there is little protein sequence homology beyond this domain among these proteins. Unlike ERManI, all three EDEMs are ER-lumenal proteins, although the signal sequence of EDEM1 is resistant to cleavage (162). EDEM3 has two novel features including an additional protease-associated domain of unknown function and a KDEL signal for ER retention (45). Whether or how the coordination between the EDEMs and ERManI facilitates ERAD is still a convoluted issue. Due to lysosomal degradation mediated by the *N*-terminal cytoplasmic tail, ERManI is expressed at very low basal levels in cells, and its expression is not induced by UPR (86). Such proteolytically driven checkpoint control of ERManI expression may contribute to establish glycoprotein quality control at a baseline level, which maintains ER homeostasis without activation of IRE1/XBP1. However, if this basic mechanism fails to restore ER homeostasis, IRE1/XBP1 is induced to elevate expression of the EDEMs, which will increase ERAD. Unlike HCV and HBV, HIV-1 induces UPR, but barely activates the IRE1/XBP1 pathway, which may explain why HIV-1 Env is not directly targeted by EDEM proteins (93). Nevertheless, these two different arms of ERAD do not exclude the role of the EDEMs in ERManI-mediated degradation. EDEMs may accelerate the release of terminally misfolded glycoproteins from the CNX/CRT cycle, and thereby help ERManI to conduct more extensive demannosylation (163); and the association of EDEM with SEL1L may further accelerate the cytosolic delivery of misfolded proteins (164).

Moreover, EDEM1 may form a complex with ERManI, which stabilizes ERManI by the suppression of its proteolytic degradation (86). Discrepancies concerning the localization of ERManI with various labs determining colocalization with the ER, Golgi, or ER-Golgi intermediate compartments and quality control vesicles, lends credence to both current theories that ERManI is either a Golgi checkpoint in quality control that will return misfolded proteins back to the ER for further processing, or that it resides in quality control vesicles with glycoprotein substrates as part of the CNX/CRT cycle (24, 165).

Conclusions

It is well established that viruses have evolved to manipulate host UPR and ERAD to optimize their replication, whether they are 'tuning' host quality control to ensure the proper folding of their envelope glycoproteins, circumventing ERAD in order to prevent degradation of their viral envelope glycoproteins, or hijacking ERAD to dispose of host proteins. There are still many questions left to be answered, including the identities of the dislocons that each envelope glycoprotein is targeted to, the motifs or patterns that allow α1,2-mannosidases to differentiate between native and misfolded glycoproteins, why some viral proteins are disproportionately targeted (HCMV gH), and the roles that the UPR and ERAD play in vivo during viral infections. These exciting areas merit more extensive studies.

CHAPTER 2 - ERManI (Endoplasmic Reticulum Class I α-Mannosidase) Is Required for HIV-1 Envelope Glycoprotein Degradation via Endoplasmic Reticulum-associated Protein Degradation Pathway

Tao Zhou, Dylan A. Frabutt, Kelley W. Moremen, and Yong-Hui Zheng

This research was originally published in the Journal of Biological Chemistry, 2015 September; Volume 290(36), pages 22184-22192 © the American Society for Biochemistry and Molecular Biology.

I worked with Dr. Tao Zhou to publish this article for which we were listed as co 1st authors. As cited in the article, Dr. Zhou performed the experiments in figures 2.2-5 and I designed and performed the experiments in figure 2.6. Additionally, my hands also performed experiments 2.4D, replicated the results of 2.4A, 2.4B, 2.4C, 2.4E, and performed the DNA sequencing for 2.5A, and 2.5C, which were designed and performed under Dr. Zhou and Dr. Zheng's mentorship.

Summary

Previously, we reported that the mitochondrial translocator protein (TSPO) induces HIV-1 envelope (Env) degradation via the endoplasmic reticulum (ER)-associated protein degradation (ERAD) pathway, but the mechanism was not clear. Here we investigated how the four ER-associated glycoside hydrolase family 47 (GH47)α -mannosidases, ERManI, and ER-degradation enhancing α-mannosidase-like (EDEM) proteins 1, 2, and 3, are involved in the Env degradation process. Ectopic expression of these four α-mannosidases uncovers that only ERManI inhibits HIV-1 Env expression in a dose-dependent manner. In addition, genetic knock-out of the ERManI gene MAN1B1 using CRISPR/Cas9 technology disrupts the TSPO-mediated Env degradation. Biochemical studies show that HIV-1 Env interacts with ERManI, and between the ERManI cytoplasmic, transmembrane, lumenal stem, and lumenal catalytic domains, the catalytic domain plays a critical role in the Env-ERManI interaction. In addition, functional studies show that inactivation of the catalytic sites by site-directed mutagenesis disrupts the ERManI activity. These studies identify ERManI as a critical GH47 α-mannosidase in the ER-associated protein degradation pathway that initiates the Env degradation and suggests that its catalytic domain and enzymatic activity play an important role in this process.

Introduction

Viral Env glycoproteins bind to receptors and mediate the entry of virions into cells to initiate infection. Unlike viral structural and enzymatic proteins, Env is produced through the host secretory pathway, where Env is folded into a natural conformation in the ER and delivered to the cell surface (166). Notably, the efficiency of HIV-1 Env folding is very low: almost 85% Env proteins are retained in the ER and degraded (137-139). The degradation mechanism remained unknown until we recently demonstrated that Env is targeted to the ERAD pathway for degradation (141) ERAD is a host quality control mechanism for protein folding (23). It specifically delivers misfolded proteins to the SEL1L-containing translocon pore complex on the ER membrane and elicits their retro-translocation to the cytoplasm and subsequent degradation by the ubiquitin/proteasome system. Class I α-mannosidases belong to the carbohydrate-active enZymes (CAZy) GH47 (167), which consists of seven members: ERManI, EDEM1, EDEM2, EDEM3, and Golgi mannosidase IA, IB, and IC (43). Although the enzymatic activity of EDEM1, EDEM2, and EDEM3 has not been demonstrated in vitro, the others specifically cleave the α 1,2-linked mannose residues during protein N -glycosylation. In addition, they also play an important role in the ERAD pathway. N-Glycosylation involves a number of enzymes and chaperones in the ER and requires the dedicated ERAD pathway to server as surveillance system. When nascent glycoprotein precursors enter the ER lumen, they are covalently modified with pre-assembled oligosaccharides on Asn residues in a consensus Asn-X-(Ser/Thr) motif (19). TheN-linked oligosaccharides contain 14 sugars consisting of 2 N-acetylglucosamine (GlcNAc), 9

mannose (Man, 4 are α1,2-linked), and 3 terminal glucose (Glc) residues distributed on three extended Man branches A, B, and C (Fig 2.1). The sequential removal of the two outermost Glc residues on branch A by glucosidases I and II allows client proteins to interact with ER chaperones calnexin and calreticulin. In conjunction with other chaperones and thiol-disulfide oxidoreductases, precursors are folded and oligomerized into native proteins. During this process, ERManI cleaves the outermost Man residue on branch B on native proteins (Fig 2.1).

After further removal of the last Glc residue on branch A by glucosidase II, native glycoproteins are released from calnexin/calreticulin and transported to their final destinations. Noticeably, the glycoprotein folding in the ER is error-prone. If glycoproteins display non-native conformation, they are then reglucosylated by the UDP Glc:unfolded glycoprotein glucosyltransferase and subject to additional rounds of re engagement with the chaperone machinery until folding is achieved. However, if proteins are terminally misfolded, accumulation of misfolded proteins activates the unfolded protein response. Misfolded proteins are then guided to the ERAD pathway for degradation. ERManI and EDEM1 play an indispensable role in ERAD. Genetic knock out of the ERManI gene MAN1B1 orthologue Mns1p and EDEM1 orthologue Htm1p in Saccharomyces cerevisiae showed a clear involvement of these two genes in this pathway (77), (168). In mammalian cells an inhibition of ERAD is achieved by inhibiting the CAZy GH47 α-mannosidase activity with kifunensine or by small interfering RNA-mediated gene knockdown (48, 144, 169). In addition, both ERManI and EDEM1 accelerate misfolded glycoprotein degradation

in a dose-dependent manner (83, 144, 169) It has been suggested that EDEM1 extracts misfolded proteins from the calnexin/calreticulin cycle (163, 170) and misfolded proteins are targeted to the ER-derived quality control compartment where ERManI is enriched (24, 48). Although ERManI prefers to cleave the outermost Man residue on branch B, it may continue to cleave the other α 1,2- linked Man residues on branches A and C under conditions of overexpression (25). Thus, ERManI and possibly the EDEM proteins may catalyze more extensive demannosylation, which constitutes a signal of protein misfolding, resulting in misfolded proteins being degraded via ERAD. Recently, we reported that the mitochondrial translocator protein TSPO induces HIV-1 Env glycoprotein degradation via ERAD in the human $CD4^+$ T cell line CEM.NKR (NKR), resulting in a potent HIV-1 restriction (141). TSPO associates with the mitochondrial permeability transition pore complex by interacting with one of its components, the voltage-dependent anion channel protein (171). Mitochondrial permeability transition pore establishes the mitochondrial transmembrane potential ($\Delta\psi_m$), which allows carrier proteins to exchange small molecules between the mitochondrial matrix and cytoplasm for energy production and controls the integrity of the mitochondrial membrane (142). The goal of this study was to elucidate how HIV-1 Env is degraded via the ERAD pathway, and we identified ERManI as a critical initiator for the Env degradation, resulting in inhibition of HIV-1 replication.

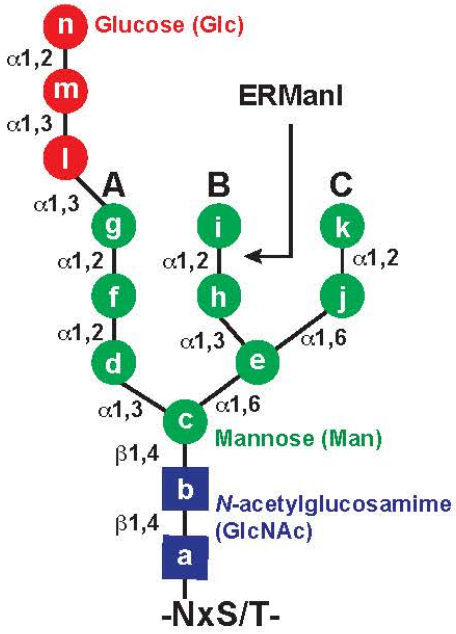

Figure 2.1. Schematic presentation of the N-linked core oligosaccharide structure. The core is composed of two N-acetylglucosamine (GlcNAc, blue squares), nine mannose (Man, green circles), and three glucose (Glc, red circles) residues. A, B, and C are three oligosaccharide branches. The ERManI preferred cleavage site is indicated.

Results

TSPO Triggers Env Degradation via ERAD in the Human T Cell Line NKR

The human $CD4^+$ T cell line NKR is nonpermissive for HIV-1 replication due to TSPO overexpression, which causes rapid Env turnover by ERAD (141). This is further demonstrated in its permissive clone N5-P and non-permissive clone N2-NP, which were obtained by limiting dilution of NKR cells (140). N2-NP cells expressed significantly higher TSPO levels than N5-P (Fig 2.2A), resulting in 8-fold more TSPO expression (Fig 2.2B). After HIV-1 infection, levels of Env expression were much lower in N2-NP cells than in N5-P cells (Fig 2.2C), resulting in 10-fold Env reduction (Fig 2.2D). In addition, treatment of these infected cells with an ERAD inhibitor kifunensine (KIF) significantly increased the Env expression in N2-NP cells (Fig 2.2, C and D); KIF also increased HIV-1 replication in N2-NP cells but not in N5-P cells (Fig 2.2E). These results suggest that Env is degraded via ERAD, which is responsible for HIV-1 inhibition in N2-NP cells.

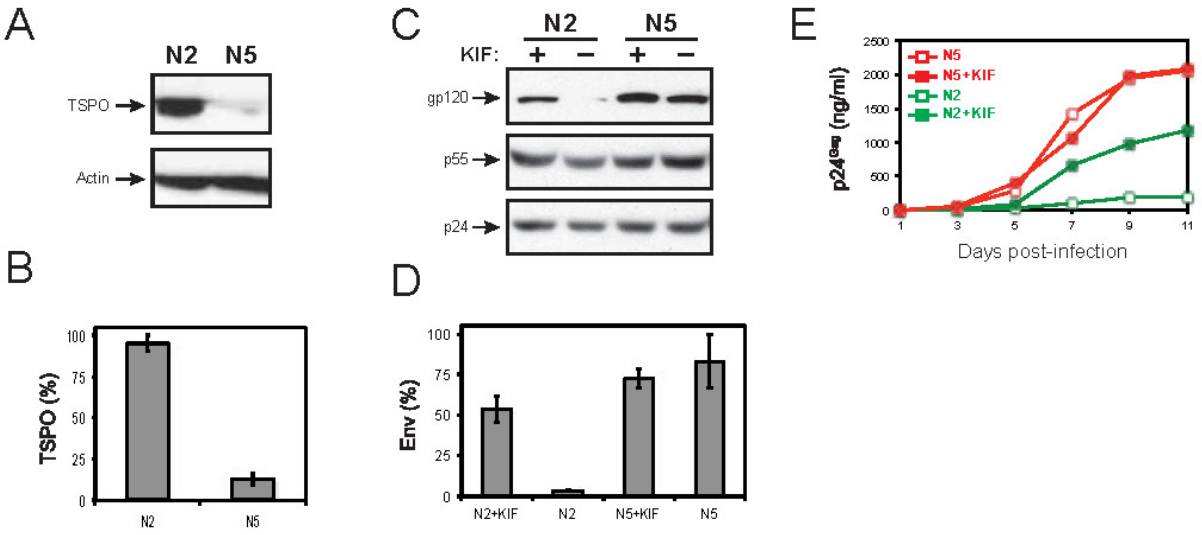

Figure 2.2. HIV-1 Env is degraded via ERAD in N2-NP cells. (A) Comparison of the endogenous TSPO expression in N2-NP and N5-P cells. Equal numbers of cells were lysed, and cellular TSPO expression was determined by western blotting using actin as a loading control. (B) Quantitation of the TSPO expression from (A), as described in the experimental procedures. The levels of TSPO expression in N2 cells were set up as 100%, and the levels in N5 cells were normalized and are presented as relative values. (C) Inhibition of HIV-1 Env expression by ERAD. N2- NP and N5-P cells were infected with HIV-1 in the presence or absence of 5 μM KIF. HIV-1 Env and Gag expression were determined by western blotting. (D) Quantitation of the Env expression from (C). The levels of HIV-1 gp120 expression in untreated N5 cells were set up as 100%, and the others were normalized and are presented as relative values. (E) Inhibition of HIV-1 replication by ERAD. N2-NP and N5-P cells were infected with HIV-1 in the presence or absence of 5 μM KIF. HIV-1 replication was determined by measuring the Gag protein levels in supernatants of infected cells by p24Gag ELISA. Error bars represent standard error measurements (SEMs) from three independent experiments.

TSPO Triggers Env Degradation via ERAD in 293T Cells

To explore the mechanism of HIV-1 Env degradation by ERAD, the endogenous TSPO activity was further investigated in 293T cells. A3 is a clonal 293T cell line where the TSPO gene was knocked out by the advantageous "clustered, regularly interspaced, short palindromic repeat (CRISPR)/CRISPR-associated- 9 (Cas9)" technology (141). When HIV-1 protein expression was compared in A3 and the wild-type (WT) 293T cells after transfection with the HIV-1 proviral vector pNL4-3, similar levels of Gag (p24, p55) were detected in both cell lines, but much more Env (gp41, gp160) proteins were detected in A3 than WT cells (Fig 2.3A , lanes 1 and 10). In fact, a 4–8-fold higher Env expression was detected in A3 cells than in WT 293T cells after comparing serially diluted samples (Fig 2.3A, lanes 3, 4, 10). Next these HIV-transfected cells were treated with increasing amounts of KIF, and the Env expression was determined. It was found that the Env expression was increased in a dose-dependent manner in WT cells (Fig 2.3B). When levels of the increase were quantified, a maximal 4-fold increase was detected, which almost reached the Env expression levels in A3 cells (Fig 2.3C). The same treatment did not increase the Env expression in A3 cells or the Gag expression in both A3 and WT cells (Fig 2.3, B and C). These results further confirmed the TSPO activity in 293T cells.

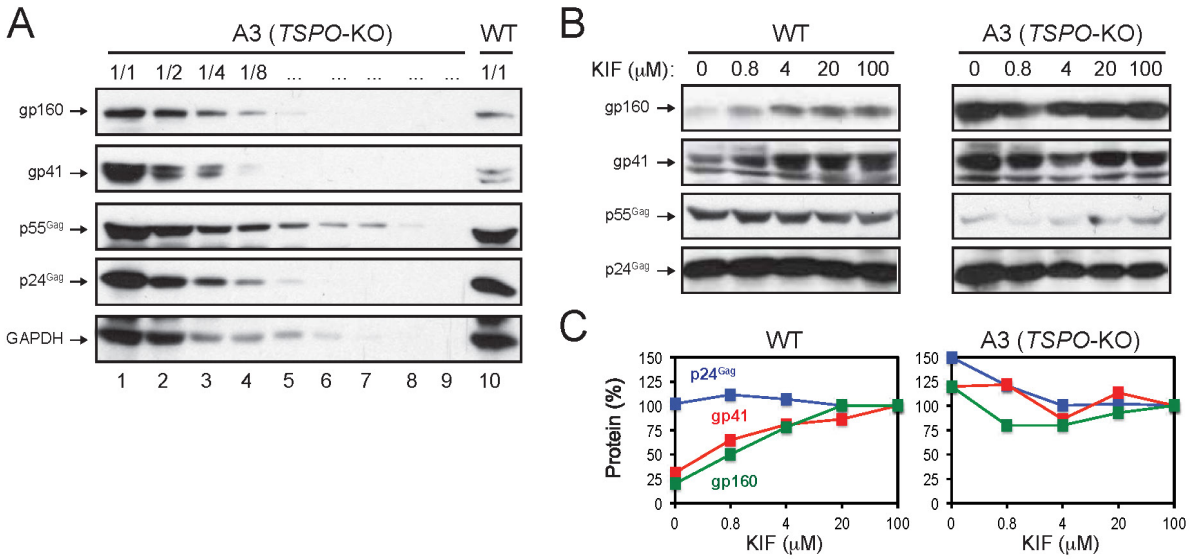

Figure 2.3. TSPO inhibits HIV-1 Env expression via ERAD in 293T cells. (A) The TSPO-knockout (KO) 293T cell line A3 and wild-type (WT) 293T cells were transfected with HIV-1 proviral clone pNL4-3. After 48 h, transfected cells were lysed and the A3 cell lysate was serially diluted. Diluted A3 and undiluted WT samples were analyzed by western blotting using indicated antibodies. (B). A3 and WT 293T cells were transfected with pNL4-3 and cultured under treatment with indicated amounts of KIF. Viral protein expression was analyzed by western blotting using indicated antibodies. (C) Quantification of Gag and Env protein expression from (B). In each cell line, levels of Gag or Env expression in samples treated with 100 uM KIF were set up as 100%, and the others were normalized to the standards and presented as relative values, respectively.

Identification of ERManI from the ERAD Pathway That Inhibits HIV-1 Env Expression

KIF is an alkaloid that specifically inhibits CAZy GH47 α -mannosidases (172). Results that KIF rescues HIV-1 Env expression in both N2-NP and 293T cells suggest that these enzymes are involved in the Env degradation. Among the seven CAZy GH47 α -mannosidases, ERManI, EDEM1, EDEM2, and EDEM3 have been found to play a role in ERAD. To understand how they are involved in HIV-1 Env degradation, 293T cells were transfected with HIV-1 proviral vector pNL4-3 plus a human ERManI, murine (m) EDEM1, mEDEM2, or mEDEM3 expression vector or a human APOBEC3A (A3A) expression vector, which served as a control. After 48 h of transfection, protein expression was determined by Western blotting. It was found that although all these enzymes were expressed, only ERManI was able to inhibit the Env gp120 and gp41 expression (Fig 2.4A, lane 4). Human EDEM proteins share an overall 90% amino acid sequence identity with their murine orthologues (52). To confirm the lack of inhibitory activity of these EDEM proteins, human EDEM proteins were ectopically expressed with HIV-1 in 293T cells, and the Env expression was determined. The A3A protein was also used as a control in this experiment. Again, like their murine orthologues and the A3A protein, these human EDEM proteins did not show any inhibitory effect on HIV-1 Env expression (1.4 B , lanes 1, 2, and 3). To verify the ERManI activity, 293T cells were transfected with fixed amounts of pNL4-3 and serially diluted ERManI expression vector, and levels of Env expression were determined. It was found that ERManI could inhibit HIV-1 Env expression in a dose-dependent manner, suggesting that the Env inhibition is indeed caused by ERManI (Fig 2.4C). In addition, these

transfected cells were treated with KIF and a proteasomal inhibitor lactacystin. Both KIF and lactacystin were previously found to block the ERManI-mediated degradation of misfolded human _1 -antitrypsin (A1AT) genetic variant-null Hong Kong (NHK) (144, 169). As expected, both KIF and lactacystin also rescued the HIV-1 Env expression (Fig 2.4D). Moreover, the ERManI activity was further evaluated in a HIV-1 replication assay. HIV-1 reporter viruses were produced from 293T cells after ectopic expression of WT ERManI or its catalytic mutant E330A (see below). After normalization of viral production by the Gag protein levels, equal amounts of HIV-1 were used to infect the GHOST cells, and viral infectivity was determined. It was found that unlike the E330A mutant, WT ERManI significantly reduced the HIV-1 infectivity (Fig 2.4E). Taken together, these experiments identified ERManI as a potent CAZy GH47 α -mannosidase that strongly inhibits HIV-1 Env expression via the ERAD pathway.

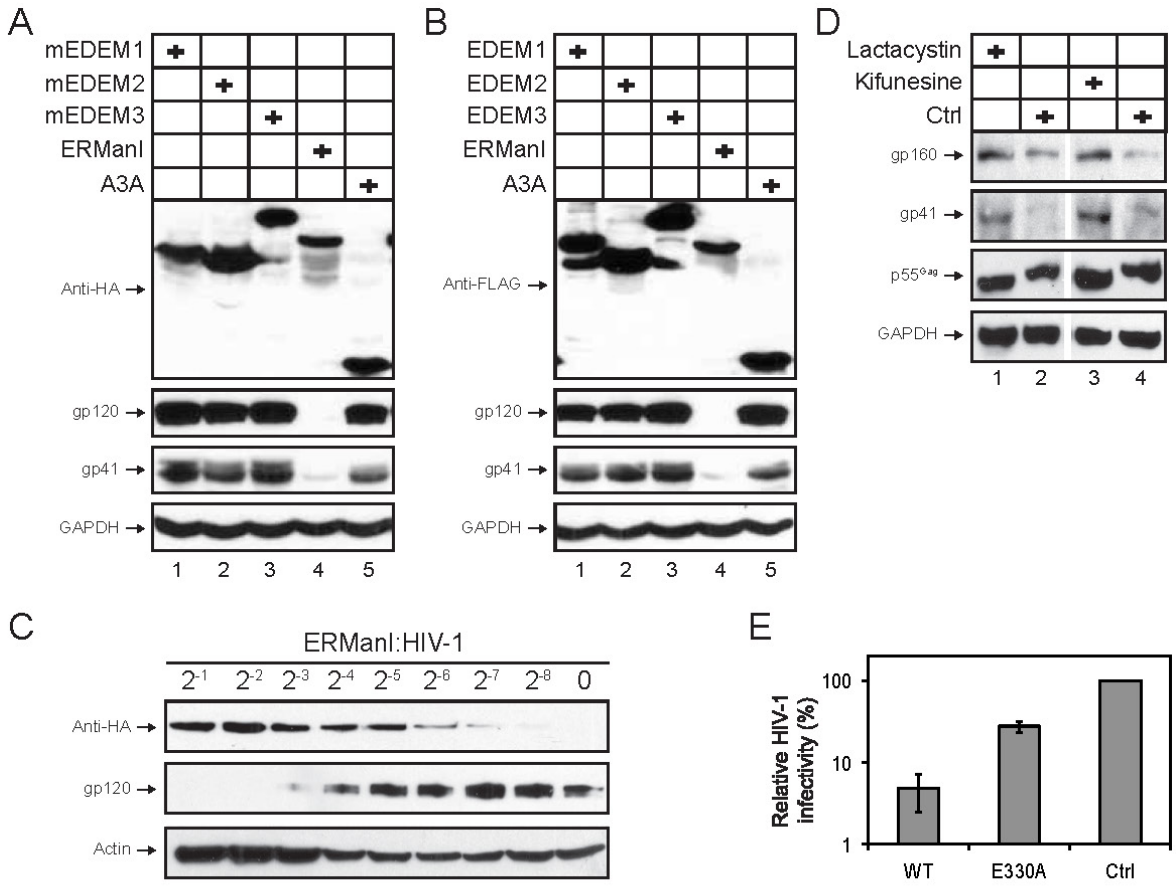

Figure 2.4. ERManI inhibits HIV-1 Env expression. (A) / (B) 293T cells were transfected with pNL4-3 and a mammalian vector expressing indicated human or murine (m) proteins, respectively. After 48 h, protein expression was determined by western blotting using indicated antibodies. (C) Titration of the ERManI anti-Env activity. 293T cells were transfected with pNL4-3 and an ERManI expression vector at indicated ratio, and protein expression was determined by western blotting. (D) 293T cells were transfected with 2.0 μg pNL4-3 and 1.0 μg ERManI expression vectors. Cells were treated with 25 μM lactacystin or 5 μM KIF for 4 h, or untreated (control, Ctrl). Protein expression was determined by western blotting using indicated antibodies. (E) ERManI reduces HIV-1 infectivity. HIV-1 luciferase (Luc) reporter viruses were produced after transfection of 293T cells with the HIV-1 proviral vector pNL-Luc and a WT ERManI, its catalytically inactive mutant E330A, or a control (Ctrl) vector. Viruses were normalized by p24Gag ELISA and used to infect GHOST cells. After 48 h, cells were lysed and viral infectivity was determined by measuring the Luc activity. Error bars represent SEMs from three independent experiments.

Knock-out of ERManI Disrupts TSPO Activity

To demonstrate the role of ERManI in TSPO-induced Env degradation, the ERManI gene MAN1B1 was knocked out in 293T cells using the CRISPR/Cas9 technology (173, 174). MAN1B1 is located on human chromosome 9, which has 13 exons. A specific 19-nucleotide gRNA was designed to target the exon 4 and inactivate this gene (Fig 2.5A). A clone, E7, which did not show any ERManI expression, was identified by Western blotting (Fig 2.5B). When an 83-bp DNA fragment was amplified from the targeted locus in E7 cells by PCR, a small deletion was identified (Fig 2.5C). After cloning and sequencing the DNA fragment, a 5-bp deletion was found (Fig 2.5A). These results demonstrate that MAN1B1 is successfully knocked out in these E7 cells. Next, HIV-1 protein expression was compared in E7 and WT 293T cells after ectopic expression of TSPO. Cells were transfected with a fixed amount of pNL4-3 and increasing amounts of TSPO expression vector, and the protein expression was determined by Western blotting. It was found that although TSPO could inhibit the Env (gp41, gp120) expression in WT cells in a dose-dependent manner, resulting in a maximal 10-fold reduction of Env expression, this activity was almost completely lost in E7 cells (Fig 2.5, D and F). To confirm that MAN1B1 KO was responsible for the loss of the TSPO activity, the TSPO activity was tested again in E7 cells after the ERManI expression was restored by co-transfection with an ERManI expression vector. It was found that TSPO became able to reduce the Env expression in E7 cells in a dose-dependent manner, indicating that the TSPO activity was restored (Fig 2.5E, lanes 4–6, and F). In addition, the TSPO activity was stronger in WT cells than in E7 cells, which could result from the endogenous

ERManI activity. Taken together, these results demonstrate that ERManI plays an indispensable role in HIV-1 Env degradation via the ERAD pathway.

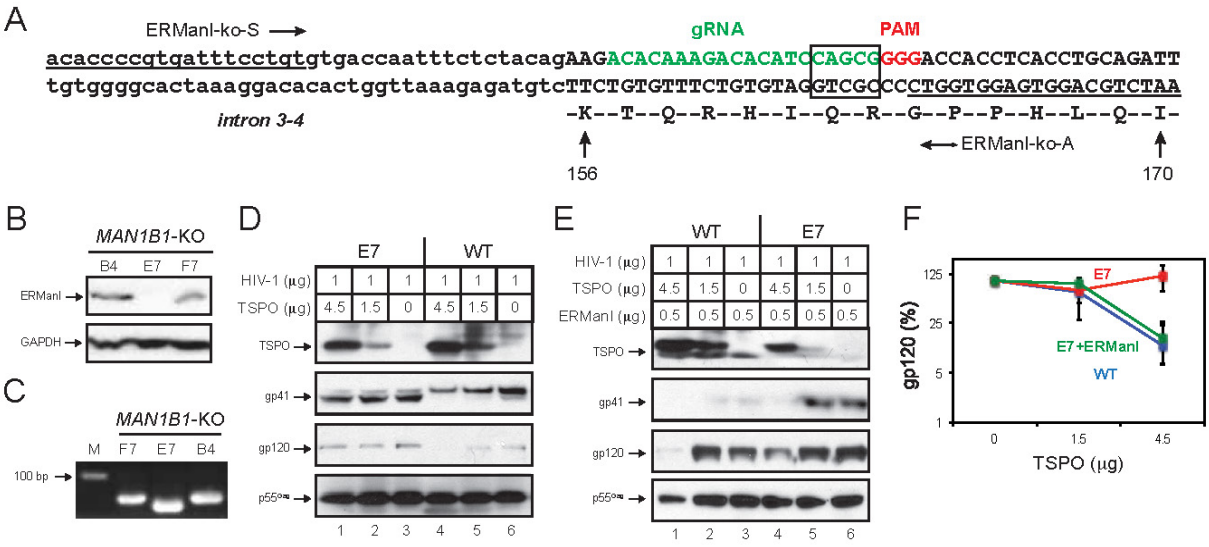

Figure 2.5. Role of the endogenous ERManI protein in the TSPO inhibitory activity. (A) Schematic illustration of MAN1B1. Numbers indicate the nucleotide or amino acid positions in the ERManI open reading frame. The intron 3-4 sequence is shown in lower case and the exon 4 sequence is shown in upper case. The 19-bp guide RNA (gRNA) target sequence is shown in green, and the protospacer-adjacent motif (PAM) is shown in red. The sense primer ERManI-ko-S and antisense primer ERManI-ko-A sequences that were used to amplify this gene locus are underlined. A 5-bp deletion detected in MAN1B1-KO cells is boxed. (B) Analysis of the endogenous ERManI protein expression inthree 293T clones (B4, E7, F7) isolated after transfection with Cas9 and MAN1B1 gRNA expression vectors by western blotting. (C) Analysis of the MAN1B1 gene locus by PCR. An 83-bp DNA fragment was PCR-amplified from the MAN1B1 locus using primers ERManI-ko-S and ERManI-ko-A, and analyzed by 10% TBE-polyacrylamide gel. M, maker. (D)/(E) Influence of MAN1B1 KO on HIV-1 Env inhibition. WT and E7 cells were transfected with indicated amounts of HIV-1 proviral vector pNL4-3 and TSPO expression vector in the absence (D) or presence (E) of an ERManI expression vector. Viral and cellular protein expressions were analyzed by western blotting. (F) Quantification of the Env expression in (D) and (E). The levels of HIV-1 gp120 expression in un-transfected cells were set up as 100%, and the others were normalized and are presented as relative values. Error bars represent SEMs from three independent experiments.

Mapping of the Critical ERManI Determinants for HIV-1 Env Inhibition

Human ERManI is a 79.5-kDa, type II membrane protein. It has 699 amino acids and consists of an N-terminal cytoplasmic domain (CD), a transmembrane (TM) helix, a lumenal stem domain, and a lumenal catalytic domain (Fig 2.6A) (146) (147). The catalytic domain contains seven residues critical for the catalytic activity and protein stability, which includes Glu-330, Arg-334, Glu-397, Asp-463, Cys-527, Cys-556, and Glu-599 (see "Discussion"). To understand how these residues contribute to the HIV-1 Env inhibitory activity, they were targeted for site-directed mutagenesis by generating seven single and E599A. When these mutants were ectopically expressed with HIV-1 provirus in 293T cells, it was found that all these mutants were expressed at similar levels as the WT protein (Fig 2.6B). Nevertheless, even though they were expressed, their inhibitory activity on Env expression was decreased to the similar levels as the control protein A3A (Fig 2.6B). These results suggest that the catalytic domain is required for the ERManI inhibition of HIV-1 Env expression. To confirm the role of the catalytic domain in HIV-1 Env inhibition, two previously described ERManI catalytic domain deletion mutants (FL-1–240 and FL-1–240/ΔDPS) were employed (152). Both mutants lack the lumenal catalytic domain, and the FL-1–240/ΔDPS mutant has an additional deletion of a highly conserved decapeptide sequence (DPS) in the lumenal stem domain (Fig 2.6A). When these mutants were tested for Env inhibition together with the WT ERManI, the ERManI E330 mutant, and the human A3A protein, it was found that only the WT ERManI exhibited the Env inhibitory activity, whereas A3A, FL-1–240, FL-1–240/ΔDPS, and E330A were all inactive (Fig 2.6C). These results further confirmed the

indispensible role of the catalytic domain in the ERManI activity. To understand how ERManI inhibits HIV-1 Env expression, the interaction between ERManI and HIV-1 Env was studied. A3A, WT ERManI, FL-1–240, or FL-1–240/ΔDPS was co-expressed with HIV-1 Env in 293T cells, and proteins were immunoprecipitated by an anti-FLAG antibody. It was found that the WT ERManI could pull down the HIV-1 Env precursor gp160, whereas A3A, FL-1–240, or FL-1–240/ΔDPS could not (Fig 2.6D). These results demonstrate that ERManI interacts with Env and suggest the luminal catalytic domain is involved in this interaction.

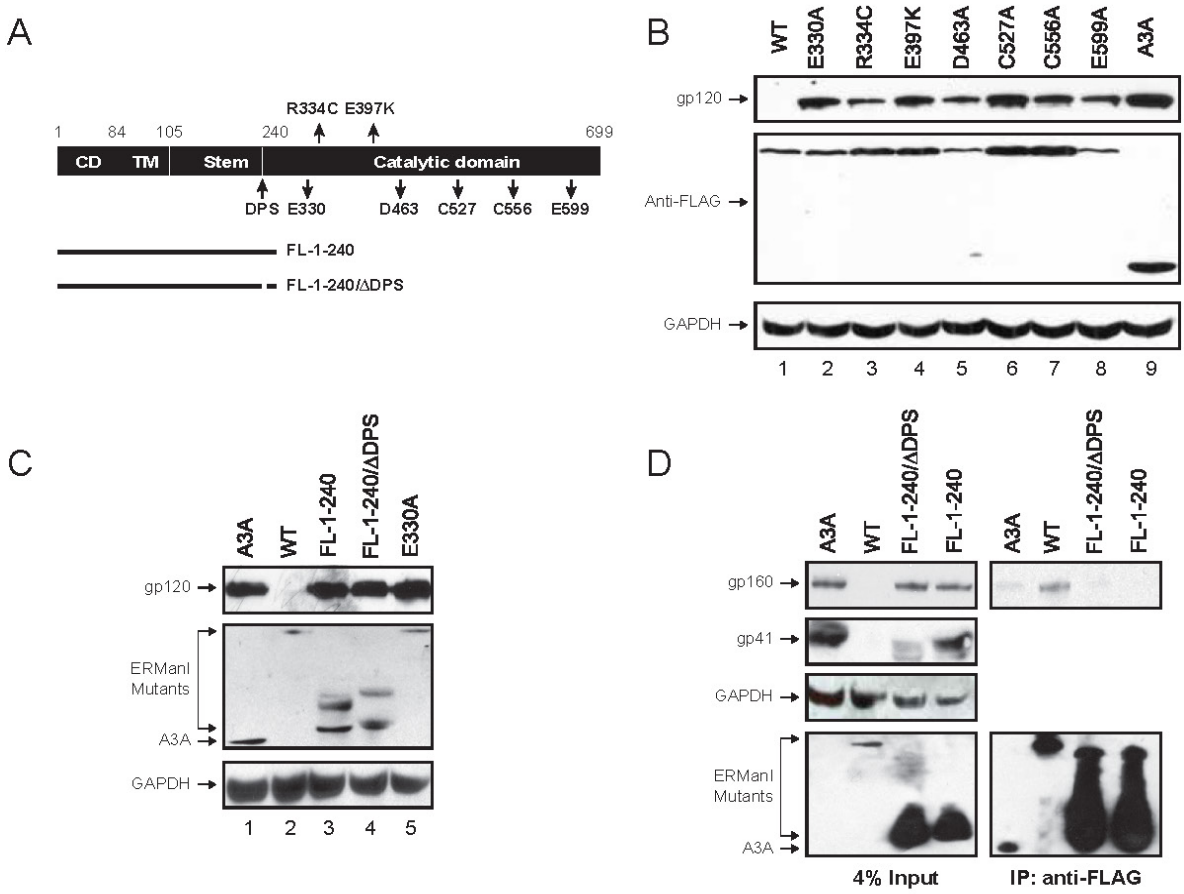

Figure 2.6. Mapping of critical ERManI determinants for Env inhibition. (A) Schematic description of the ERManI protein. The cytoplasmic domain (CD), transmembrane (TM) domain, lumenal stem domain, and lumenal catalytic domain are indicated. Numbers are amino acid positions that divide these domains. Three catalytic residues, two conserved cysteine residues, two genetic mutations, and the decapeptide sequence (DPS) are indicated. In addition, two catalytic domain deletion mutants FL-1-240 and FL-1-240/ΔDPS are also illustrated. (B) Mapping of critical ERManI residues for Env inhibition. 293T cells were transfected with pNL4-3 plus a vector expressing indicated ERManI mutants at 1:1 ratio. Viral and cellular protein expression was determined by western blotting. (C) Mapping of the critical ERManI domain for Env inhibition. 293T cells were transfected with pNL4-3 plus a vector expressing indicated ERManI mutants at 2:1 ratio. Viral and cellular protein expression was determined by western blotting.. (D) Interaction between ERManI and HIV-1 Env. 293T cells were transfected with pNL4-3 and an indicated ERManI deletion mutant expression vectors. After 48 h, proteins were immunoprecipitated with anti-FLAG M2-agarose beads. Proteins in cell lysate (Input) and in association with beads (IP) were analyzed by western blotting. A3A was used as a control in (B), (C), and (D).

Discussion

In this report we studied the molecular mechanism of TSPO induced HIV-1 Env degradation via ERAD and identified ERManI as a critical initiator for the degradation. Env is expressed through the classical secretory pathway, in which it needs to be properly folded in the ER (166). The Env folding involves cross-linking of 20 cysteine residues, which is dependent on heavy N-glycosylation and the most oxidizing redox status in the ER (175). It has been suggested that the oxidative protein folding in the ER is controlled by mitochondria, likely via regulating the ER redox status through releasing reactive oxygen species (176). Intracellular reactive oxygen species is mainly produced by mitochondria as a byproduct from energy production. Indeed, ER contains a specialized subcompartment that is called the mitochondrial-associated ER membrane, which physically connects ER to mitochondria (177). In mammalian cells, mitochondrial-associated ER membrane is supported by a protein complex consisting of voltage-dependent anion channel and several other proteins (178). As introduced earlier, TSPO is a mitochondrial protein (179) that interacts with voltage-dependent anion channel (171). We speculate that TSPO overexpression reduces the oxidative redox status in the ER, likely by blocking the mitochondria-ER communication, to interfere with HIV-1 Env folding. Accumulation of misfolded Env then activate unfolded protein response, resulting in recognition of these misfolded Env proteins by ERManI and their degradation via ERAD.

We found that the catalytic domain of ERManI plays an indispensible role in inhibition of HIV-1 Env expression. The structure of this domain shows an $(\alpha\alpha)_7$ -barrel

composed of 14 consecutive helices, and Glu-330, Asp-463, and Glu-599 were proposed as potential catalytic residues (148). Mutations of Glu-330, Asp-463, and Glu-599 caused 96.5%, 99.9%, or 100% reduction in enzyme efficiency (k_{cat} /K_m), respectively (180). In addition, ERManI has two highly conserved cysteine residues Cys-527 and Cys-556, which are also conserved in three other Golgi CAZy GH47 α 1,2-mannosidases, IA, IB, and IC, but not in EDEM proteins (148). The formation of a disulfide bond between these residues was demonstrated in the yeast Mns1, which was proposed to stabilize the protein(149). Moreover, R334C and E397K mutations are identified in nonsyndromic autosomal-recessive intellectual disability (NS-ARID) patients (150), and the R334C mutation is also found in the congenital disorders of glycosylation (181).The E397K mutation was found to reduce the ERManI expression, and the R334C mutation was found to reduce the enzyme efficiency by 100% (150). We created seven ERManI mutants, E330A, R334C, E397K, D463A, C527A, C556A, and E599A, to inactivate these critical residues, and found that they all lost the Env inhibitory activity (Fig 2.6B). In addition, we tested the activity of two previously reported catalytic domain deletion mutants, FL-1–240 and FL-1–240/ ΔDPS. Although the FL-1–240 mutant still has the activity to trigger NHK degradation, the FL-1–240/Δ DPS mutant does not (152). Nevertheless, we found that they all lost the Env inhibitory activity (Fig 2.6C). Together, these results demonstrate that the catalytic activity and the catalytic domain are required for the ERManI activity. The importance of the catalytic domain was further underscored from our investigation on Env-ERManI interaction. We found that WT ERManI could pull down HIV-1 Env, whereas both FL-1–240 and FL-1–240/ΔDPS mutants could

not, suggesting that ERManI interacts with Env, and this interaction is dependent on the catalytic domain (Fig 2.6D). Therefore, it is likely that Env cycles between the ER and Golgi and interacts with ERManI in a post-ER compartment, resulting in Env degradation. Results from this report point out two remarkable differences in ERAD-mediated degradation of HIV-1 Env and misfolded host glycoproteins. First, although ectopic expression of EDEM proteins is able to accelerate the degradation of NHK and/or misfolded -secretase (45, 83, 84, 182), it is unable to inhibit HIV-1 Env expression (Fig 2.4, A and B). Second, although the ERManI catalytic domain is not required for NHK degradation, it is required for the Env degradation. Because the FL-1–240 mutant still triggers the NHK degradation but the FL-1–240/ ΔDPS mutant does not, it is suggested that instead of the catalytic domain, the conserved DPS in the stem domain is critical for the NHK degradation (152). However, because both FL-1–240 and FL-1–240/Δ DPS mutants fail to inhibit HIV-1 Env expression, it is suggested that the catalytic domain is critical for the Env degradation (Fig 2.6C). Thus, although both HIV-1 Env and NHK are degraded via ERAD, different downstream signaling cascades could be involved in their degradation. A further understanding of these differences may identify a specific pathway for inhibition of the Env expression and HIV-1 replication.

Materials and Methods

Chemicals and antibodies

Kifunensine, tunicamycin, anti-HA antibodies, anti-FLAG M2 antibodies, and anti-FLAG M2-agarose beads were purchased from Sigma. Lactacystin and anti-actin antibodies were purchased from Santa Cruz Biotechnology. The enhanced chemiluminescence detection kit was purchased from Amersham Bioscience. Monoclonal anti-glyceraldehyde- 3-phosphate dehydrogenase antibodies were purchased from Meridian Life Science. Goat anti-human TSPO antibodies and monoclonal anti-MAN1B1 antibodies (3C2) were purchased from Novus. HIV-1 proteins were detected by antibodies from the NIH AIDS Research and Reference Reagent Program, and their catalogue numbers are 1513 (HIV-1 Gag), 526 (HIV-1 gp41), and 521 (HIV-1 gp120). Horseradish peroxidase-conjugated anti-rabbit, -goat, or -mouse immunoglobulin G secondary antibodies were purchased from Pierce.

Cell lines

The human 293T cell line was purchased from ATCC. The human CEM-T4 T cell line and HIV-1 luciferase reporter GHOST cells were obtained from the NIH AIDS Research and Reference Reagent Program. The TSPO-KO 293T cell line A3 was reported before (141). The human CEM.NKR T cell line subclones N2-NP and N5-P were described before (140). CEM-T4, N2-NP, and N5-P cells were cultured in RPMI 1640 with 10% fetal bovine serum (HyClone). 293T and GHOST cells were cultured in DMEM with 10% bovine calf serum (HyClone).

Plasmids

The HIV-1 proviral vector pNL4-3 was obtained from the NIH AIDS Research and Reference Reagent Program. The HIV-1 luciferase reporter proviral vector pNL-Luc and the pcDNA3.1-TSPO-V5-His vector were described before (140, 183). Mammalian vectors expressing human ERManI, murine (m) EDEM1, mEDEM2, and mEDEM3 fused with a C-terminal HA tag were kindly provided by the Hosokawa and the Suzuki. laboratories. pCMV6-Entry vectors expressing human EDEM1, EDEM2, and EDEM3 with a C-terminal FLAG tag were purchased from OriGene. Vectors expressing human ERManI C-terminal deletion mutants FL-1–240 and FL1–240/_ DPS were provided by the Sifers laboratory. The full-length human ERManI cDNA was subcloned into the pcDNA3.1 vector by replacing the APOBEC3G cDNA in the pcDNA3.1-A3G-HA-FLAG vector that expresses an in-frame C-terminal tandem arrayed HA-FLAG tag after HindIII/NotI digestion. The human ERManI single-point mutants E330A, R334C, E397K, D463A, C527A, C556A, and E599A were directly created in the pcDNA3.1-ERManI-HA-FLAG vector using QuikChange II Site-Directed Mutagenesis kit (Agilent Technologies). The pcDNA3.3-TOPO vector expressing human codon-optimized Cas9 was obtained from the Church laboratory through Addgene (173). To express MAN1B1 guide RNA (gRNA; see Fig 2.5A), a 455-bp gBlock that contained the U6 promoter, 19-bp gRNA, gRNA scaffold, and termination signal sequences was ordered from Integrated DNA Technologies (IDT) and cloned into the pGEM-T Easy vector (Promega) after PCR amplification, according to the Church laboratory protocol (173).

Analysis of HIV-1 Infectivity

HIV-1 particles were produced from 293T cells after transfection with pNL-Luc and an ERManI expression vector. After being normalized by p24Gag ELISA, equal amounts of viruses were used to infect GHOST cells. After 48 h of infection, cells were lysed, and viral infectivity was determined by measuring the cellular luciferase activity using a firefly luciferase reporter assay kit from Promega.

Immunoprecipitation

To determine ERManI and HIV-1 Env interaction, 293T cells were transfected with the HIV-1 proviral vector pNL4-3 and ERManI expression vectors that have a FLAG tag. After 48 h, cells were lysed with a buffer (50 mM Tris-HCl, pH 7.4, 150 mM NaCl, 1% Triton X-100, 1 mM EDTA). The cytosolic fraction was rocked with anti-FLAG M2-agarose beads for 4 h at 4 °C. After extensive washing with phosphate-buffered saline, bead-associated proteins were detected by Western blotting.

Knock-out of MAN1B1 in 293T Cells by CRISPR/Cas9

A detailed protocol was described before (141). Briefly, 293T cells were transfected with a Cas9 expression vector and a MAN1B1 gRNA expression vector, and cloned by limiting dilution. Clones were screened for ERManI expression by Western blotting, and ERManI knock-out (KO) clones were identified. The MAN1B1 locus in these KO clones was further analyzed by PCR using ERManI-ko-S and ERManI-ko-A as a primer pair (see Fig 2.5A), and sequenced. A verified MAN1B1 -KO clone E7 was finally identified.

Quantitation of Protein and DNA Levels

Images from Western blots were quantitated using the ImageJ program. Protein expression levels were calculated and presented as relative values.

Acknowledgments

We thank Ying Zhang, Changqing Yu, Jiajun Zhou and Matthew A. Wexler for experimental supports. We thank the Hosokawa, Suzuki, and Sifers laboratories for providing expression vectors. We also thank the NIH AIDS Research and Reference Reagent Program for providing the other reagents

CHAPTER 3 - Innate sensing of influenza A virus hemagglutinin glycoproteins by the host endoplasmic reticulum (ER) stress pathway triggers a potent antiviral response via ER-associated protein degradation

Dylan A. Frabutt, Bin Wang, Sana Riaz, Richard C. Schwartz, and Yong-Hui Zheng

This research was originally published in the Journal of Virology, 2017 December; Volume 92(1), pages e01690-17

I would like to acknowledge Dr. Bin Wang for his creation of the ΔCNX, ΔCRT, and ΔCNX/ΔCRT knockout HEK 293T cell-lines that were utilized in this study as well as his contribution of the experiments in Figure 1, Figure 2B and 2C, and the qPCR results in figure 5D. I would also like to thank Dr. Wang, Dr. Schwartz, and Dr. Zheng for advice on the manuscript on experimental support.

Summary

Innate immunity provides an immediate defense against infection after host cells sense "danger" signals from microbes. Endoplasmic reticulum (ER) stress arises from accumulation of misfolded/unfolded proteins when protein load overwhelms the ER folding capacity, which activates the unfolded protein response (UPR) to restore the ER homeostasis. Here, we show that a mechanism for antiviral innate immunity is triggered after the ER stress pathway senses viral glycoproteins. When hemagglutinin (HA) glycoproteins from influenza A virus (IAV) are expressed in cells, ER stress is induced, resulting in rapid HA degradation via proteasomes. The ER-associated protein degradation (ERAD) pathway, an important UPR function for destruction of aberrant proteins, mediates HA degradation. Three class I α-mannosidases were identified to play a critical role in the degradation process, including EDEM1, EDEM2, and ERManI. HA degradation requires either ERManI enzymatic activity or EDEM1/EDEM2 enzymatic activity, when ERManI is not expressed, indicating that demannosylation is a critical step for HA degradation. Silencing of EDEM1, EDEM2, and ERManI strongly increases HA expression and promotes IAV replication. Thus, the ER stress pathway senses influenza HA as "non-self" or misfolded protein, and sorts HA to ERAD for degradation, resulting in inhibition of IAV replication.

Viral nucleic acids are recognized as important inducers of innate antiviral immune responses that are sensed by multiple classes of sensors, but other inducers and sensors of viral innate immunity need to be identified and characterized. Here, we used influenza A virus (IAV) to investigate how host innate immunity is activated. We found that IAV

hemagglutinin (HA) glycoproteins induce ER stress, resulting in HA degradation via ERAD and consequent inhibition of IAV replication. In addition, we have identified three class I α-mannosidases, EDEM1, EDEM2, and ERManI, which play a critical role in initiating HA degradation. Knockdown of these proteins substantially increases HA expression and IAV replication. The enzymatic activities and joint actions of these mannosidases are required for this antiviral activity. Our results suggest that viral glycoproteins induce a strong innate antiviral response through activating the ER stress pathway during viral infection.

Introduction

Innate immunity provides the most rapid host defense against microbial pathogen infection and also controls host adaptive immunity (184). Host pattern recognition receptors (PRRs) sense pathogen-associated molecular patterns (PAMPs) to elicit this immediate host defensive response, which releases type I interferons (IFNs) and proinflammatory cytokines/chemokines, resulting in an antimicrobial response. Currently, the best characterized PAMPs in viral infection are viral nucleic acids, which are sensed by several classes of PRRs (185).

As obligate intracellular parasites, viruses hijack host endoplasmic reticulum (ER) to produce a large quantity of viral glycoproteins, resulting in ER stress (186). This stress arises from accumulation of misfolded/unfolded proteins in the ER when protein load overwhelms the ER folding capacity. ER stress is sensed by three ER transmembrane receptors, including the double-stranded RNA (dsRNA)-activated protein kinase (PKR)-like ER kinase (PERK), inositol-requiring enzyme 1 (IRE1), and activating transcription factor 6 (ATF6) (187). These sensors activate a series of signaling cascades, known as the unfolded protein response (UPR), to reduce the aberrant proteins in the ER by increasing protein folding capacity, halting protein translation, and degrading misfolded proteins via the ER-associated protein degradation (ERAD) pathway. ERAD is an important mechanism by which UPR maintains ER homeostasis, which retro-transports misfolded proteins from the ER to the cytoplasm for degradation via the ubiquitin/proteasome system (188). Class I α-mannosidases, which specifically cleave the four α1,2-linked mannose residues distributed

on the three sugar branches A, B, and C of *N*-glycan, play an important role in ERAD (43). These enzymes consist of seven members, including the ER class I α-mannosidase (ERManI), ER-degradation enhancing α-mannosidase-like (EDEM) proteins 1, 2, and 3, and Golgi class I mannosidases (GolgiMan) IA, IB, and IC. If glycoproteins are folded properly in the ER, only the outmost mannose residue on branch B is cleaved, which allows native proteins to enter the Golgi and complete *N*-glycosylation. However, if glycoproteins are terminally misfolded, the remaining three α1,2-mannose residues are cleaved in the ER, triggering misfolded protein degradation via ERAD (42).

Influenza A viruses (IAVs) are enveloped negative-sense RNA viruses that cause severe respiratory illness (189). Hemagglutinin (HA) and neuraminidase (NA) are two major viral glycoproteins on the viral surface, which divide IAVs into a number of subtypes (190). HA is a primary determinant for IAV pathogenesis, and is subject to *N*-glycosylation via 5 to 14 Asn-X-Ser/Thr motifs in the ER (9). The HA precursor HA_0 proteins are processed into surface HA_1 subunits that contain a receptor-binding domain, and transmembrane HA_2 subunits that contain a fusion peptide. HA_1 and HA_2 are linked by a disulfide bond, and assemble as homo-trimers to mediate IAV entry. Here, we report that HA is sensed by the ER stress pathway, which triggers a robust innate anti-IAV response via ERAD.

Results

Induction of ER stress by IAV infection

To determine whether IAV infection induces ER stress, we analyzed expression of the binding immunoglobulin protein (BiP), which is a master UPR regulator that is induced upon ER stress (191). A549 cells were infected with H1N1 A/WSN/33 virus at a multiplicity of infection (MOI) of 1, and BiP expression was measured by real time quantitative (q) PCR at 0, 12, and 36 h post-infection. BiP mRNAs were increased ~3-fold by the infection (Fig.3.1A), indicating an induction of UPR by IAV. To determine the downstream signaling pathway, we analyzed the IRE1 pathway in these infected cells, which was reportedly activated during IAV infection (100, 192). IRE1 is an ER-transmembrane protein that has both endonuclease and Ser/Thr kinase activities. IRE1 is activated upon binding to unfolded proteins, which in turn activates a transcription factor X-box binding protein 1 (XBP1) by unconventionally splicing a 26-nucleotide intron out of the *XBP1* mRNA. XBP1 then translocates to the nucleus and up-regulates ER chaperones to promote ER folding capacity and ERAD components to increase misfolded protein degradation (28). We directly measured XBP1 mRNA splicing by PCR at 0, 12, and 36 h post-infection. The spliced form of XBP1 mRNA was increased by 2-fold at 36 h post-infection (Fig.3.1B). These results demonstrate that UPR is induced and IRE1 is activated upon IAV infection.

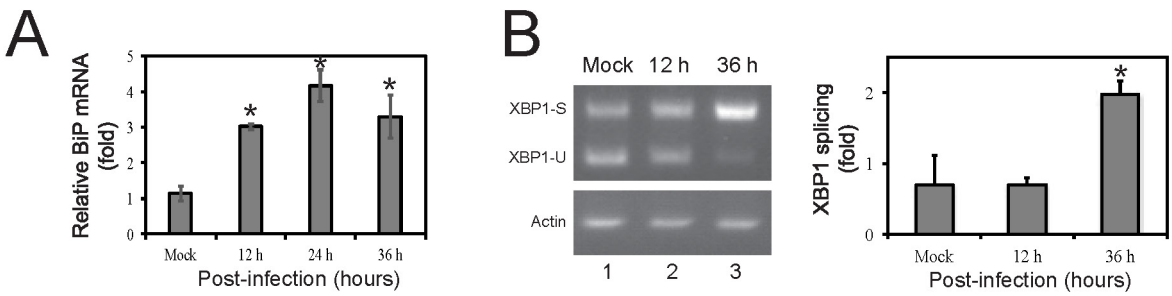

Figure 3.1. Induction of ER stress by IAV infection. (A) The BiP expression was analyzed in H1N1 A/WSN/33 virus-infected A549 cells by real-time qPCR at the indicated time-points of post-infection. (B) XBP1 splicing was analyzed in the same H1N1 A/WSN/33 virus-infected A549 cells by PCR. The spliced (S) XBP1, unspliced (U) XBP1, and actin bands are indicated. Error bars represent standard deviations (SDs) from three independent experiments. Y-axes represent normalized fold changes, where mock infection is considered 1-fold.

Activation of the IRE1 pathway by HA

HA is one of the major IAV glycoproteins, which is productively expressed in the ER after infection. To understand how HA expression affects ER homeostasis, we studied the regulation of HA biosynthesis. Calnexin (CNX) and calreticulin (CRT) comprise a fundamental chaperone system in the ER that promotes protein folding and *N*-glycosylation (193), and were reported to interact with IAV HA (194-196). Previously, we created CNX- and/or CRT-knockout (KO) cell lines using CRISPR/Cas9 (197). We examined HA subtype 5 (H5) expression in these cells. H5 has 9 *N*-glycosylation sites. When H5 precursor expression was analyzed by western blotting, there was a pronounced decrease in HA_0 expression in double-KO (ΔΔ) cells compared to wild-type (WT) and single KO cells (Fig.3.2A, lane 4). This decrease in steady-state expression translated into lower HA_1 expression on the surface of the ΔΔ cells when analyzed by flow cytometry (Fig.3.2B). We also examined expression of IAV NA from subtype 1 (N1) that has 4 *N*-glycosylation sites, as well as the viral nucleoprotein (NP) in these cells. NA is reported to interact with CNX and CRT (198), while the non-glycosylated NP does not depend on the secretory pathway. Consistently, N1, but not NP expression, was inhibited in ΔΔ cells (Fig.3.2A). To further confirm that the HA expression defect in ΔΔ cells was caused by the absence of CNX/CRT and was not an off-target artifact, CNX/CRT were reconstituted via ectopic expression. HA expression was restored through ectopic reconstitution of CNX or CRT in a dose-dependent manner (Fig.3.2C, lanes 1 to 6, and lanes 7 to 12). Thus, the functional requirement for CNX/CRT in IAV HA and NA expression are demonstrated in these experiments.

To determine whether ER stress is elicited and UPR is activated, we chose to use a luciferase-based reporter assay to measure IRE1-meidated XBP1 activation (199). As a positive control for UPR induction, the terminally misfolded human alpha1-antitrypsin variant null (Hong Kong) (NHK) was used (144). IAV HAs from H1 and H5 subtypes, the human immunodeficiency virus type 1 (HIV-1) envelope (Env) glycoproteins from the NL43, JRFL, and SF162 strains, and NHK were ectopically expressed with the XBP1-reporter construct in WT, ΔCNX, ΔCRT, and ΔΔ 293T cells, and levels of IRE1 activation were analyzed. HIV-1 Env expression resulted in marginal IRE1 activation, whereas the activation was significantly increased by IAV HA expression in all these cells (Fig.3.2D). In addition, much higher levels of IRE1 activation by HA were observed in KO cells than WT cells (Fig.3.2D). These results demonstrate that HA alone is able to activate the IRE1 pathway, which is consistent with the previous report (192).

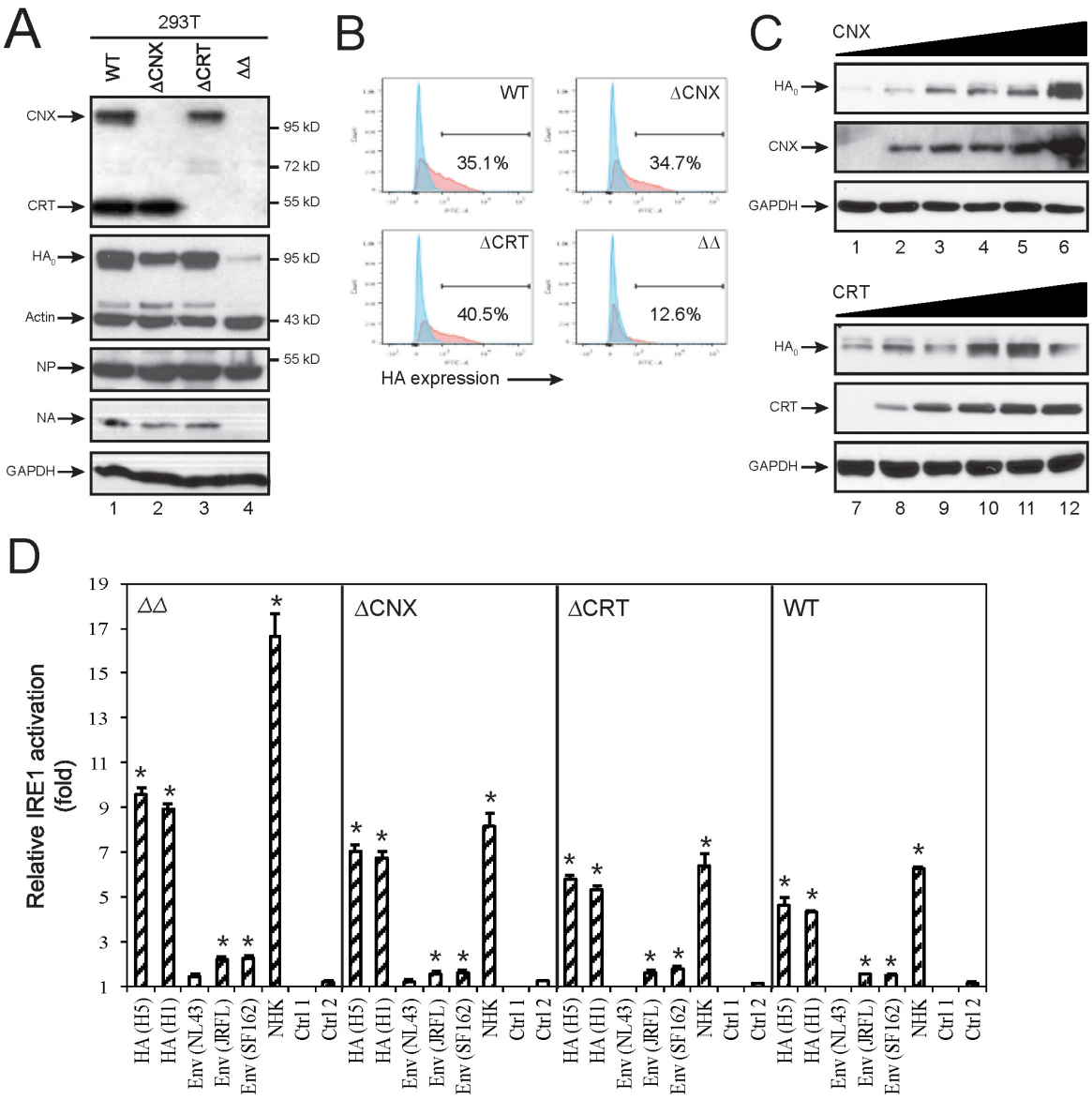

Figure 3.2. Activation of the IRE1 pathway by HA. (A) Wild-type (WT), ΔCNX, ΔCRT, or ΔΔ 293T cell lines were transfected with an IAV HA (H5), NA (N1), or NP expression vector, and protein expressions were analyzed via western blotting using indicated antibodies. (B) HA cell surface expression in WT, ΔCNX, ΔCRT, and ΔΔ 293T cells was determined by flow cytometry. (C) HA expression in ΔΔ cells was rescued by ectopic expression of CNX or CRT in a dose-dependent manner. (D) The XBP1 splicing was determined after transient transfection of the pXBP1u-FLuc reporter and viral glycoprotein expression vectors for HIV-1 and IAV into WT, ΔCNX, ΔCRT, and ΔΔ 293T cells. HA proteins from IAV subtypes H1 and H5, and Env proteins from HIV-1 NL43, JRFL, and SF162 were used. NHK, terminally misfolded human alpha1-antitrypsin variant null (Hong Kong). Control #1 (Ctrl 1) was from untransfected cells, and Ctrl 2 was from cells only transfected with the pXBP1u-FLuc vector. Displayed as the mean ± standard error of the mean (SEM), n=3, unpaired two-tailed *t*-test, *P< 0.05. Y-axis represents normalized fold changes, where Ctrl 1 is considered 1-fold.

HA degradation via ERAD

To determine how the HA expression is suppressed, we analyzed HA protein stability in ΔΔ cells. WT and ΔΔ 293T cells were transfected with an H5 expression vector and treated with cycloheximide (CHX), and protein levels were assessed after 2, 4, 6, and 8 h. HA half-life in WT cells was ~ 4 h, which was reduced to less than 2 h in ΔΔ cells (Fig.3.3A). These results suggest that HA is rapidly turned over in ΔΔ cells. To understand how HA is degraded, cells were treated with proteasome inhibitor MG132, or lysosome inhibitor bafilomycin A1. Bafilomycin A1 increased HA expression in both WT and ΔΔ cells (Fig.3.3B, lanes 5, 10), whereas MG132 selectively increased the HA expression in ΔΔ cells (Fig.3.3B, lanes 3, 8). In addition, MG132 increased the HA half-life more significantly in ΔΔ than WT cells in the stability analysis (Fig.3.3A, lanes 6, 12). These results demonstrate that HA is predominately degraded via proteasomes, indicating that HA is not folded properly in DD cells.

To test the role of ERAD in HA degradation, we treated cells with two other compounds that block ERAD at different steps. ERAD involves three major steps, including substrate recognition, retro-translocation into the cytosol, and degradation via the ubiquitin proteasome system. Class I α-mannosidases promote the recognition step by catalyzing extensive demannosylation, which can be blocked by their specific enzymatic inhibitor kifunesine (43). p97 AAA-ATPases are required for ERAD substrate retro-translocation from the ER lumen to the cytosol by catalyzing ATP hydrolysis, which is blocked by eeyarestatin I (55). Both kifunesine and eeyarestatin I blocked HA degradation

in ΔΔ cells as effectively as MG132 (Fig.3.3B, lanes 7, 9). These results demonstrate that HA is indeed rapidly degraded via ERAD in ΔΔ cells.

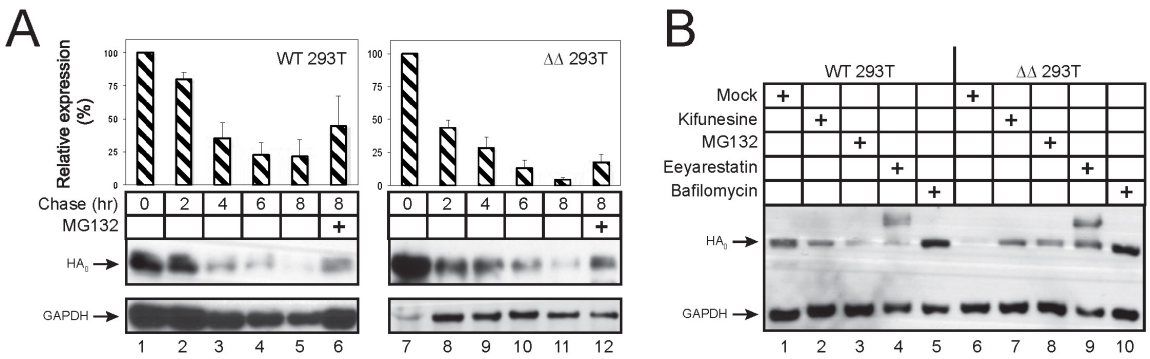

Figure 3.3. HA degradation via ERAD. (A) WT and ΔΔ 293T cells were transfected with an H5 expression vector, and the HA steady state was chased at indicated time-points by western blotting after treatment with cycloheximide (CHX) at 50 μg/ml. The relative HA expression was measured by quantification of the intensity of each protein band on the blot using ImageJ program. Error bars represent SDs from three independent experiments. Y-axes represent % changes, where the value at time zero is considered 100%. (B) After transfection of WT or ΔΔ 293T cells with an H5 expression vector, cells were incubated with MG132 (25 μM), kifunensine (5 μM), Eeyarestatin (50 μM), or Bafilomycin A1 (100 nM) for 4 h, and analyzed by western blotting.

Inhibition of HA expression by EDEM1, EDEM2, and ERManI

Having discovered HA degradation via ERAD in DD cells, we further studied the degradation mechanism in WT 293T cells. Since kifunesine rescues HA expression, we tested whether HA could be targeted by the four mannosidases in the ER, including ERManI, EDEM1, EDEM2, and EDEM3. We expressed H5 with these class I α-mannosidases, and protein expression levels were determined by western blotting. Ectopic expression of EDEM1, EDEM2, and ERManI resulted in strong 4- to 10-fold inhibition of HA expression, with EDEM1 showing the strongest effect, while EDEM3 showed a marginal effect (Fig.3. 4A, Fig.3.4B). To confirm the low activity of EDEM3, we repeated this experiment by expressing murine EDEM3 (mEDEM3) and IAV HA of another subtype, H1, that contains 6 *N*-glycosylation sites. Again, EDEM1, EDEM2, and ERManI showed similar inhibitory activities, and EDEM3 did not show any effect on the H1 expression (Fig.3.4C). To determine the specificity of EDEM1, EDEM2, and ERManI, their dose-dependent effects were determined by varying their protein expression levels. Inhibition of HA expression correlated to the levels of EDEM1, EDEM2, and ERManI expression, supporting their specific inhibitory effects (Fig.3.4D).

Because NA expression was also suppressed in ΔΔ cells, we tested whether NA could be targeted by these mannosidases. When N1, which has 4 *N*-glycosylation sites, was expressed with EDEM and ERManI proteins, we found that EDEM1 also inhibited the NA expression, but EDEM2, EDEM3 and ERManI did not (Fig.3.4E). As a comparison, we determined how EDEM and ERManI proteins inhibit expression of HIV-1 Env, which

contains ~26 *N*-glycosylation sites. Similarly to what we previously reported (145), only ERManI inhibited Env expression (Fig.3.4F, lane 1).

Next, we used a single-cycle viral replication assay to confirm these results by generating HA-pseudotyped HIV-1 infectious particles. HIV-1 pseudovirions were produced from 293T cells after cotransfection of the Env-deficient HIV-1 proviral vector pNLΔEnv with IAV H5, IAV N1, and EDEM or ERManI expression vectors. After normalization of virus production by HIV-1 $p24^{Gag}$ ELISA, viral infectivity was determined. The infectivity of these HIV-1 pseudoviruses was strongly inhibited by ERManI, EDEM1, and EDEM2, but not EDEM3, with EDEM1 showing the strongest activity; the infectivity of natural HIV-1 with authentic Env was only inhibited by ERManI (Fig.3.4G). These results demonstrate that EDEM1, EDEM2, and ERManI specifically inhibit IAV HA expression, suggesting that these class I mannosidases play an important role in the intracellular degradation process. In addition, the lower levels of ERManI expression suggest a higher specific activity on IAV HA substrate than do EDEM1 and EDEM2.

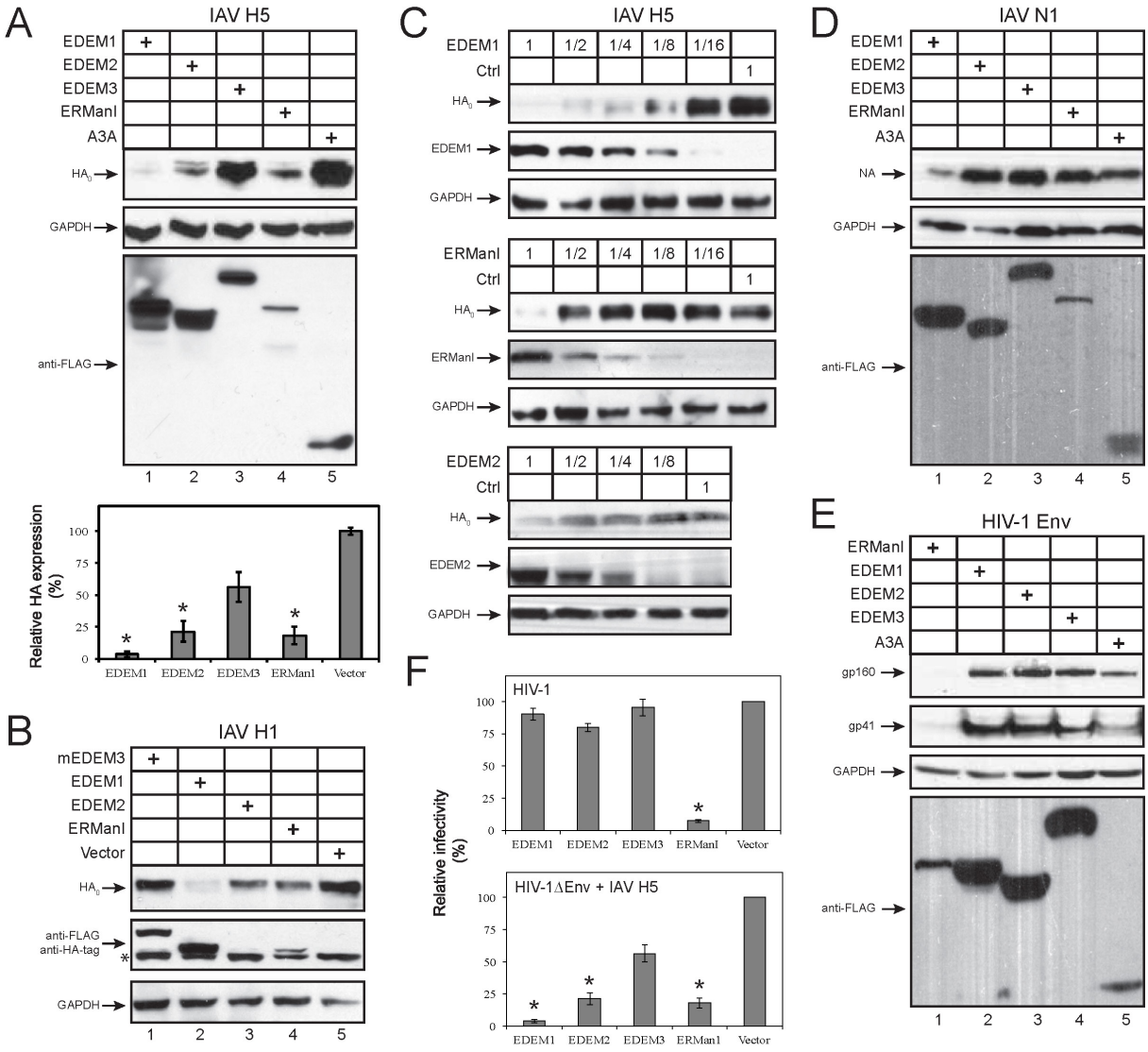

Figure 3.4. Inhibition of HA expression by EDEM1, EDEM2, and ERManI. (A) 293T cells were transfected with an H5 expression vector and a vector expressing EDEM1, EDEM2, or ERManI with a C-terminal FLAG tag. After 48 h, cells were lysed and analyzed via western blotting. APOBEC3A (A3A) was used as a control. (B) The HA expression on western blots in (A) was quantified with ImageJ program and presented as relative values. Displayed as the mean ± SD, n=3, unpaired two-tailed *t*-test, *P< 0.05. (C) A similar experiment was conducted by replacing H5 with H1, and human EDEM3 with murine EDEM3 (mEDEM3). An unspecific band is labeled with an asterisk, which overlaps with the EDEM2 band. (D) 293T cells were transfected with a fixed amount of an H5 and increasing amounts of an EDEM1, EDEM2, or ERManI expression vector (μg), and the HA expression was analyzed via western blotting. (E) The effect of EDEM and ERManI on IAV N1 expression was similarly determined. (F) The effect of EDEM and ERManI on HIV-1 Env expression was similarly determined. (G) Effect of EDEM and ERManI on single-cycle viral replication. HIV-1 with authentic Env or HIV-1 pseudoviruses with IAV H5 and N1 were produced by transfection of an EDEM or ERManI expression vector plus pNL4-3 or pNL-GFP proviral vector, respectively. The infectivity of natural HIV-1 was

Figure 3.4. (Cont'd)

determined after infection of the HIV-1 luciferase reporter cell line TZM-b1 cells and measurement of the intracellular luciferase activity; the infectivity of HA-pseudotyped HIV-1 was determined after infection of MDCK cells and measurement of the intracellular GFP expression. Displayed as the mean ± SEM., n=3, unpaired two-tailed *t*-test, *P< 0.05. Y-axes in (B) and (G) represent % changes, where the value from the vector control is considered 100%.

Requirement of ERManI, EDEM1, and EDEM2 catalytic activity for HA degradation

Previously, we reported that class I α-mannosidase activity is required for ERManI inhibition of HIV-1 Env expression (145). In contrast, this catalytic activity is not required for ERManI inhibition of the misfolded human NHK protein expression (152). To better understand the EDEM and ERManI inhibitory mechanism, we tested whether catalytic activity is required for inhibition of HA expression. We compared their inhibitory effects in the presence of kinfunesine, as well as the proteasome inhibitors lactacystin and MG132. Kifunesine blocked HA degradation by ERManI, EDEM1, and EDEM2 as effectively as lactacystin and MG132 (Fig.3.5A). Thus, ERManI, EDEM1, and EDEM2 catalytic activities are required for HA degradation.

Next, we mutated the putative catalytic residues in these proteins and tested whether their activities could be disrupted. Although EDEM class I α-mannosidase activities have not been demonstrated *in vitro*, the three ERManI catalytic residues (E330, D463, E599) are well conserved in EDEM1 (E225, D370, E493) and EDEM2 (E117, D252, E372) (52). Previously, we created three ERManI catalytic mutants E330A, D463A, and E599A (145). Analogous EDEM1 catalytic mutants E225A, D370A, and E493A, and EDEM2 catalytic mutants E117A, D252A, and E372A were created. When these mutants were compared to their WT proteins, all EDEM1 and EDEM2 catalytic mutants were still able to inhibit HA expression, whereas the ERManI mutants lost inhibitory activity against HA expression (Fig.3.5B). These results suggest that ERManI requires its catalytic activity to inhibit HA expression, but EDEM1 and EDEM2 do not.

To reconcile these conflicting results, we tested these EDEM1 and EDEM2 catalytic mutants again in a previously reported ERManI-KO cell line (145). When HA was expressed with these mutants, the two EDEM1 mutants D370A and E493A and two EDEM2 mutants D252A and E373A lost their inhibitory activity, although the EDEM1 E225A and EDEM2 E117A mutants were still as active as their WT proteins, (Fig.3.5C), indicating the requirement for their catalytic activity in this cell line. This result suggests that the catalytic activity of EDEM1 and EDEM2 becomes indispensable for inhibition of HA expression when ERManI is not present. ERManI, EDEM1, EDEM2, and EDEM3 expression were all detectable in the human lung epithelial cell line A549 by qPCR, indicating that all these four mannosidases are expressed in these cells (Fig.3.5D). Thus, ERManI, EDEM1, and EDEM2 likely all play a role in targeting HA to ERAD for degradation.

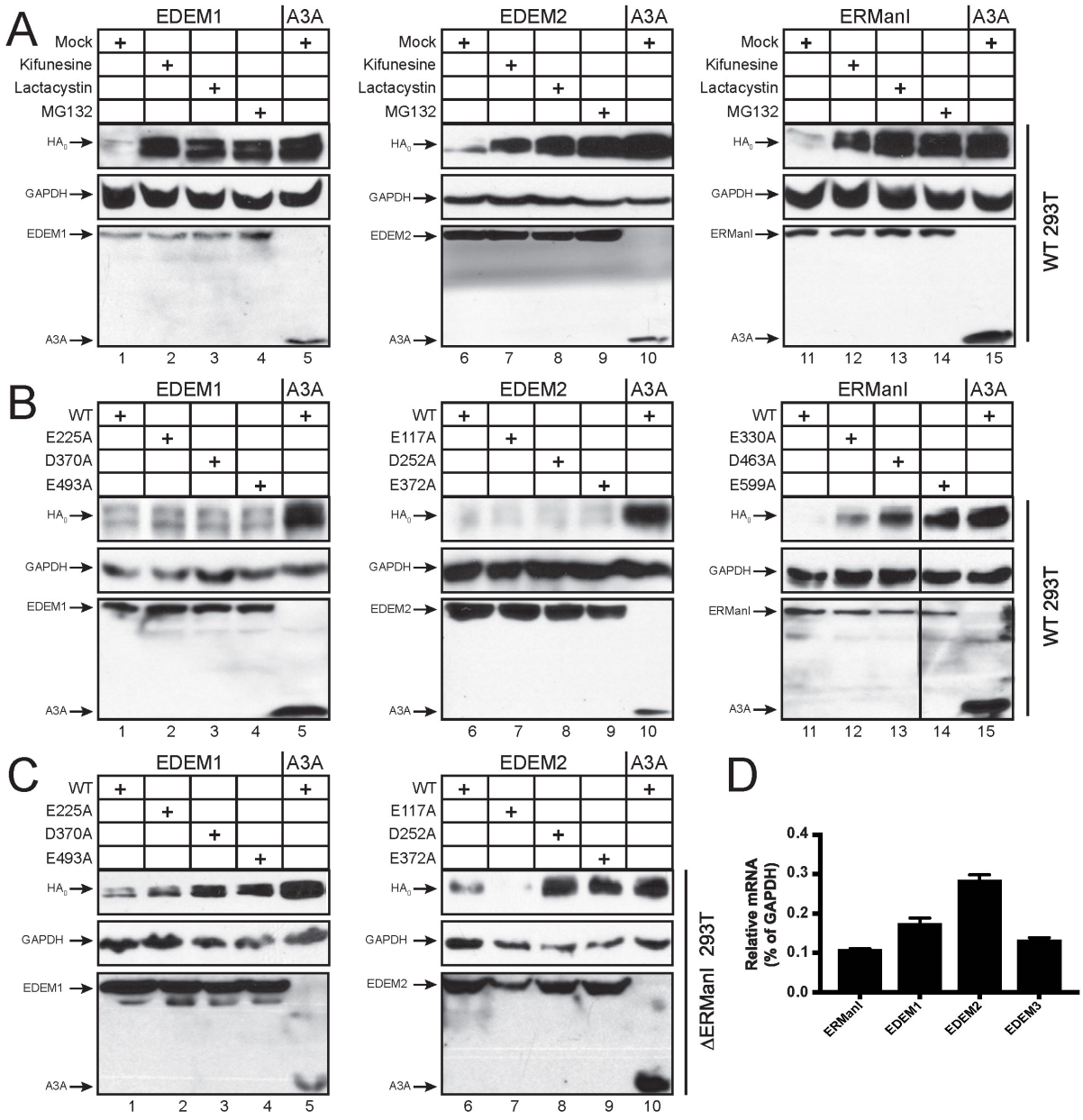

Figure 3.5. Requirement of mannosidase activity for HA inhibition. (A) 293T cells were transfected with an H5 and indicated EDEM and ERManI expression vector. After 24 h, cells were treated with kifunensine (5 μM), lactacystin (25 μM), or MG132 (25 μM) for 6 h, and protein expressions were analyzed by western blotting. (B) 293T cells were transfected with an H5 and indicated EDEM and ERManI WT or catalytic mutant expression vector, and protein expression was analyzed by western blotting. (C) ERManI-KO 293T cells were transfected with an H5 and indicated EDEM WT or mutant expression vector, and protein expression was analyzed by western blotting. (D) The relative expression of ERManI, EDEM1, EDEM2, and EDEM3 in the human lung epithelial cell line A549 was determined by real-time qPCR. Displayed as the mean ± SEM n=3, unpaired two-tailed *t*-test, *P< 0.05. Y-axis represents relative mRNA levels (%) after normalization to the levels of GAPDH.

Inhibition of HA expression by endogenous EDEM1, EDEM2, and ERManI

To further validate the inhibitory effects of ERManI, EDEM1, and EDEM2, we used short-hairpin (sh) RNAs to silence their expression. Two sets of shRNAs specific to each enzyme were expressed from a lentiviral vector, and their gene knockdown (KD) efficiencies were determined by western blotting. Compared to a scrambled shRNA control (ctrl-shRNA), these specific shRNAs effectively reduced EDEM1, EDEM2, or ERManI expression, respectively (Fig.3.6A, lanes 1 to 9).

After confirming their knockdown efficiencies, we tested whether these specific shRNAs increase IAV HA and HIV-1 Env expression in the DD cells. When these shRNAs were expressed with HA or Env, all of them increased HA expression, with the EDEM1-shRNAs having the most potent effect (Fig.3.6B, lanes 1 to 3). HIV-1 Env expression was slightly increased by the ERManI-shRNAs (Fig.3.6B, lane 7). These results are consistent with our previous findings that HA is targeted by EDEM1, EDEM2, and ERManI, whereas HIV-1 Env is only targeted by ERManI.

Next, we created A549 cell lines stably expressing these shRNAs via lentiviral transduction. When HA was expressed in these A549 cells, its expression was effectively increased by the EDEM2- and ERManI-shRNAs, and less effectively by the EDEM1-shRNAs (Fig.3.6C, lanes 2 to 4). We also created a triple-KD A549 cell line silencing all three genes. When HA expression was tested in these triple-KD cells, a much stronger increase in HA expression was observed (Fig.3.6C, lane 5). To understand why the EDEM1-shRNAs did not show a stronger effect, these shRNAs were also stably expressed in

293T cells via lentiviral transduction. When HA expression was tested, the EDEM1-shRNAs exhibited a similar efficiency in enhancing expression as the EDEM2- and ERManI-shRNAs (Fig.3.6C, lanes 6 to 9). These results further confirm the specific inhibition of HA expression by EDEM1, EDEM2, and ERManI.

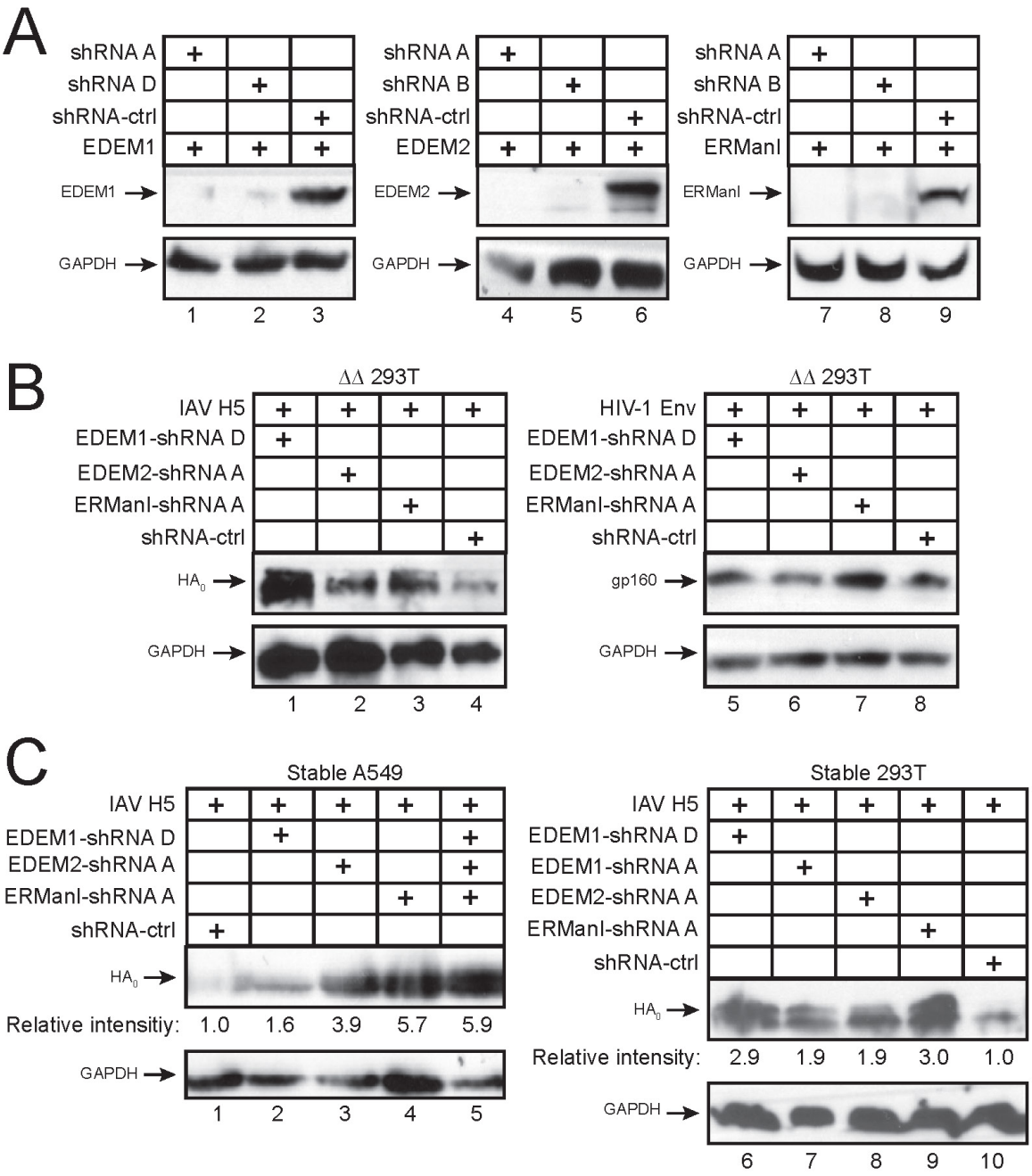

Figure 3.6. Inhibition of HA expression by endogenous EDEM1, EDEM2, and ERManI. (A) WT 293T cells were transfected with an EDEM1, EDEM2, and ERManI expression vector plus a lentiviral vector expressing the specific shRNAs or a scrambled shRNA as a control (ctrl). Protein expression was analyzed by western blotting. (B) ΔΔ 293T cells were transfected with an H5 or HIV-1 proviral vector plus a lentiviral vector expressing indicated shRNAs. Protein expression was analyzed by western blotting. (C) WT A549 and 293T cells were stably transduced with a lentiviral vector expressing indicated shRNAs, and the HA expression in these cells was analyzed by western blotting.

Inhibition of IAV replication by EDEM1, EDEM2, and ERManI

After establishment of the stable A549 silencing cell lines, we infected these cells with A/WSN/33 IAV (an H1N1 IAV in which the HA has 6 and the NA has 4 *N*-glycosylation sites) at a MOI of 0.5 (200). Viral supernatants were collected at 12, 24, 36, and 48 h post-infection, and viral replication was determined by measuring hemagglutination titers using turkey blood cells or by determining the plaque forming units (PFUs) after infecting MDCK cells. Single-KDs increased hemagglutination titers maximally by 2- to 4-fold, whereas the triple-KD increased the titers by 5-fold at 36 h post-infection (Fig.3.7A). Notably, more prominent effects were detected from the plaque assay. During the entire infection, the triple-KD exhibited the strongest effect by increasing PFUs 10- to 24-fold; single-KDs also increased PFUs 3- to 7-fold, and the ERManI-KD had the strongest effect (Fig.3.7A; note the log scale). The triple-KD doesn't appear significantly different from the ERManI-KD. However, the difference is more evident at 48 hours. Like the hemagglutination titers, PFUs dropped significantly at 48 hours, which is likely caused by the cytopathic effect from viral infection. To confirm that enhancement of viral replication is linked to increased HA expression via the shRNAs, we determined expression of EDEM1, EDEM2, and ERManI, as well as viral proteins HA, NP, and non-structural protein 1 (NS1) in these infected cells by western blotting at 24 and 48 h post-infection. The expression of EDEM1, EDEM2, and ERManI was effectively reduced during the infection by their respective shRNAs (Fig.3.7B). In addition, only the expression of HA, but not NP or NS1, was significantly increased by these shRNAs. Importantly, the triple-KD and ERManI-KD

increased the HA expression more strongly than the other two single-KDs. Taken together, these results identify EDEM1, EDEM2, and ERManI as critical host factors that are able to inhibit IAV replication by blocking the expression of HA and possibly NA as well.

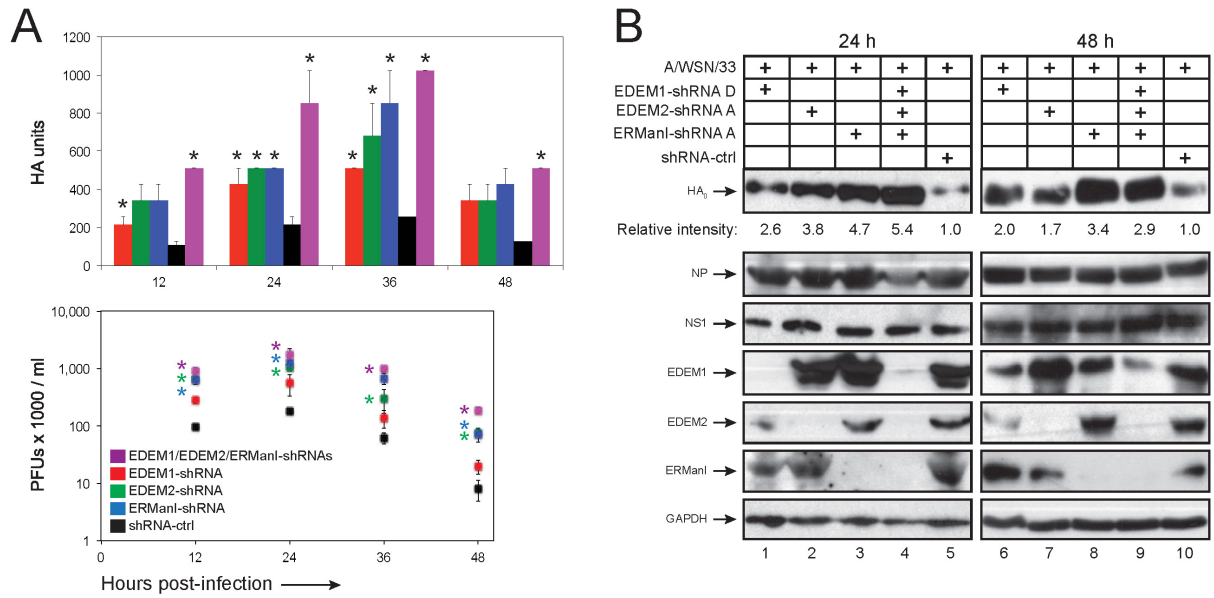

Figure 3.7. Inhibition of IAV replication by EDEM1, EDEM2, and ERManI. (A) Stable A549 cell lines expressing indicated shRNAs were infected with H1N1 A/WSN/33 viruses at an MOI of 0.5. Viral supernatants were sampled at the specified time-points. Viral titers were determined by a hemagglutination assay using turkey red blood cells and plaque forming cell assay after infecting MDCK cells. Displayed as the mean ± SD, n=2, unpaired two-tailed *t*-test, *P< 0.05. (B) Infected cells at 24 h and 48 h from the same infection experiments were collected and analyzed by western blotting using indicated antibodies. Relative intensity of HA_0 was measured using ImageJ software.

Discussion

The ER is responsible for not only translation, but also proper folding of secreted proteins, which account for one-third of total cellular proteins. To secrete native and fully functional proteins, the ER is equipped with multiple chaperone systems and folding enzymes that promote protein maturation. Nevertheless, protein folding is complex and susceptible to errors, resulting in accumulation of misfolded/unfolded proteins that induce ER stress (201). Accordingly, eukaryotic cells have evolved UPR as an evolutionarily conserved stress response mechanism to maintain the ER homeostasis. Production of viral proteins places an added burden on the folding machinery, and ER homeostasis is easily disrupted by productive viral replication. Consequently, UPR is frequently induced in virally infected cells to support cellular function and, at the same time, benefit chronic viral infection (186). Notably, UPR signaling cascades have been found to intersect with inflammatory and interferon pathways, so it is speculated that the UPR should have an additional function for sensing viral infection as part of the innate immune antiviral response (202). Recently, Hrincius *et al*. reported that HA is sensed by an ER stress pathway, resulting in inflammatory responses that cause acute lung damage in IAV infected mice (192). Here, we present evidence that UPR sensing of HA triggers a direct anti-IAV response by targeting HA degradation via ERAD. Collectively, our findings strongly suggest that host cells detect HA as a misfolded or "non-self" protein, as proposed by Hrincius *et al*., and that ER mannosidases target HA to ERAD for degradation.

ERAD is a host quality control mechanism that specifically targets misfolded glycoproteins for degradation, ensuring that only properly folded proteins are secreted from the ER. As obligate intracellular parasites, viruses have been found to exploit ERAD to promote viral replication (129, 203, 204). Viruses may degrade host proteins such as MHC class I and CD4 via ERAD to escape the host immune response or avoid superinfection, resulting in enhanced viral replication. In addition, viruses may produce viral proteins from, enter through, or replicate in some components of the ERAD machinery to directly promote viral replication. Here, we demonstrate that ERAD can be recruited to degrade HA expression and inhibit IAV replication.

We have identified three class I α-mannosidases ERManI, EDEM1, and EDEM2 that trigger HA degradation and inhibit IAV replication. These three enzymes are not only responsible for HA degradation in CNX/CRT KO cells, but also in WT cells. Class I α-mannosidases are responsible for cleavage of the four α1,2-linked mannose residues distributed on the three *N*-glycan branches A, B, and C. Currently, it is still not clear how extensive demannosylation is accomplished in the ER to initiate ERAD. ERManI cleaves the outmost mannose residue on branch B, whereas the three Golgi mannosidases cleave the other three α1,2-linked mannose residues *in vitro*. However, ERManI also cleaves these three mannose residues at high concentrations (25). Thus, in the course of viral infection, where viral proteins may be greatly overexpressed, ERManI may play a very central role, cleaving residues on branches A, B, and C. This is consistent with our finding that ERManI is the most active mannosidase in HA degradation and IAV inhibition. While our data strongly indicate

that class I α-mannosidase enzymatic activity is required for HA degradation, inactivation of the catalytic residues selectively disrupted the ERManI, but not the EDEM1 and EDEM2 inhibition of HA expression in WT 293T cells. This is again consistent with a central role for ERManI in directing HA to ERAD. Furthermore, inactivation of EDEM1 and EDEM2 activity only shows a phenotype in ERManI-KO cells. Collectively, our data point toward ERManI playing the key role in trimming the α1,2-Man residues and directing HA to ERAD. The fact that silencing any one of EDEM1, EDEM2, and ERManI results in an increase of the HA expression and IAV replication does, however, present a conundrum. Perhaps, this can be reconciled by a non-catalytic role for EDEM1 and EDEM2, where the interaction of HA with these mannosidases facilitates the cleavage of mannose groups by ERMan1. We found all three mannosidases expressed in human lung epithelial cells, a natural target for IAV infection, so it is plausible that these proteins can collaborate in some fashion to initiate the process of HA degradation. Thus, ERManI, EDEM1, and EDEM2 are important players in this innate antiviral response in the ER to inhibit IAV replication.

Materials and Methods

Chemicals and antibodies

The anti-FLAG antibody, kifunensine, L-(tosylamido-2-phenyl) ethyl chloromethyl ketone (TPCK)-treated trypsin, and cycloheximide were purchased from Sigma. Bafilomycin A1, MG132, and lactacystin were purchased from Santa Cruz. Eeyarestatin was purchased from Calbiochem. Concentrations of the inhibitors used are as stated here unless otherwise noted: cycloheximide (50 μg/ml), kifunensine (5 μM), eeyarestatin (50 μM), bafilomycin A1 (100 nM), lactacystin (25 μM), MG132 (25 μM). A mouse monoclonal anti-ERManI (3C2) was purchased from Novus Biologicals; rabbit polyclonal anti-EDEM1 and EDEM2 were purchased from Sigma; a goat anti-actin polyclonal was purchased from Santa Cruz Biotechnology; a mouse monoclonal anti-glyceraldehyde-3-phosphate dehydrogenase (GAPDH) was purchased from Meridian Life Science. Horseradish peroxidase (HRP)-conjugated human, rabbit, goat, horse, or mouse immunoglobulin G secondary antibodies were purchased from Pierce. HIV-1 proteins were detected by antibodies from the NIH AIDS Research and Reference Reagent Program, and their catalogue numbers are 526 (HIV-1 gp41), and 521 (HIV-1 gp120). Mouse anti-HA_2, NA, NS1, and NP were purchased from Bei Resources (NR-44222, NR-13459, NR-44426, or NR-4282, respectively).

Cell lines

Human embryonic kidney cells 293 carrying the SV40 T antigen (293T), human lung carcinoma cell line A549, and Madin-Darby Canine Kidney (MDCK) epithelial cells were

cultured in DMEM with 10% bovine calf serum (BCS), which was purchased from HyClone. ERMan1-KO 293T cells were described previously (17). 293T CNX/CRT single and double-KO cells were described previously (14). Stable 293T and A549 cell lines expressing ERManI, EDEM1, and EDEM2 shRNAs were generated through lentiviral transduction. Lentiviral particles were produced through co-transfection of the Origene pGFP-C-shLenti vectors (catalog numbers TL313302A, TL313302D, TL304849A, TL303362A), the packaging vector pCMVΔ8.9, and VSV-G expression vector. These viruses were used to infect 293T or A549 cells, and cultured in the presence of puromycin (10 μg/ml). The infection was also confirmed with fluorescent microscopy to test GFP expression. Stable knockdown cell lines were further confirmed by the expression of GFP, which was expressed from the same lentiviral vector.

Plasmids

pCMV6-Entry vectors expressing human EDEM1, EDEM2, and EDEM3; pcDNA3.1 expression vectors for human APOBEC3A (A3A), ERManI, and ERManI mutants E330A, D463A, and E599A; and the murine EDEM3-HA expression vector have been previously described (17). Plasmids expressing IAV (A/Thailand/1(KAN-1)/2004(H5N1) strain) HA (7705) and NA (7708) were provided by Gary Nabel. pHW181-PB2, pHW182-PB1, pHW183-PA, pHW184-HA, pHW185-NP, pHW186-NA, pHW187-M, and pHW-188-NS were provided by Robert G. Webster (20). pCMVΔ8.9 was provided by Didier Trono. pXBP1u-FLuc for measuring XBP1 splicing was provided by Yi-Ling Lin (199). The HIV-1 proviral vector pNL4-3 and pNL4-3.Luc.R^-E^- were obtained from the NIH AIDS

Research and Reference Reagent Program. pNL-Luc was constructed by swapping the BamH1-XhoI fragment from pNL4-3.Luc.R$^-$E$^-$. pNL-GFP was constructed by replacing the firefly luciferase gene with the enhanced green fluorescent protein gene after NotI and XhoI digestion. pcDNA-EDEM1-FLAG-HA and pcDNA-EDEM2-FLAG-HA were constructed by replacing the A3G gene in the pcDNA3.1-A3G-HA-FLAG vector that expresses an in-frame C-terminal tandem arrayed HA-FLAG tag after HindIII and NotI digestion. Using the Quickchange II Site-Directed Mutagenesis kit (Agilent), EDEM1 E225A, D370A, and E493A mutants were created in the pCMV6-Entry-EDEM1 vector, and EDEM2 E117A, D252A, and E372 mutants were created in the pcDNA-EDEM2-HA-FLAG vector. pGFP-C-shLenti lentiviral vectors expressing 4 unique 29mer shRNAs (A, B, C, D) against human ERManI (TL302262), EDEM1 (TL313302), EDEM2 (TL304849), and a scrambled control (TR30021) were purchased from OriGene.

Real-time qPCR analysis

Total RNAs were extracted from mock- or virus-infected A549 cells using RNA extraction Kit (Qiagen, Chatsworth, CA). First-strand complementary DNAs (cDNA) were synthesized using ReverTra Ace qPCR RT Master Mix (TOYOBO, Japan) according to the manufacturer's instructions. Real-time PCRs were performed using SYBR Permix Ex Taq II (TaKaRa, China) in a LightCycler 480 II real-time PCR system (Roche). Primers for EDEM1 are 5'-CAGAATAATAACTGACTCCAAGCAGC-3' and 5'-CTGTCTTTAGATTCACCCGAGGAT-3'); primers for EDEM2 are 5'-ATTCCAAAGAGTGGTTGAAGTGC-3' and

5’-CAGCCTTCTTGGAGAGCAGATGA-3’; primers for ERManI are 5’-CCAGCAAATCCACCCGTCTTAC-3’ and 5’- GGTCTTGGCTTGGGGGTCTAAT-3’; primers for BiP are 5’-AGGCTTATTTGGGAAAGAAGGTTAC-3’ and 5’-GATCCTCATAACATTTAGGCCAGC-3’; primers for GAPDH are 5’-GAGTCAACGGATTTGGTCGT-3’ and 5’- GGTGCCATGGAATTTGCCAT-3’. The thermal cycling conditions were as follows: 1 cycle of 95°C for 5min, followed by 40 cycles of 95°C for 30s, 60°C for 30s and 72°C for 20s. Fluorescence signal was acquired continuously after the last elongation step to monitor dissociation. Melting curves were obtained with MxPro software. Expression levels of the target genes were computationally transformed from Ct value and then normalized by the glyceraldehyde-3-phosphate dehydrogenase (GAPDH) expression. Results were determined by the $2^{-\Delta\Delta Ct}$ method.

XBP1 mRNA splicing assay

The assay was performed as described previously with minor modification (155). Briefly, A549 cells were infected with H1N1 WSN/33 viruses at MOI of 0.5. Total RNAs were extracted from the infected cells at 0, 12 and 24 h post infection. After reverse transcription, 2 μl of cDNAs were used as templates for amplification of the XBP1 mRNAs with the described primers (155) using 60°C as the annealing temperature. The PCR products were analyzed on a 2% agarose gel after *Pst*I digestion.

Transfection

Polyethylenimine (PEI) stock solution (1 mg/ml) was prepared by dissolving 500 mg PEI (Polysciences) into 500 ml sterilized water after adjusting pH to 4.5 with HCl and filtering

the solution through a 0.22 μM membrane. To produce HA (7705) pseudotyped HIV-1 and express various mannosidase proteins, $1x10^6$ 293T cells were seeded in each well of a 6-well culture plate 16 hr before transfection. 3 μg total DNA was diluted into 200 μl serum-free DMEM medium, and mixed with 9 μg PEI. After 15 minutes of incubation at room temperature, these transfection reagents were added directly into the supernatant of each well. Media were replaced after 6 hr and cell lysate collected at 48 hr unless otherwise noted. Viruses were collected from the supernatants and viral production was measured by $p24^{Gag}$ ELISA; protein expression was directly determined by western blotting.

Analysis of HA-pseudotyped HIV-1 infectivity

Viral particles were produced from 293T cells co-transfected with pNL-GFP, HA expression vector 7705, and NA expression vector 7708. Particles were normalized by $p24^{Gag}$ ELISA, and equal amounts of viruses were used to infect MDCK cells. After 48 hr, cells were washed 3 times with PBS, filtered through 40 micron nylon mesh, and used for flow cytometry analysis.

Analysis of HIV-1 infectivity

HIV-1 particles were produced from 293T cells after transfection with pNL4-3 and a mannosidase expression vector or vector control. After normalization by $p24^{Gag}$ ELISA, equal amounts of viruses were used to infect TZM-b1 cells. After 48 hr, cells were lysed, and viral infectivity was determined by measuring the cellular luciferase activity using the firefly luciferase reporter assay kit from Promega.

Production of H1N1 A/WSN/33 virus and hemagglutination assay

A/WSN/33 virus was produced as described before using an 8-plasmid transfection into MDCK/HEK 293T co-culture (20). Viral titer was determined via MDCK plaque assay. For infection experiments $0.5x10^6$ A549 stable knockdown shRNA cells were seeded into a 6 well plate and incubated for 6 h. Media were then replaced with Opti-MEM supplemented with 0.5μg/ml TPCK trypsin and virus was added at an MOI of 0.5. Viral supernatants were collected at 12, 24, 36, and 48 hr time points and extracted media were replaced with fresh opti-MEM (0.5 μg/ml TPCK trypsin). Hemagglutination titers were determined by a turkey blood HA-assay using two-fold dilutions of the virus. HA units were calculated from the last dilution of virus that exhibited turkey RBC agglutination. Viral titers in PFUs/ml were calculated by plaque assay using 12-well plates. Adsorption of 10-fold serial dilutions of virus was performed on MDCK monolayers and overlaid with 0.3% final concentration of agarose in Opti-MEM with 2 μg/ml TPCK trypsin. After 48 h, cells were fixed with 2% formaldehyde and stained with 0.15% crystal violet in ethanol for plaques to be detected.

Statistics

Statistical tests were performed using Microsoft Excel. Significance of differences between samples was assessed using an unpaired two-tailed students t-test. Variance was estimated by calculating the standard deviation (SD) or the standard error of the mean (SEM) in each group, as indicated in figure legends, and represented by error bars. Unless specified in the legend, all experiments were performed independently at least three times and ‘n’ indicates biological replicates, with a representative experiment being shown.

Acknowledgements

We thank Ian York and Richard N. Sifers for constructive comments on this manuscript. We thank Robert G. Webster, Yi-Ling Lin, Richard N. Sifers, Chengjun Li, the BEI Resources, and the NIH AIDS Research and Reference Reagent Program for providing various reagents.

DAF is supported by the Bertina Wentworth endowed fellowship and Russell B. Duvall endowed fellowship. BW is supported by grants from the National Natural Science Foundation (31502089), Natural Science Foundation of Heilongjiang Province (QC2017028), and Harbin Veterinary Research Institute (SKLVBP2017012), China. YHZ is supported by a grant from the "948" plan, 2014-Z10, Ministry of Agriculture, China.

CHAPTER 4 – The dispensability of ER chaperones, calnexin and calreticulin for HIV-1 envelope folding, and the role of Golgi mannosidases on viral envelope glycoproteins.

Summary

In this chapter, I will be discussing the characterization of factors that may influence HIV-1 and IAV envelope glycoprotein folding and maturation, including chaperones in the ER, and class I and class II mannosidases that reside in the Golgi apparatus. The literature describing HIV-1 folding, until this point, has contended that the ER chaperones, calnexin and calreticulum, have a crucial role in HIV-1 envelope folding and maturation. I have found that ectopic HIV-1 envelope expression in HEK 293T cells does induct the unfolded protein response (UPR), although through the PERK and ATF6 sensors, rather than through the IRE1 pathway as observed with Influenza A virus hemaggluttinin (Fig 3.2). Below, I will describe how HIV-1 envelope glycoprotein expression is not affected in the ΔCNXΔCRT (ΔΔ) HEK 293T knockout cell line. In the absence of these chaperones, there is no difference in whole-cell or cell-surface expression as well as no difference in the infectivity of viral particles produced in the knockout cell lines when compared to parental HEK 293T cells.

Given the resistance of HIV-1 envelope to the removal of ER chaperones and the ectopic expression of the EDEM family of class I α 1,2-mannosidases, sensitivity to the Golgi-localized class I and class II mannosidases was tested. No evidence was found to support the role of class II mannosidases modulating the expression of HIV-1 envelope glycoproteins, while the enzymes, Golgi Man1A and Golgi Man1C reduce the expression of both HIV-1 and IAV envelope glycoproteins when co-transfected in addition to the HIV-1 structural protein $p24^{Gag}$. The reduction of envelope expression by Golgi Man1A and Golgi Man1C is not dependent upon the glutamic acid present in the active-site of the mannosidase

homology domain. Furthermore, unlike the results from the EDEM proteins, there is no rescue of viral envelope expression when Golgi mannosidase catalytic-site mutants are expressed the E7 ERManI KO HEK 293T cell line. I also confirm that ManIA and ManIC specifically bind to IAV HA using protein immunoprecipitation in this work.

Additionally, I investigated whether the envelope degradation phenotype potentiated by ManIA and ManIC upon HIV-1 and IAV envelope glycoproteins is influenced the infectivity of viral particles. I found that, while a significant effect can be seen in systems that do not normalize viral titer, ectopic ManIA and ManIC expression does not have a significant effect on HIV-1 HA/NA pseudo-particle infectivity. This difference in infection is abrogated when the production defect in cells expressing ManIA and ManIC is accounted for.

Introduction

Calnexin and calreticulin have been associated with HIV-1 maturation mainly through immunoprecipitation studies that have shown a strong correlation between the release of HIV-1 envelope from calnexin and the binding of envelope to its host receptor (CD4) during pulse-chase experiments (205). Further studies have also characterized the discrete binding sites of calnexin and calreticulin and their molecular determinants on the HIV-1 envelope glycoprotein (206-208). Thus, in the past, the interaction between calnexin, calreticulin, and HIV-1 envelope has been comprehensively studied using methodologies that exclusively rely on protein-protein interactions.

After exposure to the ER chaperones calnexin and calreticulin and the ER-localized class I α 1,2-mannosidases, viral envelope glycoproteins undergo further mannose trimming in the Gogli apparatus The class I and class II mannosidases that are purported to be situated in the Golgi apparatus are responsible for the further trimming of the final α 1,2- or α 1,3- and α 1,6-linked mannose residues, respectively. While current models for ERAD would suggest that Golgi-situated enzymes would not be able to target glycoproteins to the conventional ERAD dislocon for degradation (chapter 1), the localization of both class I and class II Golgi mannosidases has been controversial (24, 48, 50, 85, 152, 165). Recently, Golgi ManIA has been reported to reside in quality control vesicles where they can interact with the other canonical ERAD components in the targeting and degradation of misfolded proteins (50). Given the newfound likelihood that the Golgi mannosidases could potentially participate in the conventional ERAD, it is possible that their activity would influence the targeting of viral

envelopes to degradation via ERAD. Although there is not documented controversy concerning the class II mannosidases, the fixation errors and confusion of quality control vesicles with Golgi fractions described by Dr. Lederkremer's group may have influenced the predicted localization of the class II manosidases which have previously been identified as Golgi localized (209, 210).

Results

Expression of HIV-1 envelope glycoproteins in HEK 293T and ΔΔ HEK 293T cells induces the PERK and ATF6 pathways of the UPR

While I have previously found that IRE1-mediated pathway for the unfolded protein response (UPR) was potently activated by multiple serotypes of Influenza A virus (IAV) envelope glycoproteins, ectopic expression of HIV-1 envelope glycoproteins activated the IREI pathway to a lesser extent (Fig 3.2). While investigating IAV HA UPR activation, I found that the HIV-1 envelope glycoprotein expression vectors JRFL and HXB2 (NL) are able to potently activate the PERK and ATF6 pathways of the UPR (Fig 4.1A and B). When examining the induction of expression for the chaperone BiP in transfected cell lysates an increase in the expression of BiP due to viral protein expression can be observed (Lane 9 in figure 4.1C compared to lanes 1-8). Although, the greatest induction of BiP protein expression appears to be the pNLΔgag treatments that achieved the highest expression of HIV-1 envelope (Fig 4.1C lane 5). The only structural protein expressed by the pNLΔgag vector is the viral envelope, which allows for a finer determination of what viral element is inducing stress.

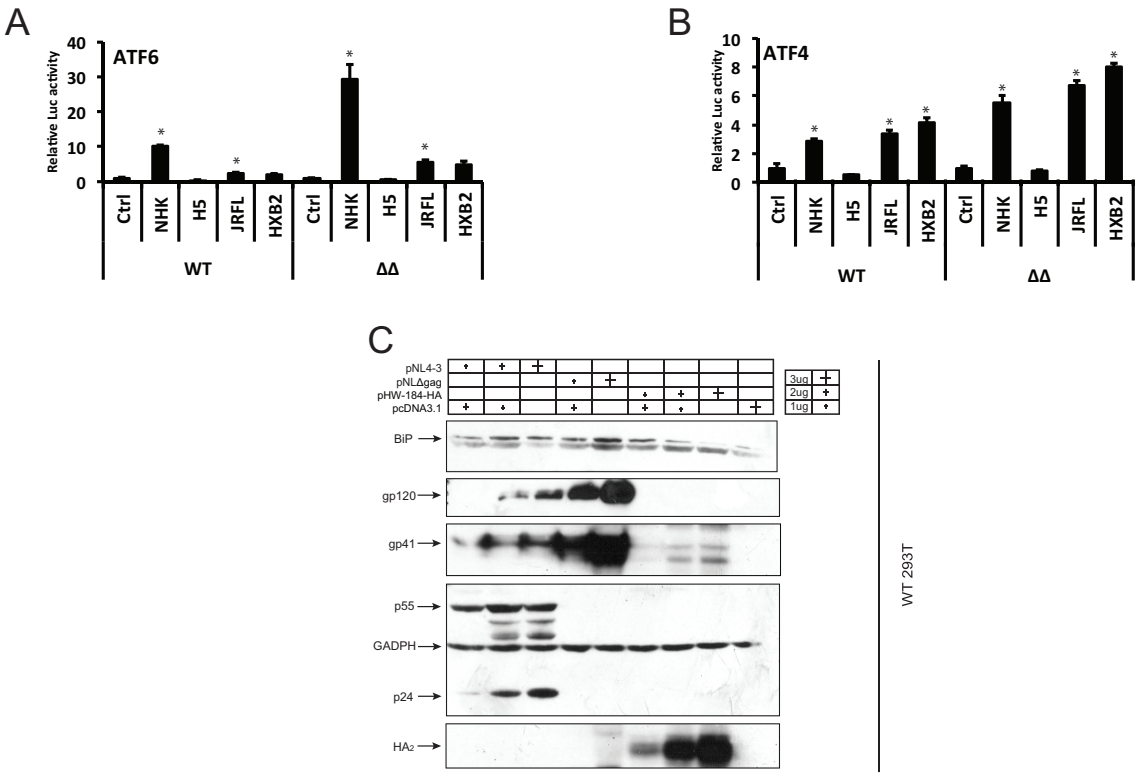

Figure 4.1. HIV-1 envelope glycoprotein expression induces the unfolded protein response in HEK 293T cells. Fold induction of the ATF6 and ATF4 UPR pathways was measured using luciferase reporter constructs co-transfected with envelope expression vectors p5xATF6-GL3 and pATF4-UTR-Fluc, respectively (A and B). Dose dependent transfections of pNL4-3, pNL4-3ΔGag, and VRC-7705 were performed as noted in the figure with pcDNA3.1 empty vector used to fill transfections mixes to 3ug. BiP expression in whole cell lysate was analyzed via Western blotting with the antibodies indicated (C). Values in (A) and (B) are displayed as the mean ± SEM., n=3, unpaired two-tailed *t*-test, *P< 0.05.

Knockout of calnexin and calreticulin does not affect HIV-1 envelope expression or function

Ectopic expression of HIV-1 envelope glycoproteins is not affected in ΔΔ HEK 293T cells and this is reflected when probing whole cell lysate (Fig 4.2A) or cell surface expression (Fig 4.2B). Given the correlation between the release of HIV-1 envelope from calnexin and CD4 binding, particle infectivity of NL4-3 virus produced in the parental or ΔΔ HEK 293T cells was tested and these data reveal that there is no difference in infectivity between the virus produced in the ΔΔ and parental cell background (Fig 4.2C). Notably, the expression of VSV Glycoprotein and HCV E1 are both inhibited in the ΔΔ cellular background, similar to IAV HA and NA (Appendix Fig 1A and 1B).

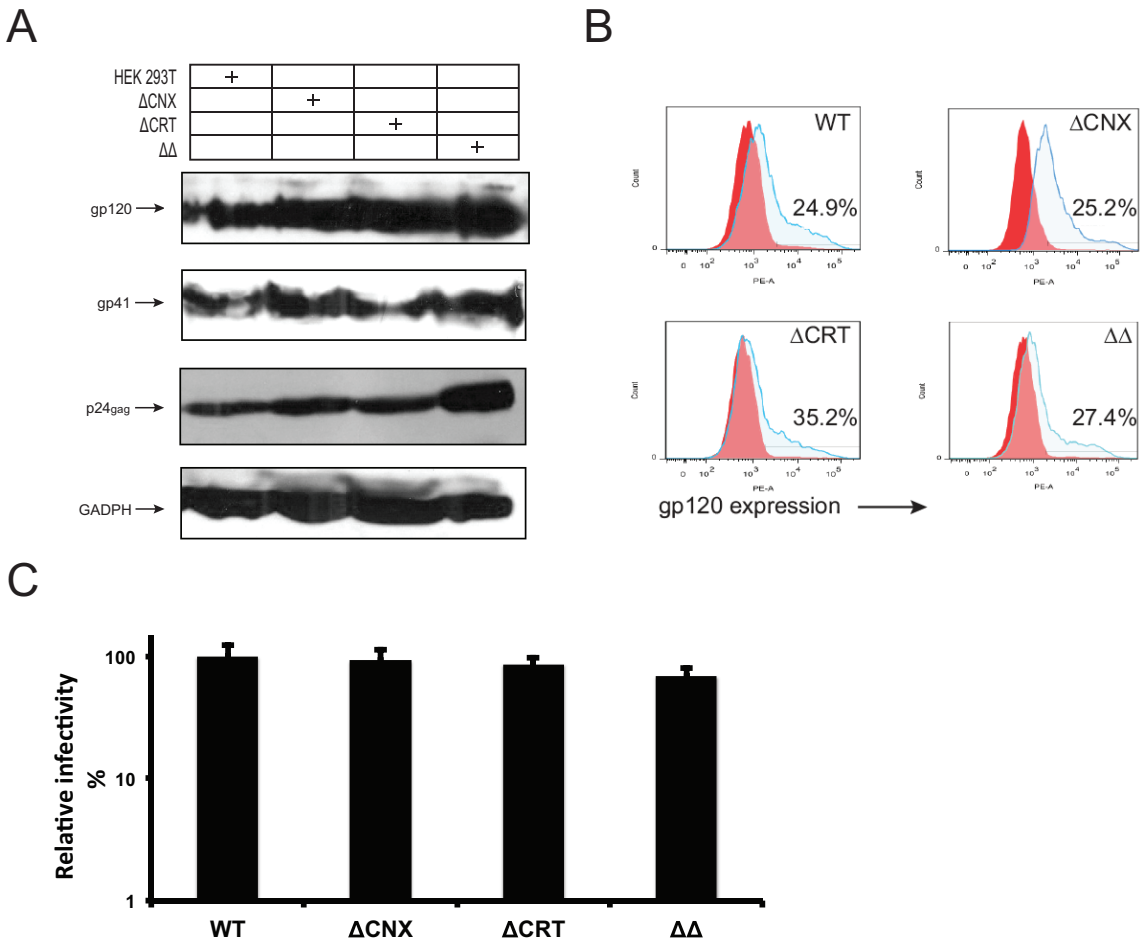

Figure 4.2. Calnexin and calreticulin are not required for HIV-1 envelope glycoprotein folding. Analysis of whole cell lysate (A) or cell surface expression (B) of the HIV-1 envelope glycoprotein after ectopic expression of pNL4-3 in parental HEK 293T, ΔCNX, ΔCRT, or ΔCNXΔCRT knockout cell lines. The $p24^{Gag}$-normalized infectivity of NL4-3 HIV-1 particles collected from cellular supernatants from each cellular background was determined after infection of the HIV-1 luciferase reporter cell line TZM-b1 cells and measurement of the intracellular luciferase activity(C). Values in (C), are displayed as the mean ± SEM., n=3, unpaired two-tailed *t*-test, *P< 0.05.

Class II mannosidases do not affect viral glycoprotein expression

Ectopic expression of Man2A1 or Man2C1 does not affect the expression of HIV-1 envelope glycoproteins, when compared to the previously established activity of ERManI in HEK 293T cell lysate (Fig 4.3A). Dose dependent expression of Man2A1 and Man2C1 did not influence the particle infectivity of HIV-1 NL virus collected from viral supernatants (Fig 4.3B). While Man2C1 appears to have a non-significant decreasing trend in infectivity with higher expression, analysis of whole cell lysates shows that there is no clear trend for envelope expression correlating with Man2C1 expression (Fig 4.3C). There is also no evidence for a MAN2A1 or MAN2C1 effect on IAV HA (Appendix Fig 2B).

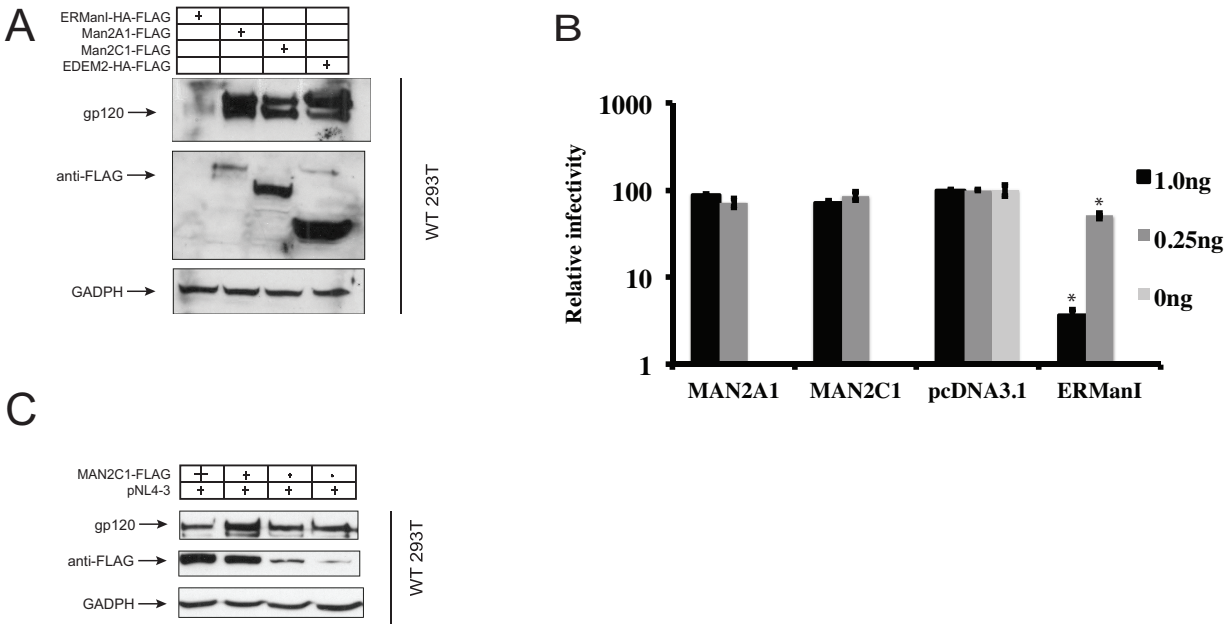

Figure 4.3. Class II mannosidases do not affect HIV-1 envelope expression or viral particle infectivity. Ectopic co-expression of ERManI, Golgi Man2A1, Golgi Man2C1, and EDEM2 with pNL4-3 was performed and whole cell lysates were analyzed using Western blotting with the antibodies indicated (A). Dose-dependent ectopic expression of Man2A1, Man2C1, or empty vector control was performed and viral supernatants were normalized by $p24^{Gag}$ ELISA and analyzed for particle infectivity (B). Whole cell lysates from the dose-dependent transfection of Man2C1 were analyzed using Western blotting with the antibodies indicated (C). Values in (B) are displayed as the mean ± SEM., n=3, unpaired two-tailed *t*-test, *P< 0.05.

Golgi class I α 1,2-mannosidases ManIA and ManIC have potent effects on HIV-1 and IAV envelope glycoprotein expression

Ectopic expression of each class I Golgi mannosidases with the HIV-1 proviral vector (Fig 4.4A) or IAV envelope expression vector VRC-7705 (Fig 4.4C) was performed to assay their influence upon viral envelope expression. Golgi ManIA and ManIC have similar effects on HIV-1 envelope as ERManI (Fig, 4.4A) and have consistent and potent effects on IAV HA (Fig 4.4C). It is notable that the mutation of the conserved glutamic acid residue in the mannosidase homology domain that has previously been successful in abrogating ERManI anti-HIV and anti-IAV envelope activity has no detectable effect in hampering Golgi mannosidase anti-HIV or anti-IAV envelope activity (Fig 4.4B and C). To determine if ERManI is also primarily responsible for envelope degradation associated with ectopic Golgi mannosidase expression, as we have reported regarding EDEM1 and EDEM2 with IAV HA, Figure 4C was repeated in the ERManI KO E7 HEK 293T cell line (Fig 4.4D). There is no detectable abrogation of Golgi ManIA or ManIC activity in the E7 KO cell line. It is notable that the ectopic expression of the Golgi mannosidases ManIA and ManIC influence the expression of HIV-1 structural proteins as evidenced by the difference in $p24^{Gag}$ expression (Fig 4.4B).

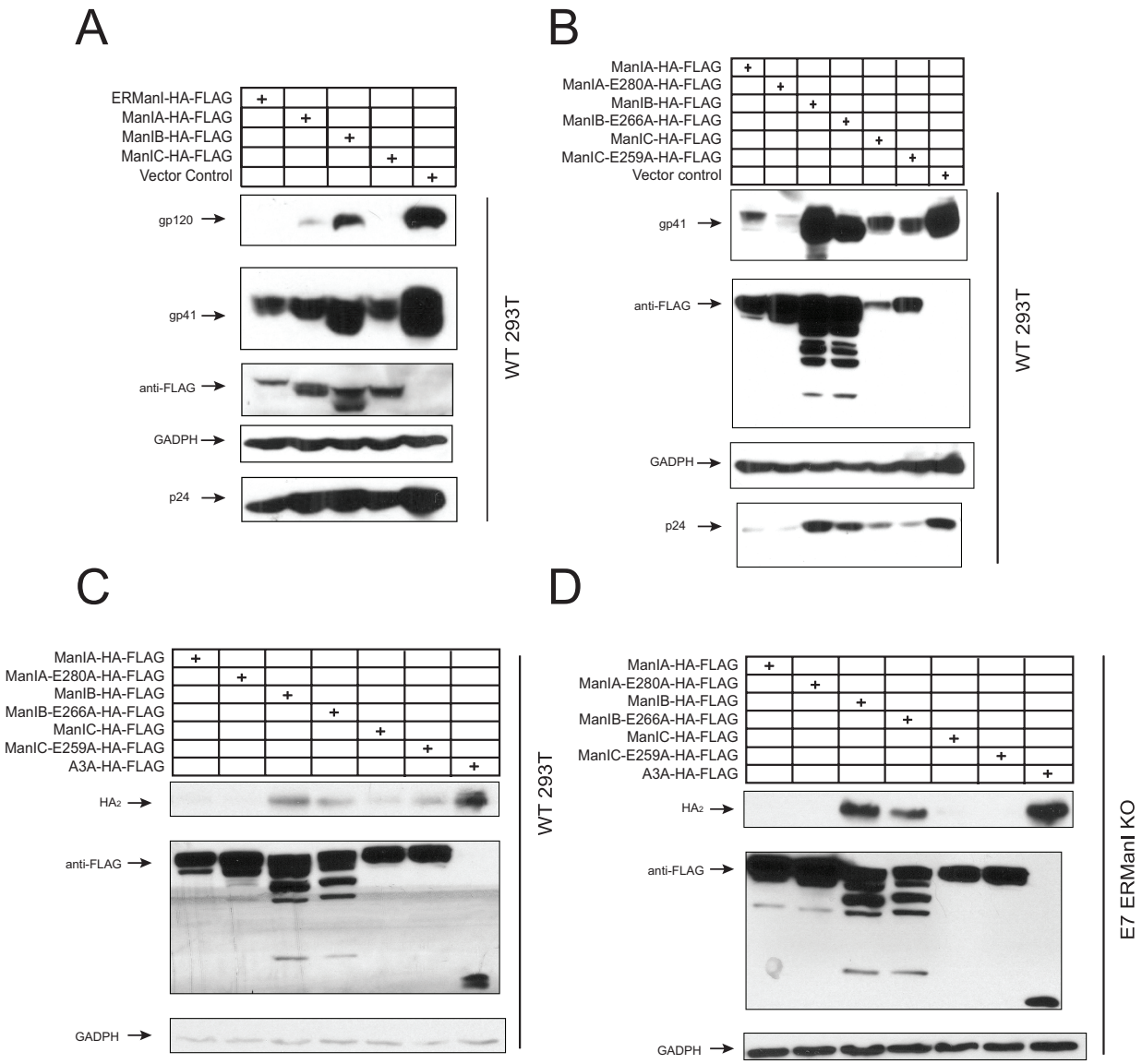

Figure 4.4. Golgi mannosidases, ManIA and ManIC, degrade IAV and HIV-1 viral envelopes using a mechanism that does not require conserved catalytic residues or endogenous ERmanI expression. Ectopic co-expression of pNL4-3 and the Golgi mannosidases ManIA, ManIB, and ManIC (A) and their catalytic site mutants (B) with ERManI as a positive control in HEK 293T cell whole cell lysate analyzed by Western blotting using the indicated antibodies. Ectopic expression of VRC-7705 HA expression plasmid with Golgi mannosidases and their catalytic site mutants in HEK 293T in parental (C) or E7 ERManI KO cells (D) was analyzed via Western blotting using the antibodies indicated.

Expression of Golgi mannosidases decreases the production of viral particles and the expression of structural genes

To determine whether there is a specific interaction between the Golgi mannosidases and IAV envelope hemagglutinin, I performed an immunoprecipitation experiment using an anti-HA_2 antibody ($HA_{2\ is}$ cleaved from HA_0 in the Golgi by the host protease Furin) (A). ERManI, ManIA, and ManIC can be strongly immunoprecipated using the HA_2 antibody, suggesting an interaction. It is notable that EDEM3 is not detected in the HA_2 pull-down, which functions as a better control for the assay's specificity than GFP. To assay the effect of the Golgi mannosidases on general IAV viral infection, I first employed an MLV-GFP packaging vector, which allowed me to pseudotype various viral envelopes onto the MLV backbone and use GFP as an indicator of productive viral infection (B). Using this system Golgi ManIA, ManIB, and ManIC or as or more effective than ERManI and significantly inhibit viral infection (B). Since the MLV-GFP system is not normalized for viral production, I moved to using the proviral vector pNL Luc, which has firefly luciferase replacing the viral Nef gene in order to make IAV HA and NA pseudo-typed HIV-1 NL Luc virions that could be titered using a $p24^{Gag}$ ELISA (C). Using this system I could assay the same virus on MDCK or TZM-bl cells to identify IAV HA (D) or HIV-1 (E) envelope infectivity. Analysis of $p24^{Gag}$ in viral supernatants confirms that ectopic expression of ManIA, ManIC, and their mutants cause a significant production defect (C), which may mean that the significant differences in infection seen using the MLV-GFP vector may not be due to differences in envelope expression (B). After performing a normalized infection of MDCK cells by the pNL Luc pseudo-particles, I found that the Golgi mannosidases had no significant effect on

IAV HA/NA pseudo-viral infectivity (D). ERManI was included as a positive control to confirm the sensitivity of the system, which succeeded with ERManI achieving a statistically significant difference from the control (D). When the aforementioned particles were used to infect TZM-bl cells to test HIV-1 envelope infectivity, a result similar to that found when infecting MDCK cells was achieved, with no significant difference between the Golgi mannosidases and the control treatment (E). Once again, ERManI confirmed the sensitivity of the system by achieving a statistically significant decrease in infectivity.

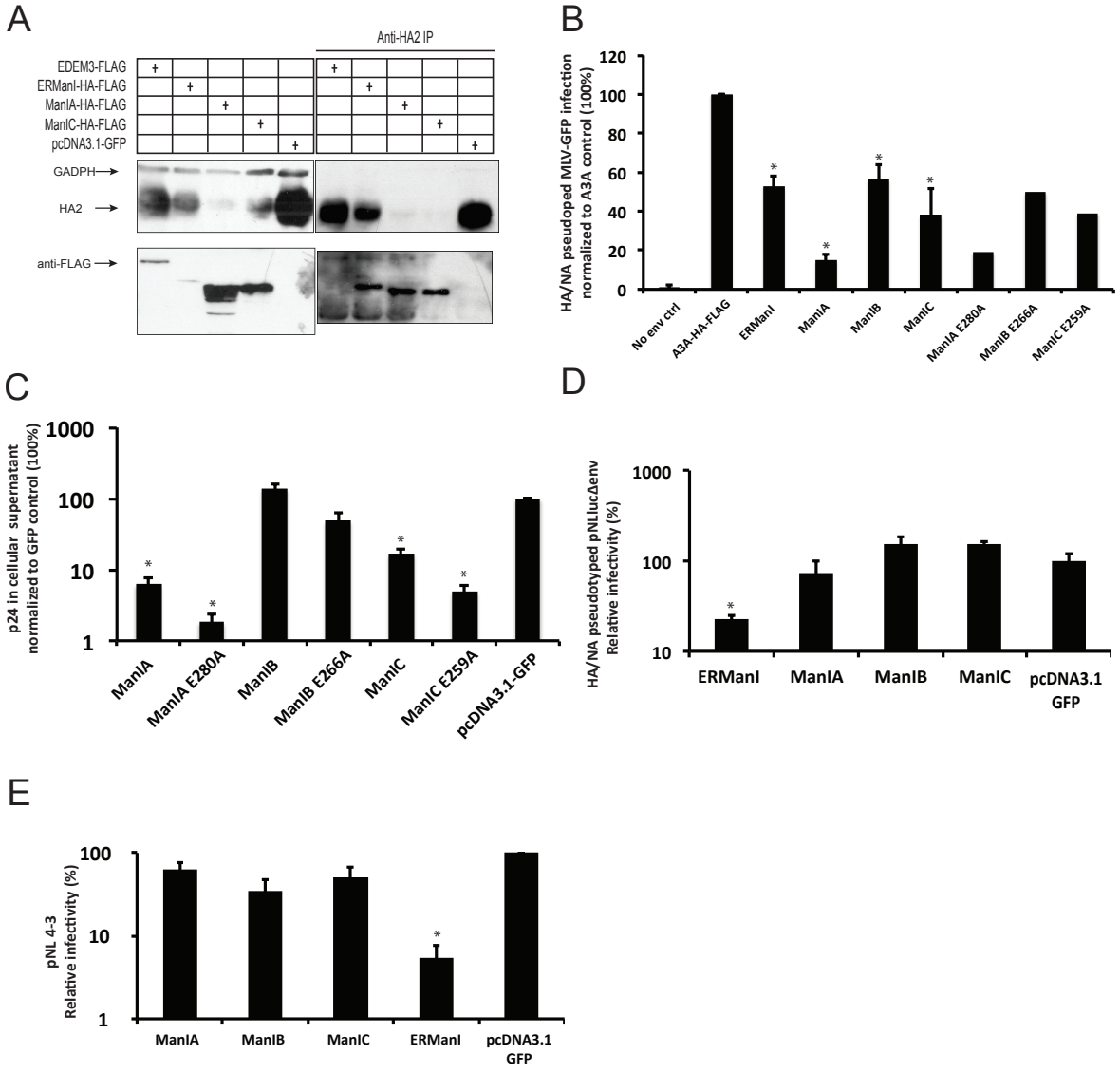

Figure 4.5. Golgi ManIA and ManIC specifically interact with IAV HA, decrease HA pseudovirion % infection and HIV-1 viral production in cellular supernatants, but have no significant effect on HIV-1 NL particle or H5N1 pseudoparticle infectivity after p24^{Gag} normalization. Ectopic expression of EDEM3, ERManI, ManIA, ManIC, and pcDNA3.1-GFP with the HA expression vector VRC 7705-HA in HEK 293T cells was performed and cells were lysed after 24 hours in order to perform protein immune-precipitation using the antibody against HA_2. Input and HA2 immunoprecipitated samples were used to perform a western blot using the antibodies indicated (A). An MLV-GFP packaging system was used to psuedotype MLV particles with IAV HA (VRC 7705) and NA (VRC 7708-NA) envelope glycoproteins. Viral supernatants were used to directly infect MDCK cells and productive infection was measured using flow cytometry (B). p24^{Gag} ELISA was performed on the supernatants collected after transfection of HEK 293T cells with the treatment plasmids indicated and pNL Luc (C). Analysis of p24^{Gag} normalized

Figure 4.5 (cont'd)

infection of MDCK cells by HA (VRC 7705) and NA (VRC 7708-NA) pseudotyped pNL Luc virions produced in backgrounds co-transfected with the plasmids indicated (D). Analysis of of $p24^{Gag}$ normalized infection of TZM-bl cells using pNL Luc virions produced in backgrounds co-transfected with the plasmids indicated. Values in (B), (C), (D), and (E) are displayed as the mean ± SEM., n=3, unpaired two-tailed *t*-test, *P< 0.05. Y-axes in (B) and (D) represent % change compared to pcDNA3.1-A3A-HA-FLAG as a control set at 100%, while the Y-axes in (C) and (E) represent % change compared to pcDNA3.1-GFP as a control set at 100%. n=1 for the Golgi mannosidase mutants ManIAE280A, ManIBE266A, and ManIC259A in (B), which are included to show that the mutations fall within the variance of the wild-type proteins.

Discussion

Given the work completed using the ER-localized class I α 1,2-mannosidases (chapters 2 and 3) and the disparate activities of the EDEM1 and EDEM2 mannosidases upon HIV-1 and IAV HA envelope glycoproteins, I chose to investigate if further differences could be observed between the HIV-1 and IAV HA envelopes. As I had already identified the potent effects of the calnexin and calreticulin knockout cell lines on IAV HA and NA folding, it was prudent to test HIV-1 envelope folding in these cell lines to determine if there may be another avenue to characterize their differences. The resistance of HIV-1 envelope to the knockout of calnexin and calreticulin is notable because the current models of HIV-1 folding currently provide no explanation for this phenomenon. Additionally, I have tested HCV and VSV-G envelope expression in the ΔCNXΔCRT cell line and each has a similar phenotype to IAV HA (Appendix Fig 1A and 1B), which is notable because representatives of all three classes of viral envelope glycoproteins (Chapter 1) have requirements for CNX and CRT. It is of note that my research indicates that HIV-1 and IAV HA activate different UPR pathways; IAV activates IRE1, while HIV-1 envelope activates PERK and ATF6. One explanation for this may be the specific binding of misfolded HA to IRE1 vs HIV-1 interacting with the chaperone BiP as a client since it has been reported to take longer to fold than other viral glycoproteins (211). This extended folding may prolong the client status with BiP, which could, in turn, preferentially activate PERK and ATF6 through the titration of BiP away from these sensors. For this to be true it is important for the activation of IRE1 through direct binding of misfolded proteins to be more stimulating than the titration of BiP away from IRE1 (31).

The similar effects of the Golgi mannosidases ManIA and ManIC on both HIV-1 and IAV HA envelope glycoproteins may point to a different mechanism of degradation from the ER mannosidases. In fact, my experiments using HCV glycoproteins E1 and E2 and EIAV gp90 have had similar results concerning ManIA and ManIC degradation (Appendix Fig 1C and D). The statistically significant effects that ManIA and ManIC have on HIV-1 $p24^{gag}$ expression in whole cell lysate and viral supernatants is interesting given the non-significant effect of ManIB, which shares the same expression vector and is homologous to ManIA and ManIC. The lack of a discernable phenotype when the conserved glutamic acid residue in the mannosidase homology domain was removed from the Golgi mannosidases may suggest that a pathway other than ERAD may be involved in the degradation phenotype of ManIA and ManIC.

Materials and Methods

Chemicals and antibodies

The anti-FLAG antibody was purchased from Sigma. A goat anti-actin polyclonal was purchased from Santa Cruz Biotechnology; a mouse monoclonal anti-glyceraldehyde-3-phosphate dehydrogenase (GAPDH) was purchased from Meridian Life Science. Horseradish peroxidase (HRP)-conjugated human, rabbit, goat, horse, or mouse immunoglobulin G secondary antibodies were purchased from Pierce. HIV-1 proteins were detected by antibodies from the NIH AIDS Research and Reference Reagent Program, and their catalogue numbers are 526 (HIV-1 gp41), 521 (HIV-1 gp120), and 12033 (VRC01). Mouse anti-HA_2, was purchased from Bei Resources (NR-44222).

Cell lines

Human embryonic kidney cells 293 carrying the SV40 T antigen (293T) and Madin-Darby Canine Kidney (MDCK) epithelial cells were cultured in DMEM with 10% bovine calf serum (BCS), which was purchased from HyClone. 293T CNX/CRT single and double-KO cells were described previously (14). The infection was also confirmed with fluorescent microscopy to test GFP expression. The TZM-bl cell line was purchased from the NIH aids reagent program.

Plasmids

pCMV6-Entry vectors expressing human EDEM1, EDEM2, EDEM3, and pcDNA3.1 expression vectors for human APOBEC3A (A3A) and ERManI have been previously described (17). The pcDNA3.1 expression vectors for MAN1A1

(pcDNA3.1-Man1A-HA-FLAG), MAN1A2 (pcDNA3.1-Man1B-HA-FLAG), and MAN1C1 (pcDNA3.1-Man1C-HA-FLAG) were cloned from the cDNA of pCMV6-Entry plasmids purchased from origene into the backbone of pcDNA3.1-A3G-HA-FLAG after Kpn1 and Not1 (Man1A) or HindIII and NotI (Man1B, Man1C) restriction enzyme digestion. Golgi mannosidase mutants, pcDNA3.1-MAN1A1-E280A-HA-FLAG, pcDNA3.1-MAN1A2-E266A-HA-FLAG, pcDNA3.1-Man1C-E259A-HA-FLAG were generated using the Quickchange II Site-Directed Mutagenesis kit (agilent). MAN2A1 and MAN2C1 pCMV6-entry expression vectors were purchased from origene. Entry Plasmids expressing IAV (A/Thailand/1(KAN-1)/2004(H5N1) strain) HA (7705) and NA (7708) were provided by Gary Nabel. PHW184-HA was provided by Robert G. Webster (20). The HIV-1 proviral vector pNL4-3 and pNL4-3Δgag were obtained from the NIH AIDS Research and Reference Reagent Program. The ATF4(PERK)-expression reporter construct pATF4-UTR-Fluc was obtained from Dong-Yan Jin (the University of Hong Kong)(199); the ATF6-activation reporter construct p5xATF6-GL3 was obtained from Ron Prywes (Columbia University) through Addgene. The plasmid pNL Luc has been described before(212). The plasmid pCgp has been described before (213).

Transfection

Polyethylenimine (PEI) stock solution (1 mg/ml) was prepared by dissolving 500 mg PEI (Polysciences) into 500 ml sterilized water after adjusting pH to 4.5 with HCl and filtering the solution through a 0.22 μM membrane. To produce HA (VRC-7705) and NA (VRC 7708) pseudotyped pNL Luc HIV-1 co-expressed with various mannosidase proteins, $1x10^6$ 293T

cells were seeded in each well of a 6-well culture plate 16 hr before transfection. 3 μg total DNA was diluted into 200 μl serum-free DMEM medium, and mixed with 9 μg PEI. After 15 minutes of incubation at room temperature, these transfection reagents were added directly into the supernatant of each well. Media were replaced after 6 hr and cell lysate collected at 48 hr unless otherwise noted. Viruses were collected from the supernatants and viral production was measured by $p24^{Gag}$ ELISA; protein expression was directly determined by western blotting.

Analysis of HA-pseudotyped HIV-1 infectivity

Viral particles were produced from 293T cells co-transfected with pNL Luc, HA expression vector 7705, and NA expression vector 7708. Particles were normalized by $p24^{Gag}$ ELISA, and equal amounts of viruses were used to infect MDCK or TZM-bl cells. After 36 hours, cells were lysed, and viral infectivity was determined by measuring the cellular luciferase activity using the firefly luciferase reporter assay kit from Promega

Analysis of HIV-1 Infectivity

HIV-1 particles were produced from 293T cells after transfection with pNL4-3 and a mannosidase expression vector or vector control. After normalization by $p24^{Gag}$ ELISA, equal amounts of viruses were used to infect TZM-b1 cells. After 36 hours, cells were lysed, and viral infectivity was determined by measuring the cellular luciferase activity using the firefly luciferase reporter assay kit from Promega.

Analysis of HA-pseudotyped MLV infection

MLV particles were produced from 293T cells after transfection with pCgp and pCMV-GFP-MLV, VRC-7705 HA and VRC-7708 NA, and mannosidase expression vector or vector control. Viral supernatants were collected at 24 hours and used to infect MDCK cells. After 24 hours, positive GFP signal in target cells was measured using flow cytometry.

Cell surface staining

HIV-1 envelope cell surface staining was performed using the VRC01 antibody before cellular fixation with 2% formaldehyde. Fixed cells were washed with phosphate buffered saline and used to perform flow cytometry analysis.

Statistics

Statistical tests were performed using Microsoft Excel. Significance of differences between samples was assessed using an unpaired two-tailed students t-test. Variance was estimated by calculating the standard deviation (SD) or the standard error of the mean (SEM) in each group, as indicated in figure legends, and represented by error bars. Unless specified in the legend, all experiments were performed independently at least three times and ‘n’ indicates biological replicates, with a representative experiment being shown.

Acknowledgments

I would like to thank Dr. Tao Zhou for his help in cloning the Golgi mannosidases MAN1A1 and MAN1C1 into the pcDNA3.1-A3G-HA-FLAG plasmid backbone, and performing the site-directed mutagenesis on Golgi MAN1A1, MAN1A2, and MAN1C1, and his general

assistance and mentorship with the HIV-1 viral techniques. I would also like to thank Dr. Yong-Hui Zheng for his mentorship during this work.

CHAPTER 5 – Concluding remarks

The role of host quality control mechanisms in the endoplasmic reticulum is a neglected area of research that has an overabundance of data involving protein binding and little concerning the consequences of such. In this work, I have implicated class I α 1,2-mannosidases in the degradation of viral proteins that require the ER luminal chaperons calnexin and calreticulin for optimal protein folding (Chapters 3 and 4). This research has also identified a knowledge gap in the area of HIV-1 envelope folding, due to the insensitivity of the HIV-1 envelope glycoproteins to the knockout of calnexin and calreticulin, which would not be predicted by the current literature (205).

I can devise two models for the factors that would account for the HIV-1 resistance to the knockout of calnexin and calreticulin: First, another chaperone may have a redundant effect that compensates for the loss of calnexin and calreticulin; and second, the folding time required for each protein may be different, which will have consequences on the interactions with host quality control. To support this first model, there is another chaperone, malectin, which binds after glucosidase I cleaves the first glucose off of a client protein's N-glycans, which is before CNX and CRT binding. Therefore, investigations into malectin could help to elucidate the molecular determinants of HIV-1 envelope folding in the endoplasmic reticulum. To support the second model, there is research that supports the folding half-life for Influenza HA to be 3 minutes (214), while the similar metric for HIV-1 has been reported as 15-30 minutes (137, 215). This difference in folding time may account for the sensitivity of influenza and other viral glycoproteins such as HCV E1 and E2 and VSV Glycoprotein to the knockout of calnexin and calreticulin (Appendix Fig 1A and 1B). Corroborating this, HIV-1

leader peptides are not cleaved until a native protein conformation is reached at around 30 minutes (211) and swapping the HIV-1 gp160 signal sequence with that from influenza A hemagluttinin allows for immediate signal sequence cleavage (216). Given these findings, the calnexin and calreticulin knockout cell line may be a useful tool for determining a given viral glycoprotein's folding strategy to be used inside host cells. HIV-1 particles also contain many fewer envelope trimers per virion when compared to most other virus and even other retroviruses (Chapter 1). Therefore, this HIV-1 calnexin/calreticulin independence phenotype may be indicative of the overall viral replication and envelope packaging strategy. To build on these observations, my other work has identified differences in the activation of the unfolded protein response sensors during ectopic expression of HIV-1 and Influenza A viral glycoproteins. In my hand, expression of the Influenza envelope glycoprotein HA activates IRE1, while expression of the HIV-1 envelope activates the PERK and ATF6 pathways (Figs 3.2, 4.3).

Given my thoughts on the differences between the folding strategies undertaken by HIV-1 and Influenza A virus envelope glycoproteins in the endoplasmic reticulum, it is of interest that the empirical differences that I have noted have applied only to host interactions in the endoplasmic reticulum and not the golgi (Chapter 4). While the manipulation of Golgi mannosidase expression has potent effects on viral envelope glycoprotein expression (Fig 4.4), there is a similar effect for both HIV-1 and IAV envelopes. And although no measurable effect was observed for the class II mannosidases, it's still a consistent null effect for HIV-1 and IAV envelopes. This is consistent with the role of mannose trimming

enzymes in the Golgi apparatus as part of the remodeling process into complex glyans instead of the degradation signal in the endoplasmic reticulum.

The mannose trimming role of class I α 1,2- mannosidases upon viral glycoproteins is also controversial based on my investigations (Chapter 3). While the active site of ERManI is needed for envelope degradation to be observed in HIV-1 and IAV envelopes (chapters 2 and 3), the EDEM proteins appear to have redundant trimming activity that is only necessary in an ERManI knockout background (Fig 3.5). Additionally, the catalytic sites of the Golgi localized class I α 1,2-mannosidases, ManIA, ManIB, and ManIC, were not required for their inhibition of envelope expression in parental or ERManI knockout backgrounds (Fig 4.4). These results may suggest that the envelope degradation by the Golgi mannosidases may be through a mechanism other than ERAD, which may also explain their inhibition of HIV-1 capsid expression.

Investigations into viral envelope protein folding in the endoplasmic reticulum are useful in both further elucidating the roles of host proteins and determining the strategies that viruses use to exploit or capitalize on them. Without a more thorough understanding of ERAD, it is not possible to determine if the specific interactions between quality control machinery and viral envelope proteins are a matter of host defense or viral adaptation and optimization to a specific envelope production strategy. Thus, this field remains an important area of research, especially considering that understanding of ERAD may be crucial in tailoring viral envelope expression and glycosylation of viral envelope glycoproteins in future prophylactic endeavors.

APPENDIX

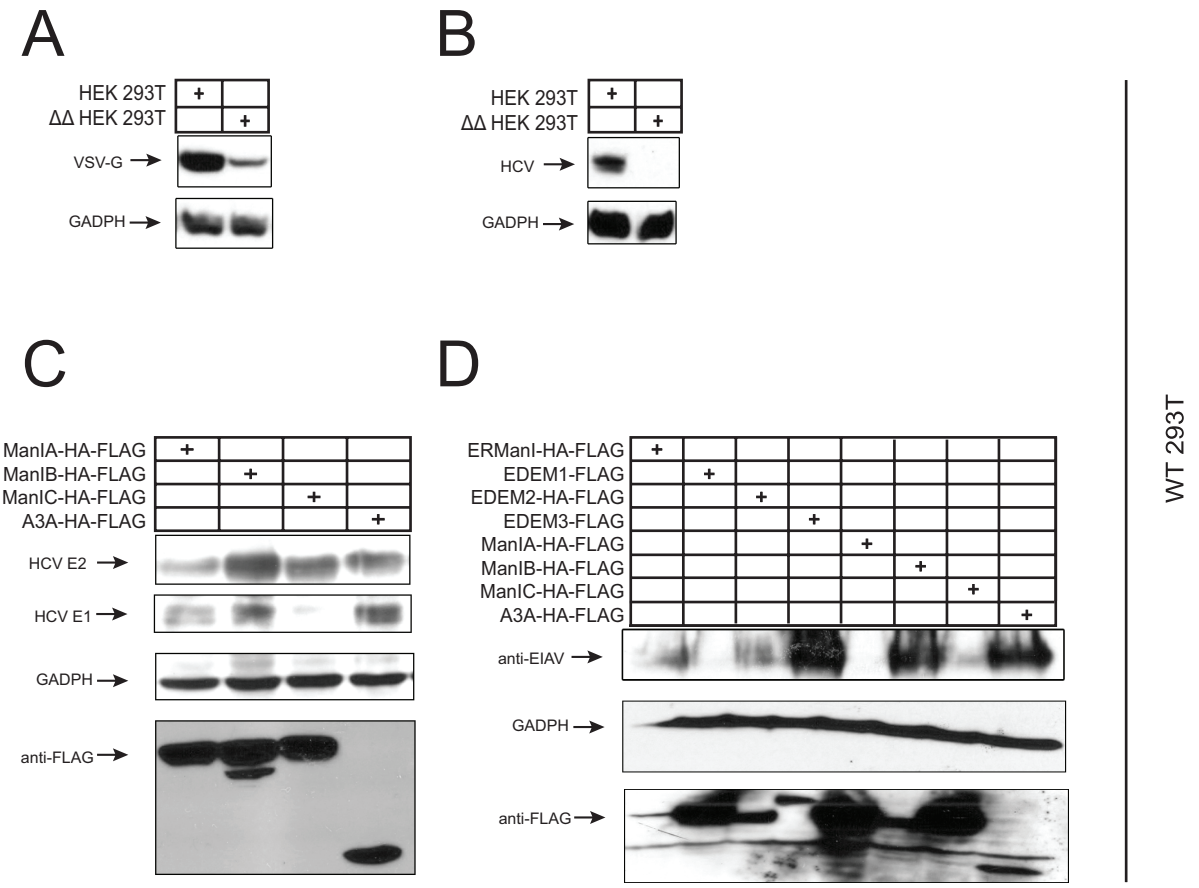

Appendix Figure 1. **ΔΔ HEK 293T cell line phenotype concerning VSV-G and HCV E1 envelope expression; ManIA, ManIB, and ManIC effects on HCV and EIAV glycoproteins.** VSV-G (pVSV-G) and HCV (HCVenv) envelope expression vectors were used to assay the expression of each glycoprotein in parental and ΔΔ HEK 293T cells (A and B). Golgi mannosidases ManIA, ManIB, and ManIC were co-expressed with the HCV or EIAV envelope glycoproteins and their activity against each evelope was determined via Western blotting (C and D). Antibodies against HCV E1 and E2 or anti EIAV sera was used to determine envelope glycoprotein expression. The band from the anti-EIAV is the correct size for the EIAV glycoprotein gp90 (90kd).

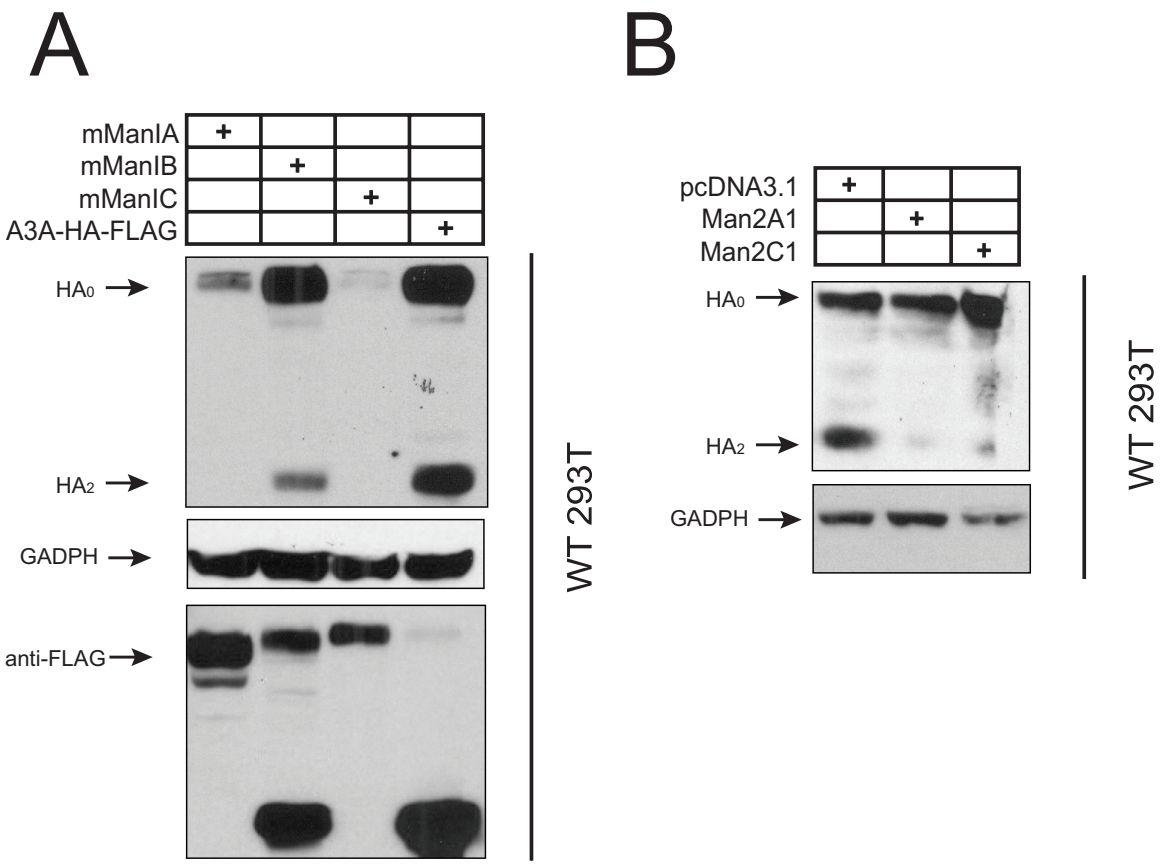

Appendix Figure 2. Anti IAV HA envelope expression effects of the Murine Golgi mannosidases mManIA, mManIB, and mManIC and Human class II α-mannosidases Man2A1 and Man2C1. The murine homologues of the Golgi class I α 1,2-mannosidases were ectopically expressed in HEK 293T cell with pcDNA3.1-A3A-HA-FLAG as a transfection control (A). Ectopic expression of Man2A1 and Man2C1 was also performed with pcDNA3.1 vector as a transfection control (B).

REFERENCES

REFERENCES

1. **(ed).** 2013. Fields virology. Wolters Kluwer/Lippincott Williams & Wilkins Health,, Philadelphia, PA.

2. **Dimitrov DS.** 2004. Virus entry: molecular mechanisms and biomedical applications. Nat Rev Microbiol **2:**109-122.

3. **Grove J, Marsh M.** 2011. The cell biology of receptor-mediated virus entry. J Cell Biol **195:**1071-1082.

4. **McDonald D, Wu L, Bohks SM, KewalRamani VN, Unutmaz D, Hope TJ.** 2003. Recruitment of HIV and its receptors to dendritic cell-T cell junctions. Science **300:**1295-1297.

5. **Tsai B.** 2007. Penetration of nonenveloped viruses into the cytoplasm. Annu Rev Cell Dev Biol **23:**23-43.

6. **Podbilewicz B.** 2014. Virus and cell fusion mechanisms. Annu Rev Cell Dev Biol **30:**111-139.

7. **Lee E, Leang SK, Davidson A, Lobigs M.** 2010. Both E protein glycans adversely affect dengue virus infectivity but are beneficial for virion release. J Virol **84:**5171-5180.

8. **Wang W, Nie J, Prochnow C, Truong C, Jia Z, Wang S, Chen XS, Wang Y.** 2013. A systematic study of the N-glycosylation sites of HIV-1 envelope protein on infectivity and antibody-mediated neutralization. Retrovirology **10:**14.

9. **Tate MD, Job ER, Deng YM, Gunalan V, Maurer-Stroh S, Reading PC.** 2014. Playing hide and seek: how glycosylation of the influenza virus hemagglutinin can modulate the immune response to infection. Viruses **6:**1294-1316.

10. **Helle F, Duverlie G, Dubuisson J.** 2011. The hepatitis C virus glycan shield and evasion of the humoral immune response. Viruses **3:**1909-1932.

11. **Lennemann NJ, Rhein BA, Ndungo E, Chandran K, Qiu X, Maury W.** 2014. Comprehensive functional analysis of N-linked glycans on Ebola virus GP1. MBio **5:**e00862-00813.

12. **Zhang M, Gaschen B, Blay W, Foley B, Haigwood N, Kuiken C, Korber B.** 2004. Tracking global patterns of N-linked glycosylation site variation in highly variable viral glycoproteins: HIV, SIV, and HCV envelopes and influenza hemagglutinin. Glycobiology **14:**1229-1246.

13. **Deshpande KL, Fried VA, Ando M, Webster RG.** 1987. Glycosylation affects cleavage of an H5N2 influenza virus hemagglutinin and regulates virulence. Proc Natl Acad Sci U S A **84:**36-40.

14. **Klenk HD, Wagner R, Heuer D, Wolff T.** 2002. Importance of hemagglutinin glycosylation for the biological functions of influenza virus. Virus Res **82:**73-75.

15. **Wagner R, Wolff T, Herwig A, Pleschka S, Klenk HD.** 2000. Interdependence of hemagglutinin glycosylation and neuraminidase as regulators of influenza virus growth: a study by reverse genetics. J Virol **74:**6316-6323.

16. **Doores KJ.** 2015. The HIV glycan shield as a target for broadly neutralizing antibodies. FEBS J **282:**4679-4691.

17. **Vigerust DJ, Shepherd VL.** 2007. Virus glycosylation: role in virulence and immune interactions. Trends Microbiol **15:**211-218.

18. **Moremen KW, Tiemeyer M, Nairn AV.** 2012. Vertebrate protein glycosylation: diversity, synthesis and function. Nature Reviews Molecular Cell Biology **13:**448-462.

19. **Helenius A, Aebi M.** 2004. Roles of N-linked glycans in the endoplasmic reticulum. Annual Review of Biochemistry **73:**1019-1049.

20. **Lamriben L, Graham JB, Adams BM, Hebert DN.** 2016. N-Glycan-based ER Molecular Chaperone and Protein Quality Control System: The Calnexin Binding Cycle. Traffic **17:**308-326.

21. **Schallus T, Jaeckh C, Feher K, Palma AS, Liu Y, Simpson JC, Mackeen M, Stier G, Gibson TJ, Feizi T, Pieler T, Muhle-Goll C.** 2008. Malectin: a novel carbohydrate-binding protein of the endoplasmic reticulum and a candidate player in the early steps of protein N-glycosylation. Mol Biol Cell **19:**3404-3414.

22. **Slominska-Wojewodzka M, Sandvig K.** 2015. The Role of Lectin-Carbohydrate Interactions in the Regulation of ER-Associated Protein Degradation. Molecules **20:**9816-9846.

23. **Meusser B, Hirsch C, Jarosch E, Sommer T.** 2005. ERAD: the long road to destruction. Nat Cell Biol **7:**766-772.

24. **Benyair R, Ogen-Shtern N, Mazkereth N, Shai B, Ehrlich M, Lederkremer GZ.** 2015. Mammalian ER mannosidase I resides in quality control vesicles, where it encounters its glycoprotein substrates. Mol Biol Cell **26:**172-184.

25. **Herscovics A, Romero PA, Tremblay LO.** 2002. The specificity of the yeast and human class I ER alpha 1,2-mannosidases involved in ER quality control is not as strict previously reported. Glycobiology **12:**14G-15G.

26. **Frenkel Z, Gregory W, Kornfeld S, Lederkremer GZ.** 2003. Endoplasmic reticulum-associated degradation of mammalian glycoproteins involves sugar chain trimming to Man6-5GlcNAc2. J Biol Chem **278:**34119-34124.

27. **Hetz C, Martinon F, Rodriguez D, Glimcher LH.** 2011. The unfolded protein response: integrating stress signals through the stress sensor IRE1alpha. Physiol Rev **91:**1219-1243.

28. **Gardner BM, Pincus D, Gotthardt K, Gallagher CM, Walter P.** 2013. Endoplasmic reticulum stress sensing in the unfolded protein response. Cold Spring Harb Perspect Biol **5:**a013169.

29. **Bertolotti A, Zhang Y, Hendershot LM, Harding HP, Ron D.** 2000. Dynamic interaction of BiP and ER stress transducers in the unfolded-protein response. Nat Cell Biol **2:**326-332.

30. **Walter P, Ron D.** 2011. The unfolded protein response: from stress pathway to homeostatic regulation. Science **334:**1081-1086.

31. **Gardner BM, Walter P.** 2011. Unfolded proteins are Ire1-activating ligands that directly induce the unfolded protein response. Science **333:**1891-1894.

32. **Han J, Back SH, Hur J, Lin YH, Gildersleeve R, Shan J, Yuan CL, Krokowski D, Wang S, Hatzoglou M, Kilberg MS, Sartor MA, Kaufman RJ.** 2013. ER-stress-induced transcriptional regulation increases protein synthesis leading to cell death. Nat Cell Biol **15:**481-490.

33. **Romisch K.** 2005. Endoplasmic reticulum-associated degradation. Annu Rev Cell Dev Biol **21:**435-456.

34. **Lemus L, Goder V.** 2014. Regulation of Endoplasmic Reticulum-Associated Protein Degradation (ERAD) by Ubiquitin. Cells **3:**824-847.

35. **Needham PG, Brodsky JL.** 2013. How early studies on secreted and membrane protein quality control gave rise to the ER associated degradation (ERAD) pathway: the early history of ERAD. Biochim Biophys Acta **1833:**2447-2457.

36. **Foresti O, Ruggiano A, Hannibal-Bach HK, Ejsing CS, Carvalho P.** 2013. Sterol homeostasis requires regulated degradation of squalene monooxygenase by the ubiquitin ligase Doa10/Teb4. Elife **2:**e00953.

37. **Wojcikiewicz RJ, Pearce MM, Sliter DA, Wang Y.** 2009. When worlds collide: IP(3) receptors and the ERAD pathway. Cell Calcium **46:**147-153.

38. **Choi K, Kim H, Kang H, Lee SY, Lee SJ, Back SH, Lee SH, Kim MS, Lee JE, Park JY, Kim J, Kim S, Song JH, Choi Y, Lee S, Lee HJ, Kim JH, Cho S.** 2014. Regulation of diacylglycerol acyltransferase 2 protein stability by gp78-associated endoplasmic-reticulum-associated degradation. FEBS J **281:**3048-3060.

39. **Lin PH, Chiang MT, Chau LY.** 2008. Ubiquitin-proteasome system mediates heme oxygenase-1 degradation through endoplasmic reticulum-associated degradation pathway. Biochim Biophys Acta **1783:**1826-1834.

40. **Vij N, Fang S, Zeitlin PL.** 2006. Selective inhibition of endoplasmic reticulum-associated degradation rescues DeltaF508-cystic fibrosis transmembrane regulator and suppresses interleukin-8 levels: therapeutic implications. J Biol Chem **281:**17369-17378.

41. **Guerriero CJ, Brodsky JL.** 2012. The delicate balance between secreted protein folding and endoplasmic reticulum-associated degradation in human physiology. Physiol Rev **92:**537-576.

42. **Hebert DN, Molinari M.** 2012. Flagging and docking: dual roles for N-glycans in protein quality control and cellular proteostasis. Trends in Biochemical Sciences **37:**404-410.

43. **Mast SW, Moremen KW.** 2006. Family 47 alpha-mannosidases in N-glycan processing. Glycobiology **415:**31-46.

44. **Ninagawa S, Okada T, Sumitomo Y, Kamiya Y, Kato K, Horimoto S, Ishikawa T, Takeda S, Sakuma T, Yamamoto T, Mori K.** 2014. EDEM2 initiates mammalian glycoprotein ERAD by catalyzing the first mannose trimming step. J Cell Biol **206:**347-356.

45. **Hirao K, Natsuka Y, Tamura T, Wada I, Morito D, Natsuka S, Romero P, Sleno B, Tremblay LO, Herscovics A, Nagata K, Hosokawa N.** 2006. EDEM3, a soluble EDEM homolog, enhances glycoprotein endoplasmic reticulum-associated degradation and mannose trimming. Journal of Biological Chemistry **281:**9650-9658.

46. **Aikawa J, Matsuo I, Ito Y.** 2012. In vitro mannose trimming property of human ER alpha-1,2 mannosidase I. Glycoconj J **29:**35-45.

47. **Hauri HP, Kappeler F, Andersson H, Appenzeller C.** 2000. ERGIC-53 and traffic in the secretory pathway. J Cell Sci **113 (Pt 4):**587-596.

48. **Avezov E, Frenkel Z, Ehrlich M, Herscovics A, Lederkremer GZ.** 2008. Endoplasmic reticulum (ER) mannosidase I is compartmentalized and required for N-glycan trimming to Man5-6GlcNAc2 in glycoprotein ER-associated degradation. Mol Biol Cell **19:**216-225.

49. **Hosokawa N, You Z, Tremblay LO, Nagata K, Herscovics A.** 2007. Stimulation of ERAD of misfolded null Hong Kong alpha1-antitrypsin by Golgi alpha1,2-mannosidases. Biochem Biophys Res Commun **362:**626-632.

50. **Ogen-Shtern N, Avezov E, Shenkman M, Benyair R, Lederkremer GZ.** 2016. Mannosidase IA is in Quality Control Vesicles and Participates in Glycoprotein Targeting to ERAD. J Mol Biol doi:10.1016/j.jmb.2016.04.020.

51. **Olivari S, Cali T, Salo KE, Paganetti P, Ruddock LW, Molinari M.** 2006. EDEM1 regulates ER-associated degradation by accelerating de-mannosylation of folding-defective polypeptides and by inhibiting their covalent aggregation. Biochem Biophys Res Commun **349:**1278-1284.

52. **Olivari S, Molinari M.** 2007. Glycoprotein folding and the role of EDEM1, EDEM2 and EDEM3 in degradation of folding-defective glycoproteins. FEBS Lett **581:**3658-3664.

53. **Christianson JC, Shaler TA, Tyler RE, Kopito RR.** 2008. OS-9 and GRP94 deliver mutant alpha1-antitrypsin to the Hrd1-SEL1L ubiquitin ligase complex for ERAD. Nat Cell Biol **10:**272-282.

54. **Munro S.** 2001. The MRH domain suggests a shared ancestry for the mannose 6-phosphate receptors and other N-glycan-recognising proteins. Curr Biol **11:**R499-501.

55. **Garza RM, Sato BK, Hampton RY.** 2009. In vitro analysis of Hrd1p-mediated retrotranslocation of its multispanning membrane substrate 3-hydroxy-3-methylglutaryl (HMG)-CoA reductase. J Biol Chem **284:**14710-14722.

56. **Suzuki M, Otsuka T, Ohsaki Y, Cheng J, Taniguchi T, Hashimoto H, Taniguchi H, Fujimoto T.** 2012. Derlin-1 and UBXD8 are engaged in dislocation and degradation of lipidated ApoB-100 at lipid droplets. Mol Biol Cell **23:**800-810.

57. **Pfeffer S, Burbaum L, Unverdorben P, Pech M, Chen Y, Zimmermann R, Beckmann R, Forster F.** 2015. Structure of the native Sec61 protein-conducting channel. Nat Commun **6:**8403.

58. **Kaiser ML, Romisch K.** 2015. Proteasome 19S RP binding to the Sec61 channel plays a key role in ERAD. PLoS One **10:**e0117260.

59. **Lilley BN, Ploegh HL.** 2004. A membrane protein required for dislocation of misfolded proteins from the ER. Nature **429:**834-840.

60. **Ye Y, Shibata Y, Yun C, Ron D, Rapoport TA.** 2004. A membrane protein complex mediates retro-translocation from the ER lumen into the cytosol. Nature **429:**841-847.

61. **Greenblatt EJ, Olzmann JA, Kopito RR.** 2011. Derlin-1 is a rhomboid pseudoprotease required for the dislocation of mutant alpha-1 antitrypsin from the endoplasmic reticulum. Nat Struct Mol Biol **18:**1147-1152.

62. **Claessen JH, Kundrat L, Ploegh HL.** 2012. Protein quality control in the ER: balancing the ubiquitin checkbook. Trends Cell Biol **22:**22-32.

63. **Hirsch C, Gauss R, Horn SC, Neuber O, Sommer T.** 2009. The ubiquitylation machinery of the endoplasmic reticulum. Nature **458:**453-460.

64. **Hampton RY, Gardner RG, Rine J.** 1996. Role of 26S proteasome and HRD genes in the degradation of 3-hydroxy-3-methylglutaryl-CoA reductase, an integral endoplasmic reticulum membrane protein. Mol Biol Cell **7:**2029-2044.

65. **Baldridge RD, Rapoport TA.** 2016. Autoubiquitination of the Hrd1 Ligase Triggers Protein Retrotranslocation in ERAD. Cell **166:**394-407.

66. **Stein A, Ruggiano A, Carvalho P, Rapoport TA.** 2014. Key steps in ERAD of luminal ER proteins reconstituted with purified components. Cell **158:**1375-1388.

67. **Shibata E, Abbas T, Huang X, Wohlschlegel JA, Dutta A.** 2011. Selective ubiquitylation of p21 and Cdt1 by UBCH8 and UBE2G ubiquitin-conjugating enzymes via the CRL4Cdt2 ubiquitin ligase complex. Mol Cell Biol **31:**3136-3145.

68. **Gardner RG, Swarbrick GM, Bays NW, Cronin SR, Wilhovsky S, Seelig L, Kim C, Hampton RY.** 2000. Endoplasmic reticulum degradation requires lumen to cytosol signaling. Transmembrane control of Hrd1p by Hrd3p. J Cell Biol **151:**69-82.

69. **Hosokawa N, Wada I.** 2016. Association of the SEL1L protein transmembrane domain with HRD1 ubiquitin ligase regulates ERAD-L. FEBS J **283:**157-172.

70. **Horn SC, Hanna J, Hirsch C, Volkwein C, Schutz A, Heinemann U, Sommer T, Jarosch E.** 2009. Usa1 functions as a scaffold of the HRD-ubiquitin ligase. Mol Cell **36:**782-793.

71. **Schulze A, Standera S, Buerger E, Kikkert M, van Voorden S, Wiertz E, Koning F, Kloetzel PM, Seeger M.** 2005. The ubiquitin-domain protein HERP forms a complex with components of the endoplasmic reticulum associated degradation pathway. J Mol Biol **354:**1021-1027.

72. **Kreft SG, Wang L, Hochstrasser M.** 2006. Membrane topology of the yeast endoplasmic reticulum-localized ubiquitin ligase Doa10 and comparison with its human ortholog TEB4 (MARCH-VI). J Biol Chem **281:**4646-4653.

73. **Wang X, Herr RA, Rabelink M, Hoeben RC, Wiertz EJ, Hansen TH.** 2009. Ube2j2 ubiquitinates hydroxylated amino acids on ER-associated degradation substrates. J Cell Biol **187:**655-668.

74. **Burr ML, Cano F, Svobodova S, Boyle LH, Boname JM, Lehner PJ.** 2011. HRD1 and UBE2J1 target misfolded MHC class I heavy chains for endoplasmic reticulum-associated degradation. Proc Natl Acad Sci U S A **108:**2034-2039.

75. **Carvalho P, Goder V, Rapoport TA.** 2006. Distinct ubiquitin-ligase complexes define convergent pathways for the degradation of ER proteins. Cell **126:**361-373.

76. **Habeck G, Ebner FA, Shimada-Kreft H, Kreft SG.** 2015. The yeast ERAD-C ubiquitin ligase Doa10 recognizes an intramembrane degron. J Cell Biol **209:**621.

77. **Jakob CA, Bodmer D, Spirig U, Battig P, Marcil A, Dignard D, Bergeron JJ, Thomas DY, Aebi M.** 2001. Htm1p, a mannosidase-like protein, is involved in glycoprotein degradation in yeast. EMBO Rep **2:**423-430.

78. **Burke J, Lipari F, Igdoura S, Herscovics A.** 1996. The Saccharomyces cerevisiae processing alpha 1,2-mannosidase is localized in the endoplasmic reticulum, independently of known retrieval motifs. Eur J Cell Biol **70:**298-305.

79. **Cali T, Galli C, Olivari S, Molinari M.** 2008. Segregation and rapid turnover of EDEM1 by an autophagy-like mechanism modulates standard ERAD and folding activities. Biochem Biophys Res Commun **371:**405-410.

80. **Wu Y, Termine DJ, Swulius MT, Moremen KW, Sifers RN.** 2007. Human endoplasmic reticulum mannosidase I is subject to regulated proteolysis. Journal of Biological Chemistry **282:**4841-4849.

81. **Bernasconi R, Molinari M.** 2011. ERAD and ERAD tuning: disposal of cargo and of ERAD regulators from the mammalian ER. Curr Opin Cell Biol **23:**176-183.

82. **Fujita E, Kouroku Y, Isoai A, Kumagai H, Misutani A, Matsuda C, Hayashi YK, Momoi T.** 2007. Two endoplasmic reticulum-associated degradation (ERAD) systems for the novel variant of the mutant dysferlin: ubiquitin/proteasome ERAD(I) and autophagy/lysosome ERAD(II). Hum Mol Genet **16:**618-629.

83. **Hosokawa N, Wada I, Hasegawa K, Yorihuzi T, Tremblay LO, Herscovics A, Nagata K.** 2001. A novel ER alpha-mannosidase-like protein accelerates ER-associated degradation. Embo Reports **2:**415-422.

84. **Olivari S, Galli C, Alanen H, Ruddock L, Molinari M.** 2005. A novel stress-induced EDEM variant regulating endoplasmic reticulum-associated glycoprotein degradation. J Biol Chem **280:**2424-2428.

85. **Benyair R, Ogen-Shtern N, Lederkremer GZ.** 2015. Glycan regulation of ER-associated degradation through compartmentalization. Semin Cell Dev Biol **41:**99-109.

86. **Termine DJ, Moremen KW, Sifers RN.** 2009. The mammalian UPR boosts glycoprotein ERAD by suppressing the proteolytic downregulation of ER mannosidase I. Journal of Cell Science **122:**976-984.

87. **Inoue T, Tsai B.** 2013. How viruses use the endoplasmic reticulum for entry, replication, and assembly. Cold Spring Harb Perspect Biol **5:**a013250.

88. **Li S, Kong L, Yu X.** 2015. The expanding roles of endoplasmic reticulum stress in virus replication and pathogenesis. Crit Rev Microbiol **41:**150-164.

89. **Chan SW.** 2014. Unfolded protein response in hepatitis C virus infection. Front Microbiol **5:**233.

90. **Lazar C, Uta M, Branza-Nichita N.** 2014. Modulation of the unfolded protein response by the human hepatitis B virus. Front Microbiol **5:**433.

91. **Fung TS, Liu DX.** 2014. Coronavirus infection, ER stress, apoptosis and innate immunity. Front Microbiol **5:**296.

92. **Rathore AP, Ng ML, Vasudevan SG.** 2013. Differential unfolded protein response during Chikungunya and Sindbis virus infection: CHIKV nsP4 suppresses eIF2alpha phosphorylation. Virol J **10:**36.

93. **Borsa M, Ferreira PL, Petry A, Ferreira LG, Camargo MM, Bou-Habib DC, Pinto AR.** 2015. HIV infection and antiretroviral therapy lead to unfolded protein response activation. Virol J **12:**77.

94. **Williams BR.** 2001. Signal integration via PKR. Sci STKE **2001:**re2.

95. **Otto GA, Puglisi JD.** 2004. The pathway of HCV IRES-mediated translation initiation. Cell **119:**369-380.

96. **Lee DY, Sugden B.** 2008. The LMP1 oncogene of EBV activates PERK and the unfolded protein response to drive its own synthesis. Blood **111:**2280-2289.

97. **Cheng G, Feng Z, He B.** 2005. Herpes simplex virus 1 infection activates the endoplasmic reticulum resident kinase PERK and mediates eIF-2alpha dephosphorylation by the gamma(1)34.5 protein. J Virol **79:**1379-1388.

98. **Zhang F, Moon A, Childs K, Goodbourn S, Dixon LK.** 2010. The African swine fever virus DP71L protein recruits the protein phosphatase 1 catalytic subunit to dephosphorylate eIF2alpha and inhibits CHOP induction but is dispensable for these activities during virus infection. J Virol **84:**10681-10689.

99. **Pavio N, Romano PR, Graczyk TM, Feinstone SM, Taylor DR.** 2003. Protein synthesis and endoplasmic reticulum stress can be modulated by the hepatitis C virus envelope protein E2 through the eukaryotic initiation factor 2alpha kinase PERK. J Virol **77:**3578-3585.

100. **Hassan IH, Zhang MS, Powers LS, Shao JQ, Baltrusaitis J, Rutkowski DT, Legge K, Monick MM.** 2012. Influenza A viral replication is blocked by inhibition of the inositol-requiring enzyme 1 (IRE1) stress pathway. J Biol Chem **287:**4679-4689.

101. **Galindo I, Hernaez B, Munoz-Moreno R, Cuesta-Geijo MA, Dalmau-Mena I, Alonso C.** 2012. The ATF6 branch of unfolded protein response and apoptosis are activated to promote African swine fever virus infection. Cell Death Dis **3:**e341.

102. **Jheng JR, Ho JY, Horng JT.** 2014. ER stress, autophagy, and RNA viruses. Front Microbiol **5:**388.

103. **Caselli E, Benedetti S, Gentili V, Grigolato J, Di Luca D.** 2012. Short communication: activating transcription factor 4 (ATF4) promotes HIV type 1 activation. AIDS Res Hum Retroviruses **28:**907-912.

104. **Leymarie O, Embury-Hyatt C, Chevalier C, Jouneau L, Moroldo M, Da Costa B, Berhane Y, Delmas B, Weingartl HM, Le Goffic R.** 2014. PB1-F2 attenuates virulence of highly pathogenic avian H5N1 influenza virus in chickens. PLoS One **9:**e100679.

105. **Pena J, Harris E.** 2011. Dengue virus modulates the unfolded protein response in a time-dependent manner. J Biol Chem **286:**14226-14236.

106. **Stahl S, Burkhart JM, Hinte F, Tirosh B, Mohr H, Zahedi RP, Sickmann A, Ruzsics Z, Budt M, Brune W.** 2013. Cytomegalovirus downregulates IRE1 to repress the unfolded protein response. PLoS Pathog **9:**e1003544.

107. **Minakshi R, Padhan K, Rani M, Khan N, Ahmad F, Jameel S.** 2009. The SARS Coronavirus 3a protein causes endoplasmic reticulum stress and induces ligand-independent downregulation of the type 1 interferon receptor. PLoS One **4:**e8342.

108. **van der Wal FJ, Kikkert M, Wiertz E.** 2002. The HCMV gene products US2 and US11 target MHC class I molecules for degradation in the cytosol. Curr Top Microbiol Immunol **269:**37-55.

109. **Hsu JL, van den Boomen DJ, Tomasec P, Weekes MP, Antrobus R, Stanton RJ, Ruckova E, Sugrue D, Wilkie GS, Davison AJ, Wilkinson GW, Lehner PJ.** 2015. Plasma membrane profiling defines an expanded class of cell surface proteins selectively targeted for degradation by HCMV US2 in cooperation with UL141. PLoS Pathog **11:**e1004811.

110. **Boname JM, Bloor S, Wandel MP, Nathan JA, Antrobus R, Dingwell KS, Thurston TL, Smith DL, Smith JC, Randow F, Lehner PJ.** 2014. Cleavage by signal peptide peptidase is required for the degradation of selected tail-anchored proteins. J Cell Biol **205:**847-862.

111. **Loureiro J, Lilley BN, Spooner E, Noriega V, Tortorella D, Ploegh HL.** 2006. Signal peptide peptidase is required for dislocation from the endoplasmic reticulum. Nature **441:**894-897.

112. **Stagg HR, Thomas M, van den Boomen D, Wiertz EJ, Drabkin HA, Gemmill RM, Lehner PJ.** 2009. The TRC8 E3 ligase ubiquitinates MHC class I molecules before dislocation from the ER. J Cell Biol **186:**685-692.

113. **van den Boomen DJ, Timms RT, Grice GL, Stagg HR, Skodt K, Dougan G, Nathan JA, Lehner PJ.** 2014. TMEM129 is a Derlin-1 associated ERAD E3 ligase essential for virus-induced degradation of MHC-I. Proc Natl Acad Sci U S A **111:**11425-11430.

114. **van den Boomen DJ, Lehner PJ.** 2015. Identifying the ERAD ubiquitin E3 ligases for viral and cellular targeting of MHC class I. Mol Immunol **68:**106-111.

115. **Mueller B, Klemm EJ, Spooner E, Claessen JH, Ploegh HL.** 2008. SEL1L nucleates a protein complex required for dislocation of misfolded glycoproteins. Proc Natl Acad Sci U S A **105:**12325-12330.

116. **Boname JM, Stevenson PG.** 2001. MHC class I ubiquitination by a viral PHD/LAP finger protein. Immunity **15:**627-636.

117. **Levesque K, Finzi A, Binette J, Cohen EA.** 2004. Role of CD4 receptor down-regulation during HIV-1 infection. Curr HIV Res **2:**51-59.

118. **Lindwasser OW, Chaudhuri R, Bonifacino JS.** 2007. Mechanisms of CD4 downregulation by the Nef and Vpu proteins of primate immunodeficiency viruses. Curr Mol Med **7:**171-184.

119. **Foster JL, Garcia JV.** 2008. HIV-1 Nef: at the crossroads. Retrovirology **5:**84.

120. **Margottin F, Bour SP, Durand H, Selig L, Benichou S, Richard V, Thomas D, Strebel K, Benarous R.** 1998. A novel human WD protein, h-beta TrCp, that interacts with HIV-1 Vpu connects CD4 to the ER degradation pathway through an F-box motif. Mol Cell **1:**565-574.

121. **Strebel K.** 2014. HIV-1 Vpu - an ion channel in search of a job. Biochim Biophys Acta **1838:**1074-1081.

122. **Magadan JG, Perez-Victoria FJ, Sougrat R, Ye Y, Strebel K, Bonifacino JS.** 2010. Multilayered mechanism of CD4 downregulation by HIV-1 Vpu involving distinct ER retention and ERAD targeting steps. PLoS Pathog **6:**e1000869.

123. **Byun H, Halani N, Mertz JA, Ali AF, Lozano MM, Dudley JP.** 2010. Retroviral Rem protein requires processing by signal peptidase and retrotranslocation for nuclear function. Proc Natl Acad Sci U S A **107:**12287-12292.

124. **Surjit M, Jameel S, Lal SK.** 2007. Cytoplasmic localization of the ORF2 protein of hepatitis E virus is dependent on its ability to undergo retrotranslocation from the endoplasmic reticulum. J Virol **81:**3339-3345.

125. **Neu U, Stehle T, Atwood WJ.** 2009. The Polyomaviridae: Contributions of virus structure to our understanding of virus receptors and infectious entry. Virology **384:**389-399.

126. **Lilley BN, Gilbert JM, Ploegh HL, Benjamin TL.** 2006. Murine polyomavirus requires the endoplasmic reticulum protein Derlin-2 to initiate infection. J Virol **80:**8739-8744.

127. **Schelhaas M, Malmstrom J, Pelkmans L, Haugstetter J, Ellgaard L, Grunewald K, Helenius A.** 2007. Simian Virus 40 depends on ER protein folding and quality control factors for entry into host cells. Cell **131:**516-529.

128. **Reggiori F, Monastyrska I, Verheije MH, Cali T, Ulasli M, Bianchi S, Bernasconi R, de Haan CA, Molinari M.** 2010. Coronaviruses Hijack the LC3-I-positive EDEMosomes, ER-derived vesicles exporting short-lived ERAD regulators, for replication. Cell Host Microbe **7:**500-508.

129. **Noack J, Bernasconi R, Molinari M.** 2014. How viruses hijack the ERAD tuning machinery. J Virol **88:**10272-10275.

130. **Zhu P, Chertova E, Bess J, Jr., Lifson JD, Arthur LO, Liu J, Taylor KA, Roux KH.** 2003. Electron tomography analysis of envelope glycoprotein trimers on HIV and simian immunodeficiency virus virions. Proc Natl Acad Sci U S A **100:**15812-15817.

131. **Zhu P, Liu J, Bess J, Jr., Chertova E, Lifson JD, Grise H, Ofek GA, Taylor KA, Roux KH.** 2006. Distribution and three-dimensional structure of AIDS virus envelope spikes. Nature **441:**847-852.

132. **Forster F, Medalia O, Zauberman N, Baumeister W, Fass D.** 2005. Retrovirus envelope protein complex structure in situ studied by cryo-electron tomography. Proc Natl Acad Sci U S A **102:**4729-4734.

133. **Grunewald K, Desai P, Winkler DC, Heymann JB, Belnap DM, Baumeister W, Steven AC.** 2003. Three-dimensional structure of herpes simplex virus from cryo-electron tomography. Science **302:**1396-1398.

134. **Loney C, Mottet-Osman G, Roux L, Bhella D.** 2009. Paramyxovirus ultrastructure and genome packaging: cryo-electron tomography of sendai virus. J Virol **83:**8191-8197.

135. **Yamaguchi M, Danev R, Nishiyama K, Sugawara K, Nagayama K.** 2008. Zernike phase contrast electron microscopy of ice-embedded influenza A virus. J Struct Biol **162:**271-276.

136. **Schiller J, Chackerian B.** 2014. Why HIV Virions Have Low Numbers of Envelope Spikes: Implications for Vaccine Development. PLoS Pathog **10:**e1004254.

137. **Fennie C, Lasky LA.** 1989. Model for intracellular folding of the human immunodeficiency virus type 1 gp120. J Virol **63:**639-646.

138. **Hallenberger S, Tucker SP, Owens RJ, Bernstein HB, Compans RW.** 1993. Secretion of a truncated form of the human immunodeficiency virus type 1 envelope glycoprotein. Virology **193:**510-514.

139. **Willey RL, Bonifacino JS, Potts BJ, Martin MA, Klausner RD.** 1988. Biosynthesis, cleavage, and degradation of the human immunodeficiency virus 1 envelope glycoprotein gp160. Proc Natl Acad Sci U S A **85:**9580-9584.

140. **Zhou T, Han Y, Dang Y, Wang X, Zheng YH.** 2009. A novel HIV-1 restriction factor that is biologically distinct from APOBEC3 cytidine deaminases in a human T cell line CEM.NKR. Retrovirology **6:**31.

141. **Zhou T, Dang Y, Zheng YH.** 2014. The mitochondrial translocator protein, TSPO, inhibits HIV-1 envelope glycoprotein biosynthesis via the endoplasmic reticulum-associated protein degradation pathway. J Virol **88:**3474-3484.

142. **Zamzami N, Kroemer G.** 2001. The mitochondrion in apoptosis: how Pandora's box opens. Nat Rev Mol Cell Biol **2:**67-71.

143. **Gatliff J, East D, Crosby J, Abeti R, Harvey R, Craigen W, Parker P, Campanella M.** 2014. TSPO interacts with VDAC1 and triggers a ROS-mediated inhibition of mitochondrial quality control. Autophagy **10:**2279-2296.

144. **Wu Y, Swulius MT, Moremen KW, Sifers RN.** 2003. Elucidation of the molecular logic by which misfolded alpha 1-antitrypsin is preferentially selected for degradation. Proceedings of the National Academy of Sciences of the United States of America **100:**8229-8234.

145. **Zhou T, Frabutt DA, Moremen KW, Zheng YH.** 2015. ERManI (Endoplasmic Reticulum Class I alpha-Mannosidase) Is Required for HIV-1 Envelope Glycoprotein Degradation via Endoplasmic Reticulum-associated Protein Degradation Pathway. J Biol Chem **290:**22184-22192.

146. **Gonzalez DS, Karaveg K, Vandersall-Nairn AS, Lal A, Moremen KW.** 1999. Identification, expression, and characterization of a cDNA encoding human endoplasmic reticulum mannosidase I, the enzyme that catalyzes the first mannose trimming step in mammalian Asn-linked oligosaccharide biosynthesis. Journal of Biological Chemistry **274:**21375-21386.

147. **Tremblay LO, Herscovics A.** 1999. Cloning and expression of a specific human alpha 1,2-mannosidase that trims Man(9)GlcNAc(2) to Man(8)GlcNAc(2) isomer B during N-glycan biosynthesis. Glycobiology **9:**1073-1078.

148. **Vallee F, Karaveg K, Herscovics A, Moremen KW, Howell PL.** 2000. Structural basis for catalysis and inhibition of N-glycan processing class I alpha 1,2-mannosidases. Journal of Biological Chemistry **275:**41287-41298.

149. **Lipari F, Herscovics A.** 1996. Role of the cysteine residues in the alpha1,2-mannosidase involved in N-glycan biosynthesis in Saccharomyces cerevisiae. The conserved Cys340 and Cys385 residues form an essential disulfide bond. J Biol Chem **271:**27615-27622.

150. **Rafiq MA, Kuss AW, Puettmann L, Noor A, Ramiah A, Ali G, Hu H, Kerio NA, Xiang Y, Garshasbi M, Khan MA, Ishak GE, Weksberg R, Ullmann R, Tzschach A, Kahrizi K, Mahmood K, Naeem F, Ayub M, Moremen KW, Vincent JB, Ropers HH, Ansar M, Najmabadi H.** 2011. Mutations in the Alpha 1,2-Mannosidase Gene, MAN1B1, Cause Autosomal-Recessive Intellectual Disability. American Journal of Human Genetics **89:**176-182.

151. **Gupta S, Fahiminiya S, Wang T, Dempsey Nunez L, Rosenblatt DS, Gibson WT, Gilfix B, Bergeron JJ, Jerome-Majewska LA.** 2016. Somatic overgrowth associated with homozygous mutations in both MAN1B1 and SEC23A. Cold Spring Harb Mol Case Stud **2:**a000737.

152. **Iannotti MJ, Figard L, Sokac AM, Sifers RN.** 2014. A Golgi-localized mannosidase (MAN1B1) plays a non-enzymatic gatekeeper role in protein biosynthetic quality control. J Biol Chem **289:**11844-11858.

153. **Zhang X, Zhou T, Frabutt DA, Zheng YH.** 2016. HIV-1 Vpr increases Env expression by preventing Env from endoplasmic reticulum-associated protein degradation (ERAD). Virology **496:**194-202.

154. **Lazar C, Macovei A, Petrescu S, Branza-Nichita N.** 2012. Activation of ERAD pathway by human hepatitis B virus modulates viral and subviral particle production. PLoS One **7:**e34169.

155. **Saeed M, Suzuki R, Watanabe N, Masaki T, Tomonaga M, Muhammad A, Kato T, Matsuura Y, Watanabe H, Wakita T, Suzuki T.** 2011. Role of the endoplasmic reticulum-associated degradation (ERAD) pathway in degradation of hepatitis C virus envelope proteins and production of virus particles. J Biol Chem **286:**37264-37273.

156. **McPherson S, Powell EE, Barrie HD, Clouston AD, McGuckin M, Jonsson JR.** 2011. No evidence of the unfolded protein response in patients with chronic hepatitis C virus infection. J Gastroenterol Hepatol **26:**319-327.

157. **Britt WJ, Mach M.** 1996. Human cytomegalovirus glycoproteins. Intervirology **39:**401-412.

158. **Compton T, Nepomuceno RR, Nowlin DM.** 1992. Human cytomegalovirus penetrates host cells by pH-independent fusion at the cell surface. Virology **191:**387-395.

159. **Zhou M, Lanchy JM, Ryckman BJ.** 2015. Human Cytomegalovirus gH/gL/gO Promotes the Fusion Step of Entry into All Cell Types, whereas gH/gL/UL128-131 Broadens Virus Tropism through a Distinct Mechanism. J Virol **89:**8999-9009.

160. **Hutchinson L, Browne H, Wargent V, Davis-Poynter N, Primorac S, Goldsmith K, Minson AC, Johnson DC.** 1992. A novel herpes simplex virus glycoprotein, gL, forms a complex with glycoprotein H (gH) and affects normal folding and surface expression of gH. J Virol **66:**2240-2250.

161. **Gardner TJ, Hernandez RE, Noriega VM, Tortorella D.** 2016. Human cytomegalovirus gH stability and trafficking are regulated by ER-associated degradation and transmembrane architecture. Sci Rep **6:**23692.

162. **Tamura T, Cormier JH, Hebert DN.** 2011. Characterization of early EDEM1 protein maturation events and their functional implications. J Biol Chem **286:**24906-24915.

163. **Molinari M, Calanca V, Galli C, Lucca P, Paganetti P.** 2003. Role of EDEM in the release of misfolded glycoproteins from the calnexin cycle. Science **299:**1397-1400.

164. **Cormier JH, Tamura T, Sunryd JC, Hebert DN.** 2009. EDEM1 recognition and delivery of misfolded proteins to the SEL1L-containing ERAD complex. Mol Cell **34:**627-633.

165. **Pan S, Wang S, Utama B, Huang L, Blok N, Estes MK, Moremen KW, Sifers RN.** 2011. Golgi localization of ERManI defines spatial separation of the mammalian glycoprotein quality control system. Mol Biol Cell **22:**2810-2822.

166. **Checkley MA, Luttge BG, Freed EO.** 2011. HIV-1 Envelope Glycoprotein Biosynthesis, Trafficking, and Incorporation. Journal of Molecular Biology **410:**582-608.

167. **Henrissat B, Davies G.** 1997. Structural and sequence-based classification of glycoside hydrolases. Curr Opin Struct Biol **7:**637-644.

168. **Jakob CA, Burda P, Roth J, Aebi M.** 1998. Degradation of misfolded endoplasmic reticulum glycoproteins in Saccharomyces cerevisiae is determined by a specific oligosaccharide structure. J Cell Biol **142:**1223-1233.

169. **Hosokawa N, Tremblay LO, You ZP, Herscovics A, Wada I, Nagata K.** 2003. Enhancement of endoplasmic reticulum (ER) degradation of misfolded null Hong Kong alpha(1)-antitrypsin by human ER mannosidase I. Journal of Biological Chemistry **278:**26287-26294.

170. **Oda Y, Hosokawa N, Wada I, Nagata K.** 2003. EDEM as an acceptor of terminally misfolded glycoproteins released from calnexin. Science **299:**1394-1397.

171. **McEnery MW, Snowman AM, Trifiletti RR, Snyder SH.** 1992. Isolation of the mitochondrial benzodiazepine receptor: association with the voltage-dependent anion channel and the adenine nucleotide carrier. Proc Natl Acad Sci U S A **89:**3170-3174.

172. **Herscovics A.** 2001. Structure and function of Class I alpha 1,2-mannosidases involved in glycoprotein synthesis and endoplasmic reticulum quality control. Biochimie **83:**757-762.

173. **Mali P, Yang L, Esvelt KM, Aach J, Guell M, DiCarlo JE, Norville JE, Church GM.** 2013. RNA-guided human genome engineering via Cas9. Science **339:**823-826.

174. **Cong L, Ran FA, Cox D, Lin S, Barretto R, Habib N, Hsu PD, Wu X, Jiang W, Marraffini LA, Zhang F.** 2013. Multiplex genome engineering using CRISPR/Cas systems. Science **339:**819-823.

175. **Feige MJ, Hendershot LM.** 2011. Disulfide bonds in ER protein folding and homeostasis. Current Opinion in Cell Biology **23:**167-175.

176. **Yang Y, Song Y, Loscalzo J.** 2007. Regulation of the protein disulfide proteome by mitochondria in mammalian cells. Proc Natl Acad Sci U S A **104:**10813-10817.

177. **Simmen T, Lynes EM, Gesson K, Thomas G.** 2010. Oxidative protein folding in the endoplasmic reticulum: tight links to the mitochondria-associated membrane (MAM). Biochim Biophys Acta **1798:**1465-1473.

178. **Kornmann B, Walter P.** 2010. ERMES-mediated ER-mitochondria contacts: molecular hubs for the regulation of mitochondrial biology. J Cell Sci **123:**1389-1393.

179. **Dellisanti C.** 2015. TSPO through the crystal looking glass. Nat Struct Mol Biol **22**.

180. **Karaveg K, Moremen KW.** 2005. Energetics of substrate binding and catalysis by class 1 (glycosylhydrolase family 47) alpha-mannosidases involved in N-glycan processing and endoplasmic reticulum quality control. Journal of Biological Chemistry **280:**29837-29848.

181. **Rymen D, Peanne R, Millon MB, Race V, Sturiale L, Garozzo D, Mills P, Clayton P, Asteggiano CG, Quelhas D, Cansu A, Martins E, Nassogne MC, Goncalves-Rocha M, Topaloglu H, Jaeken J, Foulquier F, Matthijs G.** 2013. MAN1B1 deficiency: an unexpected CDG-II. PLoS Genet **9:**e1003989.

182. **Mast SW, Diekman K, Karaveg K, Davis A, Sifers RN, Moremen KW.** 2004. Human EDEM2, a novel homolog of family 47 glycosidases, is involved in ER-associated degradation of glycoproteins. Glycobiology **14:**1139-1139.

183. **Dang Y, Wang X, Esselman WJ, Zheng YH.** 2006. Identification of APOBEC3DE as another antiretroviral factor from the human APOBEC family. J Virol **80:**10522-10533.

184. **Iwasaki A, Medzhitov R.** 2015. Control of adaptive immunity by the innate immune system. Nat Immunol **16:**343-353.

185. **Ma Z, Damania B.** 2016. The cGAS-STING Defense Pathway and Its Counteraction by Viruses. Cell Host Microbe **19:**150-158.

186. **Chan SW.** 2014. The unfolded protein response in virus infections. Front Microbiol **5:**518.

187. **Wang M, Kaufman RJ.** 2014. The impact of the endoplasmic reticulum protein-folding environment on cancer development. Nat Rev Cancer **14:**581-597.

188. **Vembar SS, Brodsky JL.** 2008. One step at a time: endoplasmic reticulum-associated degradation. Nat Rev Mol Cell Biol **9:**944-957.

189. **Knipe DM, Howley PM.** 2013. Fields virology, Sixth edition. ed. Wolters Kluwer/Lippincott Williams & Wilkins Health, Philadelphia, PA.

190. **Gamblin SJ, Skehel JJ.** 2010. Influenza hemagglutinin and neuraminidase membrane glycoproteins. J Biol Chem **285:**28403-28409.

191. **Luo S, Mao C, Lee B, Lee AS.** 2006. GRP78/BiP is required for cell proliferation and protecting the inner cell mass from apoptosis during early mouse embryonic development. Mol Cell Biol **26:**5688-5697.

192. **Hrincius ER, Liedmann S, Finkelstein D, Vogel P, Gansebom S, Samarasinghe AE, You D, Cormier SA, McCullers JA.** 2015. Acute Lung Injury Results from Innate Sensing of Viruses by an ER Stress Pathway. Cell Rep **11:**1591-1603.

193. **Caramelo JJ, Parodi AJ.** 2008. Getting in and out from calnexin/calreticulin cycles. J Biol Chem **283:**10221-10225.

194. **Hammond C, Braakman I, Helenius A.** 1994. Role of N-linked oligosaccharide recognition, glucose trimming, and calnexin in glycoprotein folding and quality control. Proc Natl Acad Sci U S A **91:**913-917.

195. **Hebert DN, Foellmer B, Helenius A.** 1996. Calnexin and calreticulin promote folding, delay oligomerization and suppress degradation of influenza hemagglutinin in microsomes. EMBO J **15:**2961-2968.

196. **Hebert DN, Zhang JX, Chen W, Foellmer B, Helenius A.** 1997. The number and location of glycans on influenza hemagglutinin determine folding and association with calnexin and calreticulin. J Cell Biol **139:**613-623.

197. **Wang B, Wang Y, Frabutt DA, Zhang X, Yao X, Hu D, Zhang Z, Liu C, Zheng S, Xiang SH, Zheng YH.** 2017. Mechanistic Understanding of N-Glycosylation in Ebola Virus Glycoprotein Maturation and Function. J Biol Chem doi:10.1074/jbc.M116.768168.

198. **Wang N, Glidden EJ, Murphy SR, Pearse BR, Hebert DN.** 2008. The cotranslational maturation program for the type II membrane glycoprotein influenza neuraminidase. J Biol Chem **283:**33826-33837.

199. **Yu CY, Hsu YW, Liao CL, Lin YL.** 2006. Flavivirus infection activates the XBP1 pathway of the unfolded protein response to cope with endoplasmic reticulum stress. J Virol **80:**11868-11880.

200. **Hoffmann E, Neumann G, Kawaoka Y, Hobom G, Webster RG.** 2000. A DNA transfection system for generation of influenza A virus from eight plasmids. Proc Natl Acad Sci U S A **97:**6108-6113.

201. **Valastyan JS, Lindquist S.** 2014. Mechanisms of protein-folding diseases at a glance. Dis Model Mech **7:**9-14.

202. **Smith JA.** 2014. A new paradigm: innate immune sensing of viruses via the unfolded protein response. Front Microbiol **5:**222.

203. **Byun H, Gou Y, Zook A, Lozano MM, Dudley JP.** 2014. ERAD and how viruses exploit it. Front Microbiol **5:**330.

204. **Frabutt DA, Zheng YH.** 2016. Arms Race between Enveloped Viruses and the Host ERAD Machinery. Viruses **8**.

205. **Li Y, Bergeron JJ, Luo L, Ou WJ, Thomas DY, Kang CY.** 1996. Effects of inefficient cleavage of the signal sequence of HIV-1 gp 120 on its association with calnexin, folding, and intracellular transport. Proc Natl Acad Sci U S A **93:**9606-9611.

206. **Ou WJ, Bergeron JJ, Li Y, Kang CY, Thomas DY.** 1995. Conformational changes induced in the endoplasmic reticulum luminal domain of calnexin by Mg-ATP and Ca2+. J Biol Chem **270:**18051-18059.

207. **Otteken A, Moss B.** 1996. Calreticulin interacts with newly synthesized human immunodeficiency virus type 1 envelope glycoprotein, suggesting a chaperone function similar to that of calnexin. J Biol Chem **271:**97-103.

208. **Papandreou MJ, Barbouche R, Guieu R, Rivera S, Fantini J, Khrestchatisky M, Jones IM, Fenouillet E.** 2010. Mapping of domains on HIV envelope protein mediating association with calnexin and protein-disulfide isomerase. J Biol Chem **285:**13788-13796.

209. **Moremen KW, Robbins PW.** 1991. Isolation, characterization, and expression of cDNAs encoding murine alpha-mannosidase II, a Golgi enzyme that controls conversion of high mannose to complex N-glycans. J Cell Biol **115:**1521-1534.

210. **Moremen KW, Touster O, Robbins PW.** 1991. Novel purification of the catalytic domain of Golgi alpha-mannosidase II. Characterization and comparison with the intact enzyme. J Biol Chem **266:**16876-16885.

211. **Land A, Zonneveld D, Braakman I.** 2003. Folding of HIV-1 envelope glycoprotein involves extensive isomerization of disulfide bonds and conformation-dependent leader peptide cleavage. FASEB J **17:**1058-1067.

212. **Zheng YH, Irwin D, Kurosu T, Tokunaga K, Sata T, Peterlin BM.** 2004. Human APOBEC3F is another host factor that blocks human immunodeficiency virus type 1 replication. J Virol **78:**6073-6076.

213. **Han JY, Zhao Y, Anderson WF, Cannon PM.** 1998. Role of variable regions A and B in receptor binding domain of amphotropic murine leukemia virus envelope protein. J Virol **72:**9101-9108.

214. **Braakman I, Hoover-Litty H, Wagner KR, Helenius A.** 1991. Folding of influenza hemagglutinin in the endoplasmic reticulum. J Cell Biol **114:**401-411.

215. **Earl PL, Moss B, Doms RW.** 1991. Folding, interaction with GRP78-BiP, assembly, and transport of the human immunodeficiency virus type 1 envelope protein. J Virol **65:**2047-2055.

216. **Snapp EL, McCaul N, Quandte M, Cabartova Z, Bontjer I, Kallgren C, Nilsson I, Land A, von Heijne G, Sanders RW, Braakman I.** 2017. Structure and topology around the cleavage site regulate post-translational cleavage of the HIV-1 gp160 signal peptide. Elife **6**.